

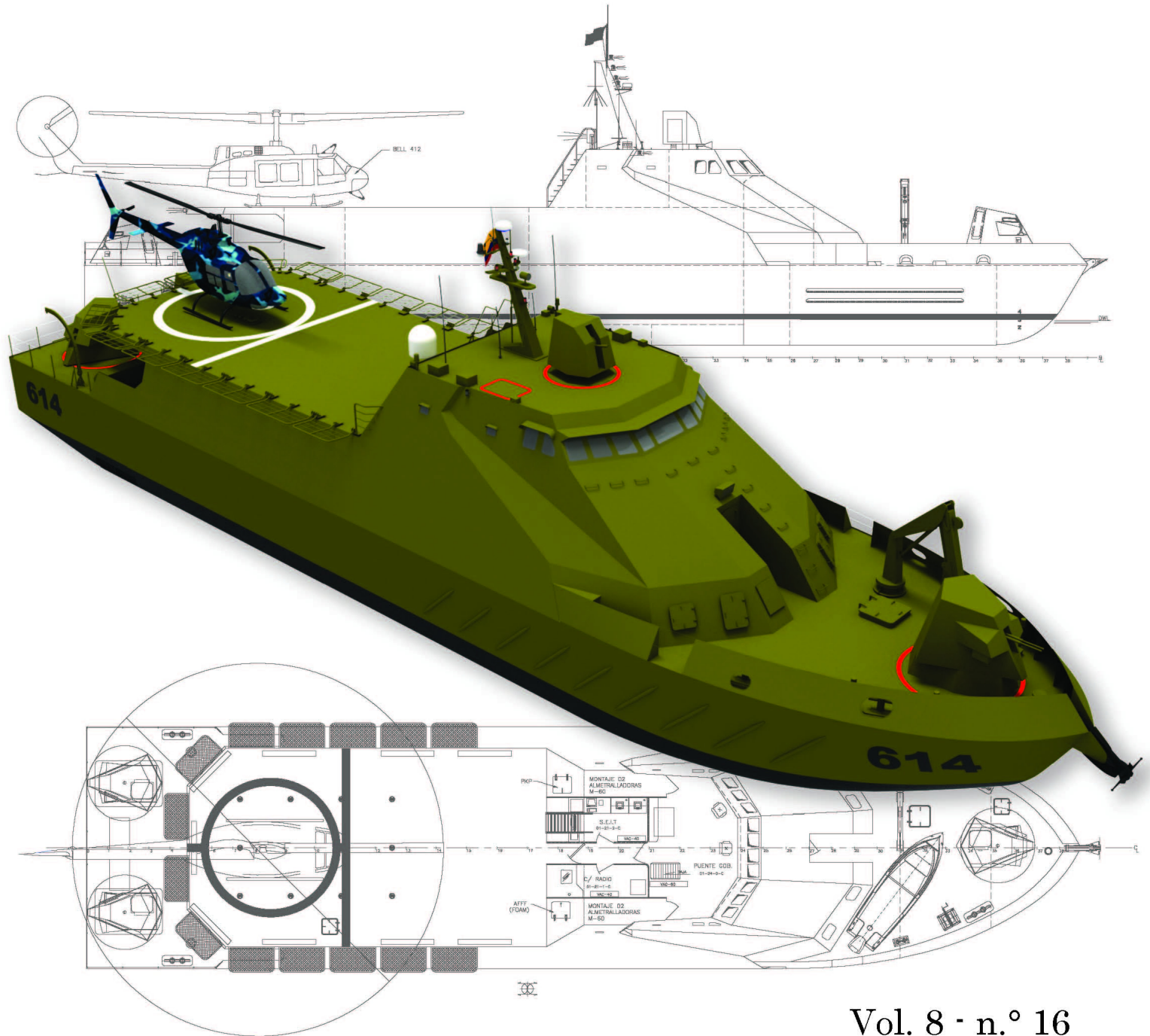
SHIP

SCIENCE & TECHNOLOGY
CIENCIA & TECNOLOGÍA DE BUQUES

ISSN 1909-8642



COTECMAR
COLOMBIA



Vol. 8 - n.º 16
(1 - 82) January 2015

SHIP

SCIENCE & TECHNOLOGY

CIENCIA & TECNOLOGÍA DE BUQUES

Volume 8, Number 16

January 2015

ISSN 1909-8642

COTECMAR

President

Rear Admiral **Jorge Enrique Carreño Moreno, Ph. D.**

Vice President of Technology and Operations

Captain **Andres Alejandro Osorio Carrillo, MBA (c)**

Manager of Science, Technology and Innovation

Commander **José Manuel Gómez Torres, MSSE & MSME**

Editor in Chief

Commander **José Manuel Gómez Torres, MSSE & MSME**

Editorial Board

Marcos Salas Inzunza, Ph. D.

Universidad Austral de Chile

Diego Hernández Lozada, Ph.D.

Universidad Nacional de Colombia

Jairo Useche Vivero, Ph. D.

Universidad Tecnológica de Bolívar, Colombia

Antonio Bula Silvera, Ph. D.

Universidad del Norte, Colombia

Juan Contreras Montes, Ph. D.

Escuela Naval Almirante Padilla, Colombia

Luis Guarín, Ph. D.

Safety at Sea Ltd.

Carlos Cano Restrepo, M.Sc.

COTECMAR, Colombia

Scientific Committee

CALM. Jorge Enrique Carreño Moreno, Ph. D.

COTECMAR, Colombia

Marco Sanjuan, Ph. D.

Universidad del Norte, Colombia

Jairo Cabrera Tovar, Ph. D.

Universidad Tecnológica de Bolívar, Colombia

Richard Luco Salman, Ph. D.

Universidad Austral de Chile

Luis Pérez Rojas, Ph. D.

Universidad Politécnica de Madrid, Spain

Rui Carlos Botter, Ph. D.

Universidad de Sao Paulo, Brazil

Ship Science & Technology is a specialized journal in topics related to naval architecture, and naval, marine and ocean engineering. Every six months, the journal publishes scientific papers that constitute an original contribution in the development of the mentioned areas, resulting from research projects of the Science and Technology Corporation for the Naval, Maritime and Riverine Industries, and other institutions and researchers. It is distributed nationally and internationally by exchange or subscription.

A publication of

Corporación de Ciencia y Tecnología para el Desarrollo de la
Industria Naval, Marítima y Fluvial - COTECMAR

Electronic version: www.shipjournal.co

Editorial Coordinator

Jimmy Saravia Arenas. M.Sc.

Layout and design

Mauricio Sarmiento Barreto

Printed by

C&D Publicidad & Marketing. Bogotá, D.C.



9

Development of a Comparison Method of Sonar Systems for Surface Platforms

Desarrollo de un método de comparación de sistemas de sonar para plataformas de superficie

Andrés Cortes Ciro, Ennio Emanuel Pinzón Villarroel

19

Fuel-Cell Integration on Board Surface Ships

Integración de celdas de combustible a bordo de buques de superficie

David Ignacio Fuentes, Hernán de Lavalle Pérez

29

Implementation of the Confirmation of Methods in the calibration of Measuring Equipment as Standardized Strategy to Assure the Quality of Measurements Made in the Construction, Repair, and Modernization of Ships and Naval Artifacts in COTECMAR

Implementación de la confirmación de métodos en la calibración de equipos de medición como estrategia normalizada para asegurar la calidad de las mediciones realizadas en la construcción, reparación y modernización de buques y artefactos navales en COTECMAR

Ronald Yesid Argote Guzmán

43

Solution to the Anti-aircraft Fire Control Problem on a Naval Platform Using the Direct Geometric Model

Solución al problema de control de tiro antiaéreo sobre una plataforma naval empleando el modelo geométrico directo

Francisco Gil, Andrés Vivas

57

Fatigue Analysis of the Structural Bottom of an Aluminum Planing Craft through Vibratory Load of the Propeller System

Análisis de fatiga del fondo estructural de una lancha planeadora en aluminio por carga vibratoria del sistema propulsor

José R. Marín, Carlos A. Cuenca

Editorial Note

Cartagena de Indias, January 23th 2015.

During 2014, COTECMAR strengthens its purpose as a Science and Technology Corporation by making important changes inside its organizational structure like creating the Vice-presidency of Technology and Operations which contains the Management of Science, Technology and Innovation as a business unit in charge of coordinating and boosting research, technological development and innovation processes in order to accomplish its corporate statement as scientific and technological leader of Colombian naval industry.

The approach of providing expert knowledge through research and its appropriate application into products has allowed COTECMAR ratify its technological character linked to industrial activity, and its calling to offer solutions to requirements of its customers. For this reason, from a research, development and innovation perspective, the business units (Production plants) are seen as laboratories where take place the identification of needs, sector problems and solutions testing, which are consequence of research and development processes. Within this virtuous circle, where market share, technological development and innovation permits to COTECMAR building and maintaining its sustainability in naval sector framed as a competitive bet in Colombia.

In this issue are found articles related to: Sonar systems to Surface platforms, Fuel cells integrations on board of ships, Confirmation of Methods in Measurement Equipment Calibration to ensure quality of ship production, anti-aircraft fire control by using direct geometric model and fatigue analysis of the structural bottom of an aluminium planning craft.

Greetings to our writers and readers, we appreciate your contributions and commitments in sustaining relationship to our spreading initiative of scientific knowledge among the naval design and architecture community.



Commander JOSÉ MANUEL GÓMEZ TORRES
Editor of the Ship Science and Technology Journal

Nota Editorial

Cartagena de Indias, 23 de Enero de 2015.

En el año 2014, COTECMAR fortalece su propósito como Corporación de Ciencia y Tecnología, realizando cambios importantes dentro de su estructura organizacional como la creación de la Vicepresidencia de Tecnologías y Operaciones y dentro de esta la Gerencia de Ciencia, Tecnología e Innovación como una unidad de negocio y encargada de gestionar y dinamizar los procesos de investigación, desarrollo tecnológico e innovación para el cumplimiento de su misión como líder científico y tecnológico de la industria naval en Colombia.

El enfoque de generar conocimiento experto a través de la investigación y su oportuna aplicación en los productos, le ha permitido a COTECMAR ratificar su carácter tecnológico vinculado a la actividad industrial, y su vocación a dar soluciones integrales a las necesidades de sus clientes. Es por ello que desde una perspectiva de investigación, desarrollo e innovación, las unidades de negocio (Plantas Productivas) son vistas como los laboratorios en los que se identifican las necesidades y problemáticas del sector y se prueban las soluciones, producto del proceso de investigación y desarrollo. Es en este círculo virtuoso, donde el mercado, el desarrollo tecnológico y la innovación le permiten a COTECMAR construir y mantener su sostenibilidad dentro del sector naval enmarcado como apuesta competitiva en Colombia.

En esta edición se encuentran artículos relacionados con: Sistemas de sonar para plataformas de superficie, Integración de celdas de combustible a bordo de buques, confirmación de métodos de calibración de equipos de medición para el aseguramiento de la calidad de los procesos de producción de buques, control de tiro antiaéreo mediante la aplicación del método geométrico directo y análisis de fatiga del fondo estructural de una lancha planeadora en aluminio.

Saludos a nuestros autores y lectores, agradecemos por sus aportes y compromiso en permanecer vinculados a nuestra iniciativa de difusión del conocimiento científico en la comunidad del diseño, la arquitectura e ingeniería naval.



Capitán de Fragata JOSÉ MANUEL GÓMEZ TORRES
Editor Revista Ciencia y Tecnología de Buques

Development of a Comparison Method of Sonar Systems for Surface Platforms

Desarrollo de un método de comparación de sistemas de sonar para plataformas de superficie

Andrés Cortes Ciro ¹
Ennio Emanuel Pinzón Villarroel ²

Abstract

This work sought to study the models of acoustic signal propagation in marine environments according to open literature currently available, by interpreting the different effects occurring during their propagation and their characteristic principal parameters; identifying models of underwater acoustic propagation that may occur and its corresponding simulation for its understanding. Software, denominated BELLFAT, was developed in Matlab, which permits predicting, evaluating, and analyzing the capabilities of an active sonar system. Such can function by taking depth, temperature, salinity in the sea of any reference area and the characteristics of the sonar to evaluate. Thus, this computational tool is established to study marine sonar systems sought to be developed or as a key piece to establish the characteristics active sonar must have for the purposes of a surface platform.

Key words: sonar systems, acoustic wave, propagation, simulation, Matlab.

Resumen

Se estudiaron modelos de propagación de señales acústicas en entornos marinos de acuerdo a la literatura abierta disponible en la actualidad, interpretando los diferentes efectos que se presentan en su propagación y sus principales parámetros que la caracterizan; se identifican modelos de propagación acústica bajo el agua que se pueden presentar y su correspondiente simulación para su entendimiento. Se desarrolló un software en Matlab denominado BELLFAT que permite predecir, evaluar y analizar las capacidades de un sistema de sonar activo. Este último puede funcionar tomando la profundidad, temperatura y salinidad en el mar de cualquier área de referencia y las características del sonar a evaluar. De esta forma, se establece esta herramienta computacional para el estudio de sistemas de sonar marítimo que se pretenda desarrollar o como pieza clave para establecer las características que debe tener un sonar activo para los propósitos de una plataforma de superficie.

Palabras claves: sistemas de sonar, onda acústica, propagación, simulación, Matlab.

Date Received: June 17th, 2014 - *Fecha de recepción: 17 de junio de 2014*

Date Accepted: August 22th, 2014 - *Fecha de aceptación: 22 de agosto de 2014*

¹ Teniente de Fragata de la Armada Nacional. Escuela Naval de Cadetes "Almirante Padilla", Colombia. e-mail: apande80@gmail.com

² Teniente de Fragata de la Armada Nacional. Escuela Naval de Cadetes "Almirante Padilla", Colombia. e-mail: ennio navy@hotmail.com

Introduction

The National Navy plans to design and construct via its own means through the Science and Technology Corporation for the Development of the Naval, Maritime, and Riverine Industry (COTECMAR), the replacement of current 'Almirante Padilla' class light frigates, through the project Strategic Surface Platform (SSP) broadly supported by the National Ministry of Defense. Their naval structure must have a vital optimum sonar system to carry out its functions in the operations area that adjust to time, environment, space, and scenario [1].

Currently, some countries have been conducting research on sonar systems through their military academic centers to construct their devices and not depend upon transnational private industry. This has generated the development of software that permits evaluating the behavior of said equipment according to the purpose and specific conditions of the marine environment. Information on the development of these programs is quite scarce and the little there is has been available through research centers that study the behavior of the sound propagation phenomenon, but not based on the parameters of a sonar system that permits predicting their performance. Among these entities, there is the Center for Marine Science and Technology at Curtin University in Australia, which openly share their development of the "acoustic toolbox" tool by Matlab for academic purposes [2]. It is called AcTUP and, along with PROPAS, is used by the Naval School's Faculty of Oceanography, are the only tools currently available in open literature.

The first section describes acoustic propagation models in underwater environments and the simulation tools now available in open literature. The second section defines the necessary parameters that characterize the Colombian marine environment and certifies data gathering at a given reference area through the National Navy's Center for Oceanographic and Hydrographic Research (CIOH, for the term in Spanish). The third section briefly describes the development of an interface in Matlab that will permit validating, studying, and evaluating the performance of active

sonar according to the information collected per the mathematical formulas defined in the text "Principles of underwater sound" by Robert Urick, considered the main bibliographical source on the topic. Thereafter, the fourth section compared the results obtained from the software developed, called BELLFAT, with the literature – permitting precision and validity. Finally, in the conclusions, this software permits implementing a comparison method of sonar systems for surface platforms in the National Navy.

Materials and Methods

This degree work was a non-experimental transactional research. As described by Aparicio and García in their research on acoustic signals in submarine environments: "diverse mathematical models exist to study acoustic propagation in underwater environments, highlighting ray-tracing models ... the ray-tracing model is based on the consideration that the wave energy can be concentrated in defined paths, so that we may think of rays rather than waves... the ray-tracing model calculates the equations followed by the rays, as well as the pressure field they generate from which transmission losses may be obtained, along with the propagation time of said rays." [3]

Parameters of Underwater Acoustic Propagation

Speed of Sound

The speed of sound in the sea is an oceanographic variable that determines several characteristics from the environment of the transmission of sound. It varies according to the season, geographic conditions, depth, and exact location of the given area. The modern experimental method in the direct measurement of the speed of sound uses laboratory techniques under carefully controlled conditions. All the methods determine the speed of sound in terms of three basic quantities, which are: temperature, salinity, and pressure [4]. We took as reference that developed by Medwin [5].

$$c = 1492.9 + 4.6T - 5.5 * 10^{-2}T^2 + 2.9 * 10^{-4}T^3 + (1.34 - 10^{-2}T)(S - 35) + 1.6 * 10^{-2}D \quad (1)$$

Limits:

- 0 ≤ T ≤ 35° (Temperature in Celsius)
- 0 ≤ S ≤ 45 (Salinity in parts per thousand)
- 0 ≤ D ≤ 1,000 (Depth in meters)

Within the observation field of the speed of sound in underwater environments, two devices are used that determine the profile of the speed of sound. One of these specialized equipments is the bathythermograph, which measures temperature in function of depth as it descends into the sea; the other is the sound profiler, which measures directly the speed of sound in terms of time over a constant fixed trajectory [4].

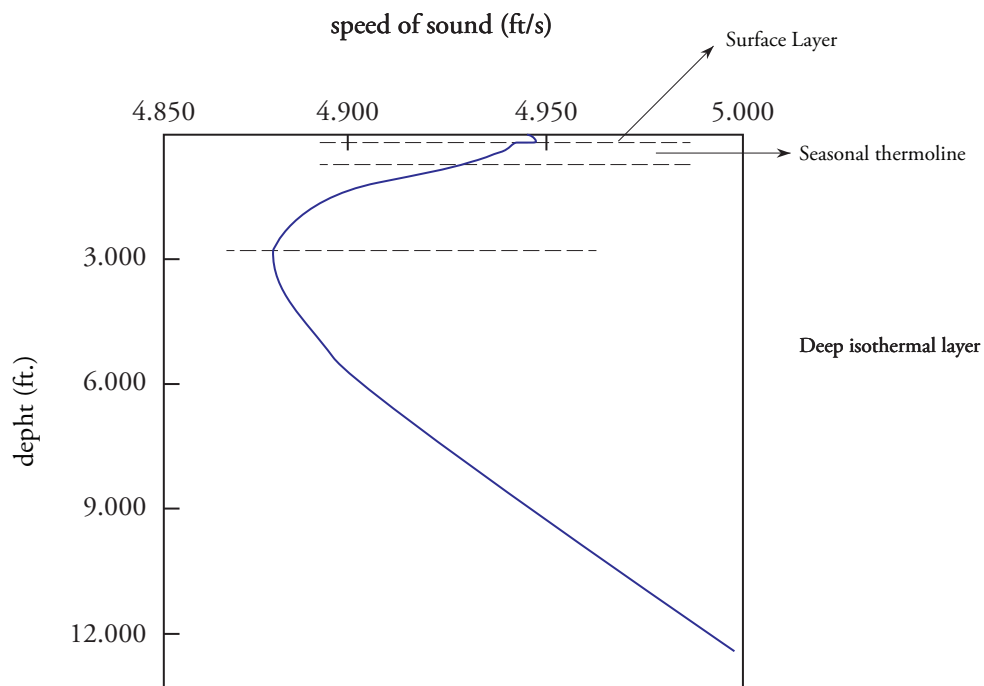
Transmission losses

When an acoustic propagation through the sea is originated, the signal's intensity is reduced, deriving in considerable loss of power. Diminished intensity indicates transmission losses (TL). The

total propagation loss is the difference between the sound intensity at a point near to the source and at a remote point. Propagation losses are due to several causes in which losses through absorption and through expansion of the wavefront stand out. These losses occur with all underwater transmissions. Transmission losses of sound depend on: [6]

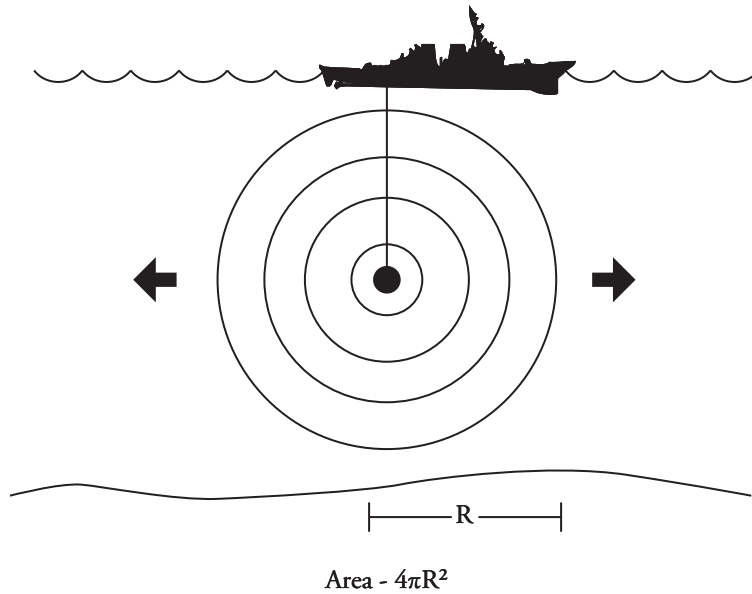
- Frequency: affects power losses; this is how the acoustic wave propagates before having lost so much energy, keeping it from making the medium vibrate.
- Expansion: wavefront expansion makes the total energy associated to the wavefront to be distributed within an increasingly greater surface, resulting in an increasingly lower intensity. In uniform and deep waters, sound originally expands in spherical manner (Fig. 2, spherical propagation) and its intensity diminishes proportionally with distance squared. The energy generated by the source is radiated equally in all directions to be distributed uniformly over the surface of a sphere surrounding the source [4].

Fig. 1. Profile of the speed of sound divided into layers.



Source: URICK, Robert. Principles of Underwater Sound. 3rd Edition. New York: McGraw-Hill, 1983.p 118

Fig. 2. Spherical propagation.



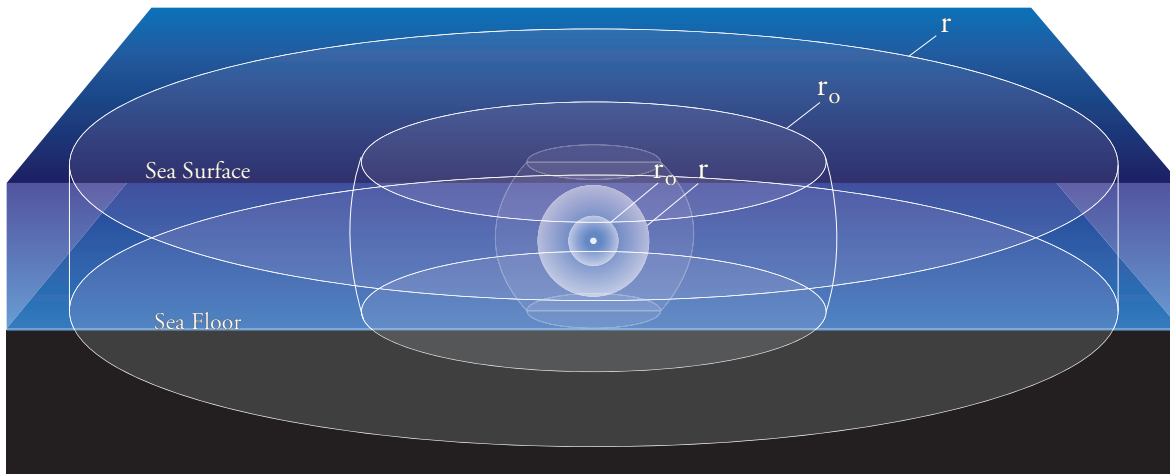
Source: http://www.fas.org/man/dod-101/navy/docs/es310/SNR_PROP/snr_prop.htm

When sound has propagated a distance approximately equal to the depth, it behaves as if it was in a conduit and the propagation becomes cylindrical where intensity diminishes directly with distance (Fig. 3). The medium has a parallel plane with upper and lower limits; the diffusion is no longer spherical, given that sound cannot cross the limiting planes [6].

- this process converts acoustic energy into heat. Hence, it represents a true loss and for sound to propagate through the underwater environment, it must be moved.

Bearing in mind all the contributions seen, transmission losses may be expressed according to equations [4]:

Fig. 3. Cylindrical propagation.



Source: <http://www.dosits.org/science/advancedtopics/spreading/>

$$TL_{spherical} = 20 \log r + \alpha r * 10^{-3} \quad (2) \quad \text{Simulation Tools}$$

$$TL_{cylindrical} = 10 \log r + \alpha r * 10^{-3} \quad (3)$$

Where distance, r , is where losses need to be measured (generally in the receptor) and α is the absorption coefficient expressed according to the equation:

$$\alpha = \frac{0.1 f^2}{1 + f^2} + \frac{40 f^2}{4100 + f^2} + 2.75 * 10^{-4} f^2 + 0.003 \quad (4)$$

where α is given in decibels per kilo-yard and f is the frequency in kilohertz.

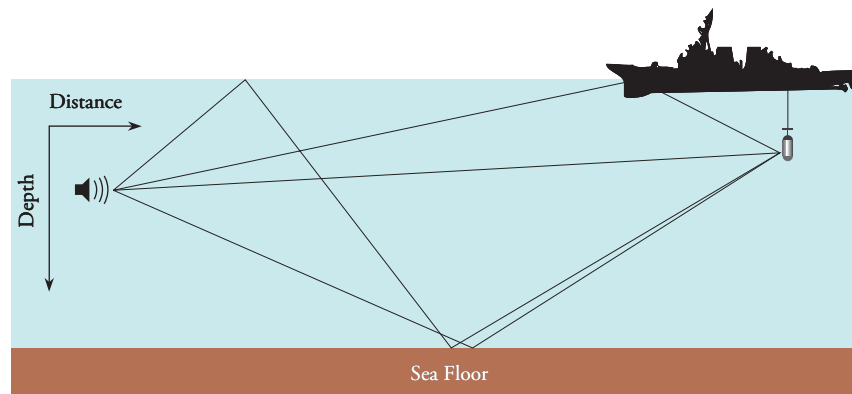
Transmission Models

Sound always travels great distances beneath the sea through some form of the surface duct (multiple paths, Figure 4). When sound travels in a duct, or sound channel, propagation is prevented in all directions and remains confined between the sound channel's dividing lines [4]. These models are mainly classified into the surface channel, the sound channel, rebounds on the bottom, the convergence zone, and propagation in shallow waters.

Currently, simulation tools of sonar performance in open literature is null; however, an application exists (AcTUP v2.2L) that works with Matlab and permits analyzing the behavior of the sound propagation phenomenon in underwater environments, but not based on the measurement parameters that characterize a sonar system [2]. AcTup has been evolving during the last 15 years and through the Centre for Marine Science and Technology (CMST) at Curtin University in Australia who kindly share the application through their web page for the academic community. This program permits analyzing the operation of the different acoustic propagation models (Fig. 5) and tracing their results.

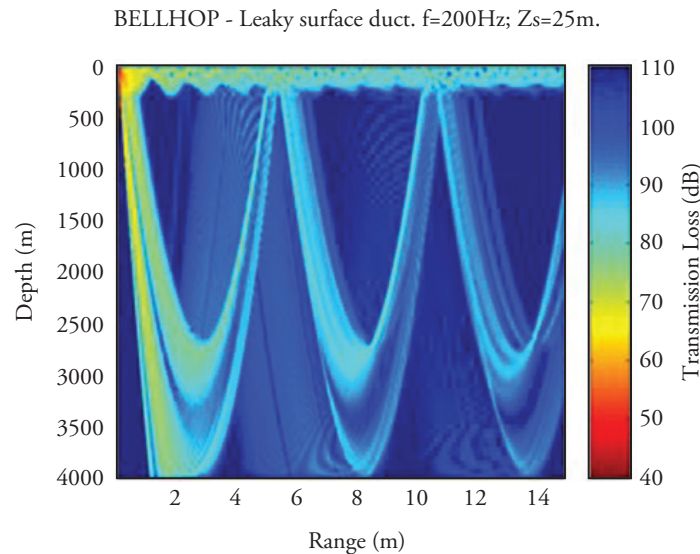
Another tool, similar to the one already described exists, but it is not available in open literature. It may be accessed through the Faculty of Physical Oceanography at the Almirante Padilla Naval School of Cadets; this tool is called PROPAS and was developed in Fortran programming language. Unfortunately, this programming language is not currently very popular and hinders its execution.

Fig. 4. Representation of multiple paths.



Source: APARICIO, Joaquín and GARCIA, Enrique. Models of Acoustic signal propagation in underwater environments. Department of Electronic Engineering. Universidad de Extremadura. Madrid. p. 2

Fig. 5. Sample of acoustic propagation using AcTUP.



Source: <http://cmst.curtin.edu.au/products/actoolbox.cfm>

Necessary Parameters for Characterization of the Colombian Marine Environment

In the observation field of the speed of sound in the underwater environment two devices are used that determine the profile of the speed of sound. One of these specialized devices is the bathythermograph, which measures temperature in function of depth as it descends in the sea; the other device is the sound velocity profiler directly measures the speed of sound in terms of time over a constant fixed trajectory. Physical characteristics of the marine environment, like density, pressure, and salinity affect mostly speed of sound. [4].

Colombia is the only country in South America with borders on two oceans and has a strategic geographic position, which allows it to have links with the rest of the countries in the northern and southern hemispheres. The Caribbean coast has a longitude of 1600 km and a marine area of 589,169 km². The Pacific coast has a longitude of 1300 km and a marine area of 339,500 km², which makes a total of 2900 km of coastline and 928,660 km² of marine territories [7].

Colombian Caribbean

This area is located in what is denominated as the Colombian pan with depths up to 4000 m. Its climate is regulated by the changing location of the Inter-Tropical Convergence Zone (ICZ) and by the effect of the trade winds from the north east, which determine during the year two well-defined periods: a rain period from May to November and a dry period from December to April, with some local variations in diverse sectors, given the topographical characteristics of each [7]. The Caribbean coast is characterized for having warm waters, with a mean temperature of 26 °C [8].

Colombian Pacific

The weather in the Colombian Pacific is notably influenced in a region of low atmospheric pressure, where the trade winds converge forming the Inter-Tropical Convergence Zone. This causes air masses with differences in temperature and humidity to rise and form clouds that generate continuous and high precipitations and variable winds. Precipitations in the north may reach 8000 mm per year. The tides are regular semidiurnal, which means there are two high tides and two low tides

during the day, with an approximate period of 12.25 hours. Its range is quite high, slightly over 4 m [7]. Its waters are relatively warm with a mean temperature of 25 °C [8].

Data Collection at Sea

This thesis work based its data on the Guajira Peninsula, Latitude N 12°21'40.68" Longitude W 71° 4'37.35", during the dry period of 2011, with oceanographic data from six stations. This area was chosen because it is considered of strategic interest for the analysis of the results of active sonar in the development of the BELLFAT software. This data consists of values taken from the factors of greatest interest already exposed; this was carried out through the CIOH, which certified that these measurements were taken with suitable measurement instruments that provide reliability and validity to the information.

Software Design in Matlab that permits predicting, evaluating, and analyzing the capabilities of an active sonar

Starting from the components of the equation

of the active sonar and bearing in mind the propagation models and the parameters that characterize the given reference area, commands were designed in Matlab for BELLFAT software.

$$DT = SL - 2TL + TS - \left(\frac{NL - DI}{NVR} \right) \quad (5)$$

- SL = Noise source level
- TL = Transmission loss
- NL = Noise level
- DI = Directivity index of the system
- NVR = Noise reverberation level
- TS = Target strength
- DT = Detection threshold

Each of these characteristics comprises hundreds of mathematical formulas and considerations, as appropriate.

MATLAB Modeling

With the information obtained from the CIOH the rate of sound propagation in water (C) can be modeled, as shown in Graph 1. Therein, may be observed the changes of layers in the yellow points at depths of 65 and 198 m.

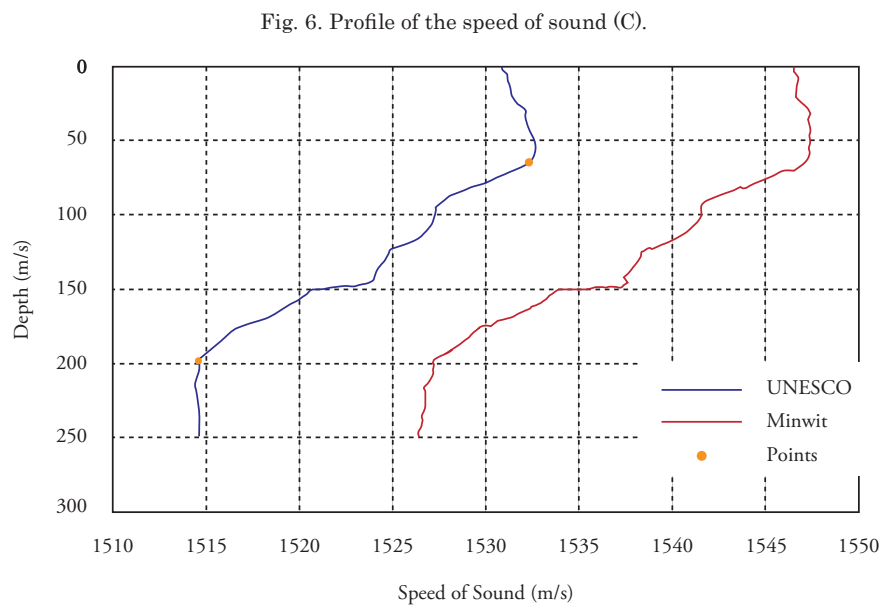


Fig. 6. Profile of the speed of sound (C).

Source: MATLAB modeling, BELLFAT program

The characteristics of a Dipping Sonar from the antisubmarine warfare (ASW) SH-60 helicopter were taken as example:

Type of arrangement: Cylindrical
 Diameter: 0.5 m
 Frequency: 8 KHz
 Depth: 210 m
 Power: 400 W

Through different user interfaces, the values to perform the calculations are located. The Fig. 7 is an example of these. Among the different mathematical operations executed, the following may be graphed, among others. (See Fig. 8)

Similarly, graphs are possible of target strength (TS), detection probability at distance, absorption coefficient, etc. Among other benefits, tables were tabulated to determine the environmental noise level and, thus, permit greater agility and ease in analyzing the sonar's behavior.

Comparison of Software results with studies available in the literature

Given that this topic is a research field that is not highly available in open literature, it is

rather complex to obtain software similar to that developed in this degree work. Nevertheless, evidence exists that some countries have basic computational tools elaborated to increase studies on these themes and enable the evolution of their processes to design these types of sensors, some of which are named ahead:

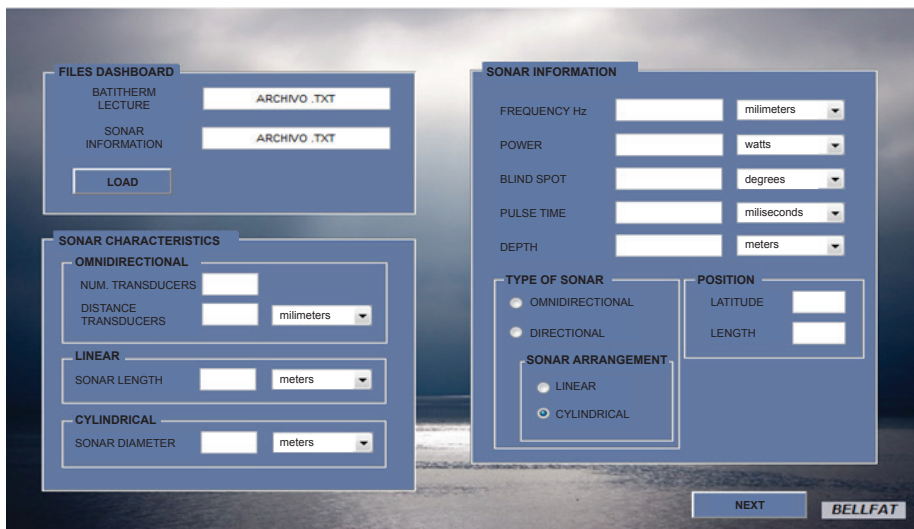
- SPARS and MODPRES from the Brazilian Navy.
- MESS from the University of Texas, USA.
- DRDO from India.

Due to this, the software was validated with exercises from the text "Principles of Underwater Sound" by Robert J. Urick, providing results and precise graphics in the different exercises taken as reference.

Conclusions

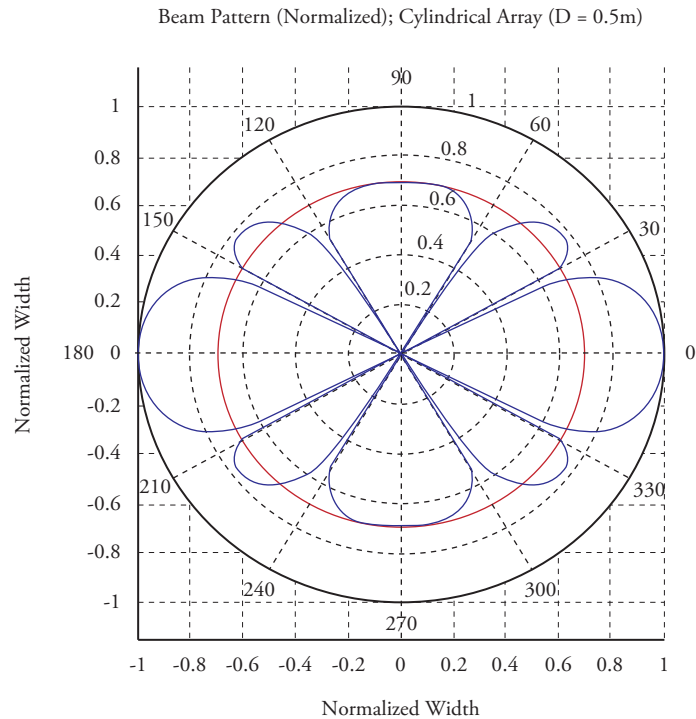
Different acoustic propagation models were identified, which are presented with the profile of the speed of sound in underwater environments, understanding the different phenomena that originate them in the different layers that make up the ocean. Likewise, the study identified simulation tools for the analysis of these factors in open literature; however, none

Fig. 7. Dynamic interface N° 1 program in MATLAB - BELLFAT.



Source:

Fig. 8. Polar-shaped beam pattern.



Source: MATLAB modeling, BELLFAT program.

was found directly related to the study of sonar performance.

This work also identified the necessary parameters that characterize the Colombian marine environment and, through the Oceanographic and Hydrographic Research Center, relevant data were acquired on depth, pressure, and salinity of a given area for our analyses. This Center certified that the measurement instruments permit providing validity and reliability to the data needed to determine the profile of the speed of sound; information of upmost importance to study sonar systems.

Based on the data gathered and studying the equation of the active sonar, a user interface was designed in Matlab, which permits predicting, evaluating, and analyzing the capabilities of an active sonar, managing to facilitate research on the matter to the academic community.

The BELLFAT software is an assessment tool for the performance of active sonar systems

and, hence, its use may be implemented as an appropriate method to study these themes in the Colombian Navy. The BELLFAT software permits becoming a computational tool to be considered in the Electronic Naval Engineering program at Colombian Naval Academy "Almirante Padilla" (ENAP) and the Marine Science program at Noncommissioned Officers' Academy "ARC Barranquilla" (ENSB), increasing their knowledge and improved basic approach of the theme.

References

- [1] GOMEZ TORRES, JOSE M: Warship Combat Systems Selection Methodology Based on a Discrete Event Simulation. Monterrey, 2010, 151 h. Thesis (Master of Science Mechanical Engineering). Naval Postgraduate School. Faculty of Naval Engineering. Department of Systems Engineering.
- [2] CURTIN UNIVERSITY TECHNOLOGY. Centre for Marine Science and Technology.

- Available in <http://cmst.curtin.edu.au/>
- [3] APARICIO, JOAQUÍN y GARCIA, ENRIQUE. Modelos de propagación de señales acústicas en entornos subacuáticos. Departamento de Ing. Electrónica. Universidad de Extremadura. Madrid. Available in: http://www.geintra-uah.org/system/files/models_de_propagacion_de_senales_acusticas_en_entornos_subacuaticos_i_y_ii-vdef.pdf
- [4] URICK, ROBERT. Principles of Underwater Sound. Third Edition. New York: McGraw-Hill, 1983.
- [5] MEDWIN, H. Speed of Sound in Water for Realistic Parameters. Journal of the Acoustical Society of America. 1975. p. 58
- [6] LABORATORIO DE PROCESADO DE IMAGEN. Available in: http://www.lpi.tel.uva.es/~nacho/docencia/ing_ond_1/trabajos_04_05/io9/public_html/sonar.html
- [7] EL OCÉANO EN LAS CIENCIAS NATURALES Y SOCIALES. Características Generales de los espacios Oceánicos y zonas costeras colombianas. Bogotá D.C.: Cassa Creativa Ltda., 2001. Available in: <http://www.cco.gov.co/ciencias%20naturales/unidad%20nueve.pdf>
- [8] MAJLUF, PATRICIA. Los Ecosistemas Marinos y Costeros. Proyecto Estrategia Regional de Biodiversidad para los Países del Trópico Andino, 2002. Serie de Informes: p. 9. ATN/JF-5887/RG (CAN BID). Available in: <http://www.comunidadandina.org/desarrollo/te2.PDF>

Fuel-Cell Integration on Board Surface Ships

Integración de celdas de combustible a bordo de buques de superficie

David Ignacio Fuentes ¹
Hernán de Laval Pérez ²

Abstract

Given the high levels of air pollution around the world, produced by the emission of greenhouse gases, the shipbuilding industry is in search of a "zero emissions" ship. To achieve this, research groups, have focused on the further investigation of the fuel cells. These devices can produce energy by only using hydrogen and oxygen as main power sources, having the next advantages features: low noise production, no emissions, and high efficiency. They can also be integrated with other systems. As Jules Verne wrote in his "The Mysterious Island", one day water will be used as fuel. The hydrogen and oxygen that constitute it, used alone and simultaneously, produce inexhaustible heat source and light intensity much greater than that of coal.

Key words: Alternative energy, fuel cells, greenhouse effect gases, generator, PEMFC.

Resumen

Teniendo en cuenta los altos índices de contaminación atmosférica alrededor del mundo, producida por la emisión de gases de efecto invernadero, la industria de la construcción naval está en la búsqueda del buque de "cero emisiones"; para el logro de este noble objetivo, los grupos de investigación sobre el tema han enfocado como objetivo las celdas de combustible. Estos dispositivos tienen la capacidad de producir energía sólo con el uso del hidrógeno y el oxígeno, además, producen poco ruido, ninguna emisión y alta eficiencia; mientras que pueden integrarse con otros sistemas. Tal y como lo visionó Julio Verne en su obra "La Isla Misteriosa", creo que el agua se usará un día como combustible, que el hidrógeno y el oxígeno que la constituyen, utilizados aislada y simultáneamente, producirán una fuente de calor y de luz inagotable y de una intensidad mucho mayor que la de la hulla.

Palabras claves: Energía alternativa, celdas de combustible, gases efecto invernadero, generador, PEMFC.

Date Received: May 21th, 2014 - *Fecha de recepción: 21 de mayo de 2014*
Date Accepted: June 30th, 2014 - *Fecha de aceptación: 30 de junio de 2014*

¹ Teniente de Navío . Escuela Naval de Cadetes "Almirante Padilla", Colombia. e-mail: fondexx@hotmail.com
² Teniente de Navío . Escuela Naval de Cadetes "Almirante Padilla", Colombia. e-mail: delavalleperez@gmail.com

Introduction

The naval construction industry is committed to the scientific search for new forms of alternative and clean energy to be in tune with the 1973 international convention to prevent pollution from ships, which was modified by the 1978 protocol, also known as MARPOL 73/78. The final objective is a ZERO-EMISSIONS ship; inasmuch as this progress is produced, interest for fuel cell technology has extended significantly. An increasing number of research groups have felt the need to participate in said projects, their need for a single, complete, and up-to-date exposition to the technology and its applications have become evident, and it is widely registered in research on the theme around the world in different disciplines. While fuel cells are the key component to develop the production of a cleaner energy alternative, it is essential to understand their characteristics.

How do fuel cells function?

Fuel cells are devices with the capacity to produce energy, while hydrogen (which acts as fuel) and oxygen (which acts as oxidant) are supplied to electrodes. These devices have the following principal characteristics: low noise level, little or no emission of contaminating gases, and high efficiency; in addition, it may be integrated with other systems for them to work as principal or secondary input source. A fuel cell functions much like a battery, "its functioning is based on the electrochemical reactions between a fuels, in this case a gas rich in hydrogen, and an oxidant, in this case oxygen from the air, with no intermediate combustion cycle. It produces energy in the form of electricity and heat and as sub-product, it generates water 100% pure; does not emit pollutants".¹

Fuel cells are composed of two electrodes, the cathode (positive) and the anode (negative), with an intermediate membrane (catalyst). Hydrogen enters through the anode and is divided in the

catalyst into H⁺ positive ions and electrons, oxygen from the air enters through the cathode and in the presence of the catalyst is divided into O²⁻ negative ions; the positive hydrogen ions leave through the electrolyte in direction to the cathode leaving the free electrons in the anode and upon properly connecting the anode and the cathode, the electrons left by the hydrogen will travel this path, producing current. In the negative pole, the oxygen, with the ions left by the hydrogen and the electrons turn into water.

Theoretically, the voltage produced by a fuel cell ranges between 1 and 3 V, but in reality "it will be from 0.6 to 0.85 V due to losses produced within the cell"²; to achieve the desired voltage, a bank is formed, that is, a set of cells that when correctly connected provide the voltage mentioned. Normally, the cell's output voltage is of continuous current, which is why at the cell output or that of a set of cells an inverter or transformer must be installed to turn it into alternate current for its use and distribution.

Why use fuel cells?

A fuel cell is an environmentally friendly source of energy; additionally, fuel cell systems do not contain moving pieces, making them more reliable and efficient. These fuel cells emit ultra-low emissions or zero emissions, have high energy conversion efficiency, low noise level, low vibration, and low or null levels undesired exhaust gases, except if hydrogen is produced through a reformed hydrocarbon process, which has carbon compounds as sub-products³.

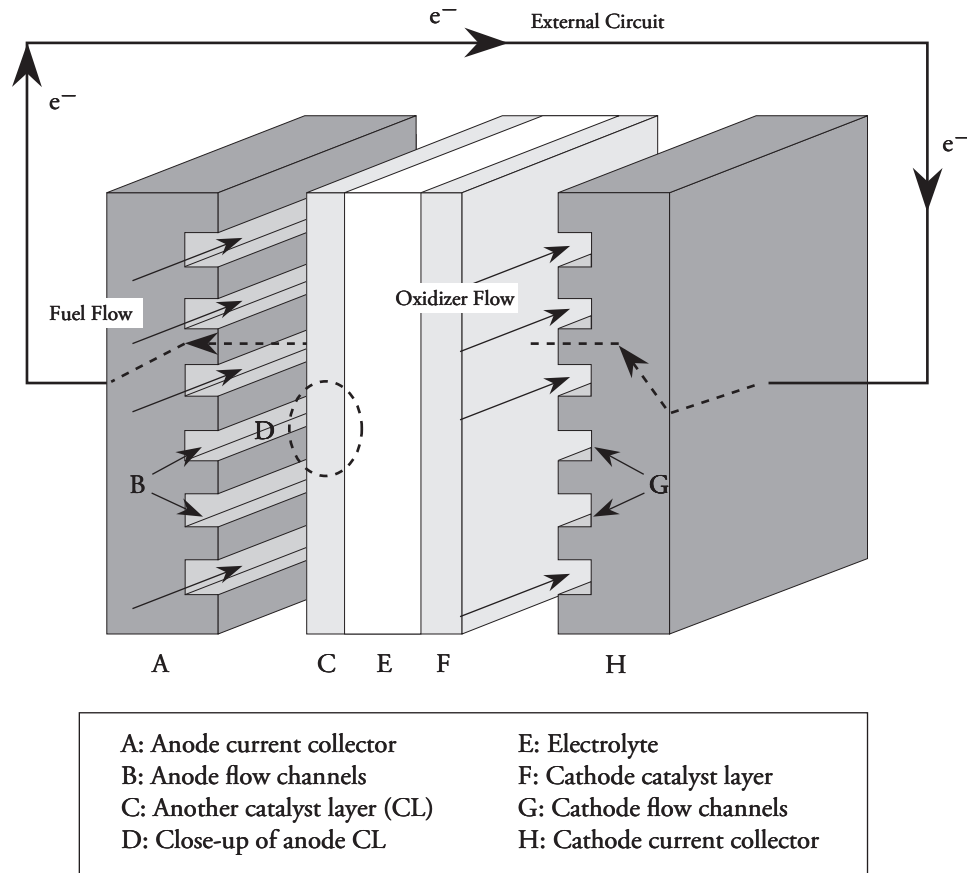
Fuel cells can deliver around 10 times more electric energy than that delivered by a lithium-ion battery, with the same volume. The fuel of the cells does not degrade over time and may function in a broad range of temperatures (80 to 1600 °C); it can be quite safe and without elimination problems,

¹ DOMÍNGUEZ, Juan José. Celdas combustibles (I). En: Anales de mecánica y electricidad. Madrid: Asociación de ingenieros de ICAI. Marzo-abril, 2002 p. 14.

² DOMÍNGUEZ, Juan José. Celdas de combustible (I). En: Anales de mecánica y electricidad. Madrid: Asociación de ingenieros de ICAI. Marzo-abril, 2002 p. 15.

³ Luckose, L (et al). Fuel cell propulsion system for marine applications. 1st edition. The United States: Elsevier publications, 2011. p 01.

Fig. 1. Schematic diagram of an individual fuel cell.



Source: Fuel cell adoption on board merchant ships, p. 17.

and may also provide high energy density, which would lengthen operation times. Fuel cells convert more chemical energy from the fuel in electric energy than that of a diesel generator motor due to its electrochemical isothermal reaction and from which is subtracted the loss of energy through radiation; these have greater efficiency at partial charge and few maintenance requirements. Unlike motors or batteries, fuel cells do not need recharging because they maintain a fuel flow reacting internally in the cell, which is why in some groups these are called flow batteries. These attributes of the cell's fuel make it attractive for the propulsion of an environmentally friendly ship project.⁴

⁴ Luckose, L (et al). Fuel cell propulsion system for marine applications. 1st edition. The United States: Elsevier publications, 2011. p. 2.

Type of fuel cells

A variety of fuel cells are in different stages of development, the most common classification of fuel cells is by the type of electrolyte used in the cells, thus: polymer electrolyte membrane fuel cells (PEMFC), alkaline fuel cells (AFC), phosphoric acid fuel cells (PAFC), molten carbonate fuel cells (MCFC), and solid oxide fuel cells (SOFC). For marine propulsion, the fuel cell is selected based on the following criteria. In the first place, the fuel cell selected must fit in the space assigned within the ship for propulsion systems, to adjust to the space available; likewise, it must have a high energy density. The fuel cell must operate at low temperatures, given that this helps to quickly start the system, control current residues, and it must allow the crew to operate near the device; lastly, the type of fuel cell must be available in the

market. The characteristics mentioned influence upon the type of fuel cell and their application is recommended in the ship project.

Bearing in mind the factors mentioned, PEMFC offer the best option to integrate fuel cells on board units afloat, given that these operate at low temperatures (60 – 80 °C), which impacts upon a fast start up and shutdown, will work even when they have not reached their normal operating temperature, do not present corrosion problems because their electrolyte membrane is a solid polymer, and have a long life (50,000 hours). The PEMFC modules have an output power of 30 to 40 KW and have operated successfully in class 212 submarines from the German and Italian navies. These PEMFC attributes make them suitable to function on board the ship.

Application on board

In the commercial marine sector, fuel cells were initially used on board yachts and fishing boats; thereafter, these systems have been brought to cargo and passenger ships⁵. The United States navy, since the 1960s, through its research and development programs, has sought its implementation in warships; in Germany, since

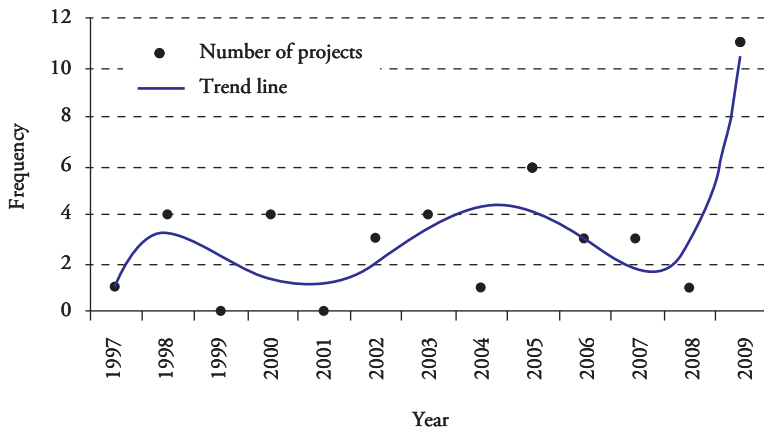
⁵ VOGLER, Finn. and WÜRSIG, Gerd. New Developments for Maritime Fuel Cell Systems, Germany: Germanischer Lloyd AG. p. 5.

the 1970s, it was observed that fuel cells are an effective way of producing energy and power on board their submarines without need to recharge their batteries through diesel combustion; this was the first time this was tested on a submarine with crew and 100% naval equipment, complying with all the power requirements needed on board. In the 1980s, the Canadian Department of Defense conducted important research for the use of these power production media on board floating units. In 1996, Germany again implemented a fuel cell system on a fishing fleet to make this trade more environmentally friendly. Work is in progress throughout the world on the best way to produce energy and power for ships without damaging the environment. Fig. 2 shows the number of research projects on fuel cells on board surface units; it may be noted that in 2009 research projects increased considerably, which indicates the rising optimism and acceptance of this form of energy production.

Options to integrate fuel cells onto surface ship

Starting from an all-electric ship (AES), systems may be found where the vessel has two propulsion modes, one would be a propulsion system where power is provided by a diesel generator motor through a transformer; another form of supplying the propulsion power needed by the ship may be from two battery banks that conveniently

Fig. 2. Research projects on fuel cells.



Source: Fuel Cell Adoption on board merchant ships, p. 19.

connected deliver the necessary power to move the electric motor; these modes of operation have some limitations that yield as a result reduced operational efficiency. As mentioned, propulsion power is supplied by the diesel generator motor and by the batteries; this generator motor produces electricity through the combustion of diesel fuel. Said process has as sub-product harmful emissions onto the environment. Additionally, the diesel generator also has problems of limited energy production and sensitivity to harmonic current consumption⁶. Furthermore, batteries have disadvantages, for example, taking as reference the batteries in Colombian submarines, such require recharge times of approximately two hours and their use time is limited, approximately eight hours; in addition, the battery's charge system introduces harmonic distortion on the AC side of the power system. Impedance of the diesel generator in combination with non-sinusoidal current feedback of the battery chargers produces voltage distortion that limits the functionality of the power system.

Option 1 – Replace one or several batteries with fuel cells.

The principal advantage of option 1 is a lower

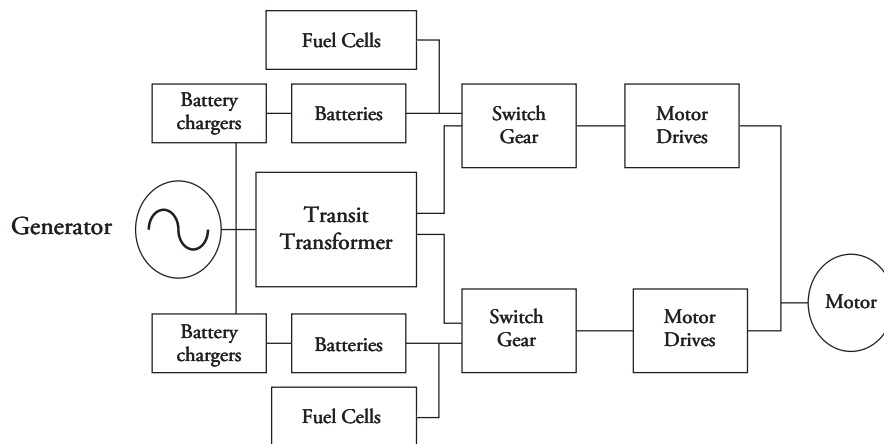
dependence on power supplied by the fuel cell. Each battery bank replaced by a fuel cell module must comply with the same voltage and current requirements as the pre-existing battery bank; in summary, this option has fuel cells in parallel with batteries, which impacts upon the system's response time due to source differences. Currently, fuel cells are not directly controlled causing disarrangement between the fuel cell and battery impedances, which makes it difficult to implement power systems that have fuel cells in parallel with the batteries.

The voltage of the fuel cell module varies between 440 – 800 V; depending on the charge condition, it requires a complex control system to adjust the voltage of the fuel cell module to coincide with the battery voltages. Another disadvantage for this option is that the space available by eliminating a series of batteries is not sufficient to house the fuel cell modules and the power conditioning system.

The efficiency of the power system with this option is low and emissions are high because the diesel generator is still in the system; besides, this option does not solve the problem of harmonic distortion from the battery's charge system and the operation time of the batteries is limited; Fig. 3 shows a power flow diagram for option 1.

⁶ U.S. Congress, Office of Technology Assessment, Marine Applications for Fuel Cell Technology – A Technical Memorandum, OTA-TM-O-37 (Washington, DC: U.S. Government Printing Office, February 1986). p. 8

Fig. 3. Power flow diagram for option 1.



Source: fuel cell propulsion systems for marine applications. 2011. First edition. p 04.

Option 2 – Substitute all the series of batteries with fuel cells.

This option permits completely eliminating the batteries and the continuous current charge system, leaving the propulsion totally dependent on the fuel cells and on the diesel generator motor. The principal advantage of this option is the use of fuel cells instead of batteries, thereby, avoiding the problem of charge times and limited use times of the batteries, also solving the problem of harmonic distortion introduced by the battery charge system. Another advantage is that the system’s power density increases given that the fuel cells have a better power density than the batteries.

However, option 2 has some inconveniences; first, the space available after eliminating the battery banks cannot accommodate the fuel cell modules, the fuel storage system, and conditioning of the system’s power; the efficiency of the power system in option 2 is low due to the presence of the diesel generator. As with option 1, in this option emissions are high because the diesel generator is still part of the system; the power flow diagram is shown in Fig. 4.

Option 3 - Replace the whole energy system with fuel cells.

This option allows the energy system to work with only fuel cells. The main advantage of this option is having a power system completely operated by a renewable source of energy; this option makes the energy system highly reliable. The operating

temperature of the power system is below⁷ 80°C. All the battery banks have to be replaced by fuel cell modules and a DC – DC converter to isolate the system.

Option 3 turned out to be a highly efficient power system with low emissions, given that it is fully dependent on fuel cells. By implementing option 3, it is possible to avoid the problem of harmonic distortion introduced onto the system by the battery charger; in addition to solving the problem of voltage distortion. It is important to keep in mind some technical considerations in executing this option; firstly, fuel cell modules must be connected in parallel to satisfy the needs of the system’s current, upon connecting the fuel cells to a bus⁸ in parallel, a high possibility exists that the current is sent back to the fuel cell modules, which can reduce the useful life and service efficiency of the fuel cell modules, thereby, current return should not be permitted to the fuel cell modules⁹.

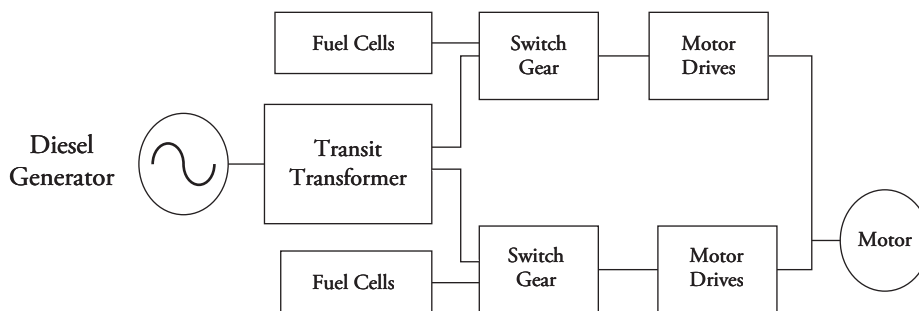
To simplify the analysis of the fuel cell modules during the conformation of the banks, it is assumed that the modules have similar characteristics, such as equal impedance, equal capacity of charge delivery, and equal response time; nevertheless,

⁷ BRANDON, Nigel and THOMPSETT, Dave. Fuel cell compendium. First edition. London: Elsevier Inc. 2005. p. 89.

⁸ El bus (o canal) es un sistema digital que transfiere datos entre los componentes de un sistema o entre sistemas.

⁹ W. Shireen, H. Nene “Active Filtering of Input Ripple Current to Obtain Efficient and Reliable Power from Fuel Cell Sources,” in proceedings of IEEE International Telecommunications Energy Conference , pp.1- 6 (2006).

Fig. 4. Power flow diagram for option 2.

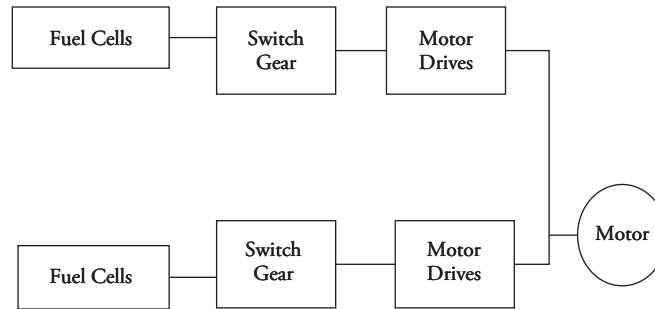


Source: fuel cell propulsion systems for marine applications. 2011. First edition. p 05.

given that the impedance does not coincide, some modules deliver more current in the bus than the rest, which is why a control system must be

installed, Fig. 5 shows the power flow diagram for option 3.

Fig. 5. Power flow diagram for option 3.



Source: fuel cell propulsion systems for marine applications. 2011. First edition. p 05.

Selection of the fuel cell integration option

new power system that is totally dependent on fuel cells.

The comparison parameters show the advantages and disadvantages of each option, the complexity of the control system to implement the options, efficiency, and emission levels. The comparison of the three fuel cell integration options is shown in Table 1.

As a precaution, when the fuel cells work in parallel, a diode must be installed or any other protection in series with the fuel cell modules to block any current circulating among them¹⁰. Keep in mind insertion of the diodes adds further losses to the system. Fig. 6 illustrates an example of a fuel cell integration bus for option 3.

Comparison of the three options shows that option 3 is the most advantageous; option 3 completely substitutes the power system in the ship with a

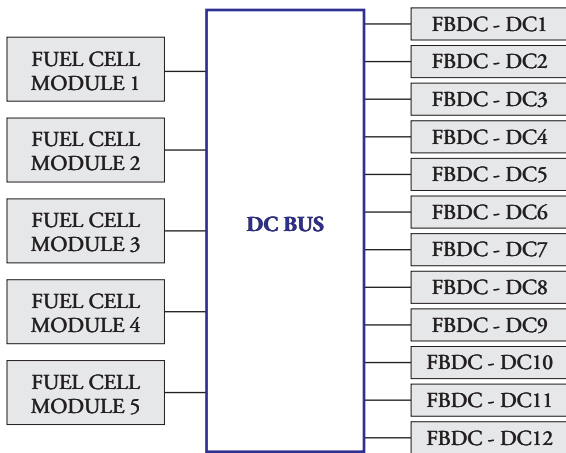
¹⁰ B. Ozpineci, L. M. Tolbert, Z. Du, "Multiple Input Converters for Fuel Cells," IEEE Industry Applications.

Table 1. Comparison of fuel cell integration options.

	Option 1	Option 2	Option 3
Advantages	Less dependence on fuel cells	Without batteries or battery charge system	Power system totally operated with renewable energies
Disadvantages	Fuel cells in parallel with batteries; the diesel generator is still in the system.	The generator is still in the system	Requires 8 fuel cell modules and a 12-V DC-DC converter
Complexity of the control system	High	Low	Low
Space	Not sufficient	Not sufficient	Adequate
Efficiency	Low	Low	High
Emissions	High	High	Low
Harmonic distortion	High	Low	Low

Source: Elaborated by the authors based on fuel cell propulsion systems for marine applications. 2011. First edition. p. 05.

Fig. 6. Example of the fuel cell integration bus for option 3.



Source: fuel cell propulsion systems for marine applications. 2011. First edition. p 05.

Environmental impact of the system

The environmental impacts of the system functioning with fuel cells are practically zero, inasmuch as the yield of the chemical reaction taking place within the PEM-type cell is pure water. These devices operate silently, hence, they do not produce noise pollution and are environmentally friendly, given that they do not produce emissions,

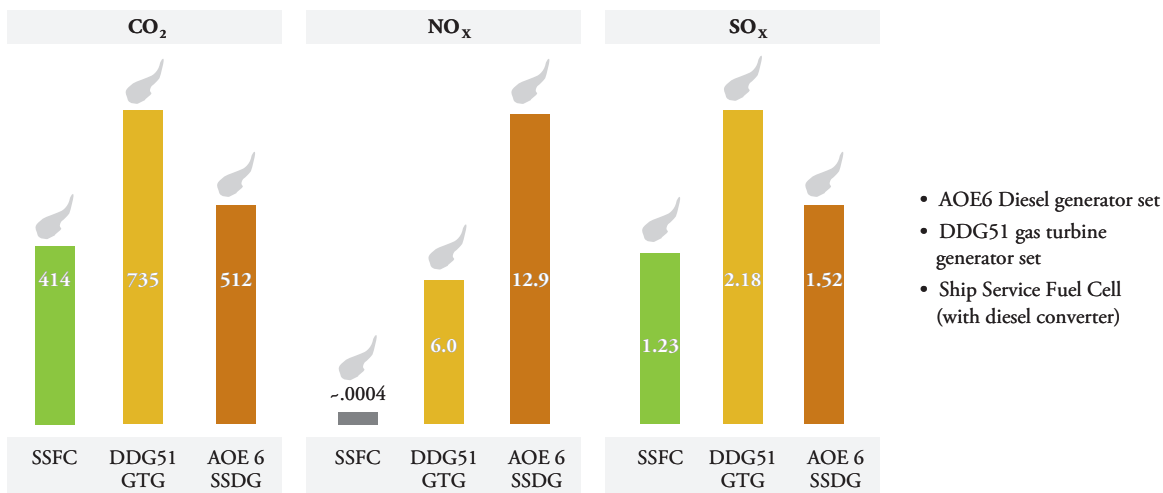
like greenhouse gases that are inclined to contribute to global pollution; another favorable point is the reuse of the resulting water for services on board the unit or even for refrigeration of the cell's own modules, thus, helping to maintain an operating temperature between 60 and 70°C.

The electrodes of all fuel cells function with hydrogen, no matter what fuel is being supplied to the fuel cell system. In indirect input fuel cells, the hydrogen carrier (methanol, ammonia, hydrazine, etc.) must first be converted with certain efficiency, also producing secondary products (equivalent to amounts of CO₂, in case of hydrocarbon conversion).

By using a fuel cell system in a ship, in any case, pollution through emissions will be further reduced due to the high conversion efficiency. Table 2 shows a comparison of emissions per type of energy production. These comparisons show that the PEM fuel cell is the most suitable for these types of vessels.

The advantages in CO reduction, in general, are quite believable for the case where coal, oil, or natural gas are used by power stations primarily for electricity production and then used for electrolysis to produce hydrogen. Of course, specific circumstances must be carefully labeled

Table 2. Comparison of emissions by type of system. (gm/HP Hr @100% of power)



Source: <http://www.fuelcelltoday.com/analysis/industry-review/2011>.

to reach valid comparisons. Only energy values¹¹ are indicative of the actual efficiency of the whole conversion chain. No CO₂ pollution exists with electric energy production through hydraulic, nuclear, wind energy or from solar installations.

However, energy considerations will also count with the CO₂, which was produced during the cement production for the water dam or for nuclear containment, through silicon fusion, etc. The risk is that these calculations go too far, which may be counterproductive for any technology. A hypothetical case is, for example, the issue of what part of the energy used for roadway and bridge construction should be counted as CO₂ source due to the existence of automobiles or trains as necessary means of transport.

Conclusions and Recommendations

Fuel cells are a promising technology and, upon considering all the types of fuel cells, it is noted that PEMFC are the most suitable cells for naval applications because of their low operating temperature, long operation times, and fast service time.

In relation to the environmental impact of fuel cells, their operation on board units afloat would be completely environmentally friendly, given that as such their functioning is due to a soundless electrochemical reaction occurring within the modules. The result of these reactions is pure water (H₂O) and CO₂ in minimum quantities, this latter only in cases implementing fuel cells that obtain hydrogen from methanol conversion. Regarding the working temperature of 50°C, which besides being ergonomically viable for its operators is a key factor for tactical and combat operations due to its low thermograph signature; likewise, its low noise level will reduce the ship's acoustic signature and improve the sound conditions of engine rooms. Fuel cell technology needs to be installed massively to make it more commercial.

Given the versatility of the fuel cells, these may not only be used as energy generation for propulsion, but may also be installed as energy generation for different services on board, like navigation equipment, galleys, on board comfort, among others.

It is worth to continue studying the possibility of implementing this technology, not only in power production on board, but in the production of electricity to units away from urban centers to preserve the environment and, thus, give future generations a healthier world.

References

- [1] DOMÍNGUEZ, JUAN JOSÉ. Celdas combustibles (I). En: Anales de mecánica y electricidad. Madrid: Asociación de ingenieros de ICAI. Marzo-abril, 2002 p. 14-18.
- [2] BRANDON, NIGEL and THOMPSETT, DAVE. Fuel cell compendium. First edition. London: Elsevier inc. 2005. 639 p.
- [3] VOGLER, FINN. and WÜRSIG, GERD. New Developments for Maritime Fuel Cell Systems, Germany: Germanischer Lloyd AG. 10 p.
- [4] U.S. CONGRESS, Office of Technology Assessment, Marine Applications for Fuel Cell Technology – A Technical Memorandum, OTA-TM-O-37 (Washington, DC: U.S. Government Printing Office, February 1986). 39 p.
- [5] LUCKOSE, 1 (*et al*). Fuel cell propulsion system for marine applications. 1st edition. USA: Elsevier publications, 2011. 7 p.
- [6] B. OZPINECI, L. M. TOLBERT, Z. DU, "Multiple input converters for fuel cells," IEEE Industry applications society annual meeting, October 3 - 7, 2004, Seattle, Washington, 797 p.

¹¹ Exergy is the portion of energy that can be transformed into mechanical work; the remaining part without practical utility is called anergy or entropy.

- [7] Fuel Cell Today [online]. Hertfordshire, UK.: [Cited 06 November 2011]. Available in: <<http://www.fuelcelltoday.com/analysis/industry-review/2011/the-industry-review-2011>>

Implementation of Confirmation of Methods in Measurement Equipment Calibration as a Normalized Strategy to Ensure the Quality of Measurements Made in the Construction, Repair, and Modernization of Ships and Naval Artifacts in COTECMAR

Implementación de la confirmación de métodos en la calibración de equipos de medición como estrategia normalizada para asegurar la calidad de las mediciones realizadas en la construcción, reparación y modernización de buques y artefactos navales en COTECMAR

Ronald Yesid Argote Guzmán ¹

Abstract

The naval, maritime and riverine industry is one of the sectors, which has greater contribution to the world economy, hence, quality assurance is one of the main priorities in all maritime activities, especially the ones related to ship building. The monitoring of different variables that allows good performance of a ship involves assessing equipment in order to assure data taking with greater precision and accuracy; this is where metrology takes place as a science for studying inherent problems to measurement data collection, focusing on equipment calibration. The grade of uncertainty produced by data taking procedures of each equipment on board of ship depend on techniques and results control specifications, which are known as Methods Confirmation. The metrology laboratory at COTECMAR applied this method to guarantee quality by estimating validity and reliability of the obtained results through different measuring equipment related to ship construction and repairing.

Key words: Ship, calibration, metrology, Methods Confirmation, quality assurance

Resumen

La industria naval, marítima y fluvial es uno de los sectores que tiene mayor contribución a la economía mundial, por ende, el aseguramiento de la calidad es una de las prioridades en las actividades marítimas, especialmente en la construcción de embarcaciones. El monitoreo de las diferentes variables que permiten el buen desempeño de un buque implica la comprobación de equipos para garantizar la toma de datos con mayor precisión y exactitud posible, es aquí donde la metrología tiene lugar como ciencia por estudiar los problemas inherentes a la toma de datos de medida, enfocándose una de sus ramas a la calibración de equipos. El grado de incertidumbre o sesgo generado por la toma de medidas de cada uno de los equipos a bordo de una embarcación dependen de las técnicas y especificaciones de control de resultados, las cuales se conocen como Confirmación de Métodos. En el laboratorio de metrología de COTECMAR se implementa dicha metodología para garantizar el aseguramiento de la calidad por medio de la evaluación de validez y veracidad de los resultados obtenidos a través de los distintos equipos de medición involucrados en la construcción y reparación de buques.

Palabras claves: Embarcación, calibración, metrología, Confirmación de Métodos, aseguramiento de la calidad

Date Received: May 31th, 2014 - *Fecha de recepción: 31 de mayo de 2014*
Date Accepted: July 18th, 2014 - *Fecha de aceptación: 18 de julio de 2014*

¹ COTECMAR. Meteorology Department. Cartagena, Colombia. e-mail:

Introduction

The importance the naval, maritime, and riverine industry has gained over time is mainly due to the set of activities, processes, and results it has contributed to the development of the economy and industry at the global level. The aforementioned involves the risks to which human lives are exposed when aboard a vessel operating in the different waters of the world.

After Titanic's disaster in 1912, the safety of human life at sea has become a priority for all the countries in the world; for this reason, the shipyard industry must respond more effectively. As a result to this sad moment in history, the International Convention for the Safety of Life at Sea (SOLAS) was approved in 1914, which in its version in effect from 01 November 1974 sanctioned during the International Conference on Safety of Human Life at Sea, convened by the International Maritime Organization (IMO), and which went into effect on 25 May 1980, has as main objective to establish guidelines from every point of view to minimize the risks to which human life is exposed at sea. Taking as example chapter XI of this treaty, regulation 2 stipulates that bulk carriers and oil tankers will be object of an improved inspection program in conformity with the guidelines approved by the IMO Assembly in 1993 through resolution A.744(18)¹. The guidelines on the improved inspections program have been elaborated by the IMO as a consequence of the high number of claims occurring in recent years and from the growing concern for the aging of the global merchant fleet². The guidelines pay special attention to corrosion. The coatings and the corrosion prevention systems on the tanks must be subjected to extensive testing and plate thickness measurements must also be made. Procedures are described to certify the companies that conduct thickness measurements of hull structures; procedures are recommended for thickness measurements and thorough

recognition; and orientations are given on how to elaborate the documentation required. With the aforementioned, it can be seen that the measurements made of the different structures, parts, and/or equipment on a vessel are quite important, given that their results are a critical variable within the quality assurance of the product obtained and which is directly related to human risks on board a ship.

Enhancement of economic and social issues in Colombia is highly linked to naval, maritime and riverine development along with the safety of human life at sea; hence, Legislation 8 of 1980 was sanctioned, which considered the guidelines of 1974 and 1978 protocols, the latter is no longer in effect because of the 1988 International SOLAS Protocol pending Congressional approval for its adoption³.

By mid 1998 the Colombian Navy sought the necessary resources to bring to life the shipyard industry in Colombia and created what is today the Science and Technology Corporation for the Development of the Naval, Maritime, and Riverine Industry, COTECMAR, founded in 2000 by the Ministry of Defense, Universidad Nacional de Colombia, Corporation Universitaria Tecnológica de Bolívar, and Escuela Colombiana de Ingeniería 'Julio Garavito'⁴.

COTECMAR has as mission statement "to lead in the scientific and technological development National Navy, satisfying the needs for support and evolution of its fleet, promoting the sustainable growth of the nation's naval, maritime, and riverine industry"⁵. Within this scientific and technological development, COTECMAR, has generated and implemented a series of strategies that permit assuring the quality of its products, besides obeying with all the applicable international and national laws. Among these strategies, there is that of keeping a metrology laboratory in charge of calibrating

¹ http://www.inocar.mil.ec/web/images/lotaip/2015/literal_a/base_legal/A_Convenio_internacional_solas_1974.pdf. Instituto Oceanográfico de la Armada INOCAR. Ecuador. 2015-05-31.

² http://www.inocar.mil.ec/web/images/lotaip/2015/literal_a/base_legal/A_Convenio_internacional_solas_1974.pdf. Instituto Oceanográfico de la Armada INOCAR. Ecuador. 2015-05-31.

³ <https://www.dimar.mil.co/content/convenio-internacional-sobre-la-seguridad-de-la-vida-humana-en-el-mar>. Dirección General Marítima, Autoridad Marítima Colombiana. 2015-05-31.

⁴ <http://www.semana.com/especiales/articulo/potencia-naval/47869-3>. Revista Semana. 2001-11-05.

⁵ <http://www.cotecmar.com/conozcanos.html>. Portal COTECMAR. 2015-05-31.

the Corporation's measuring equipment, which makes sure the results of measurements made with said equipment are reliable and true.

The reliability and veracity mentioned are only obtained by implementing adequate statistical and mathematical techniques to calibration processes conducted in the laboratory. One of these techniques has to do with Confirmation of Methods, which seeks to ensure that the results of the measurements during routine analyses are sufficiently close to the real value (unknown) of the analyte content in the sample⁶. The laboratory selects the calibration methods according to current regulations (whenever pertinent), according to the requirements of the final user (client).

The purpose of this article was to show the results reached by implementing the confirmation of methods during the calibration process of equipment in the metrology laboratory at COTECMAR, as strategy for quality assurance of the results of measurements in terms of reliability and veracity.

Measurement and calibration of measuring equipment

The activity of a measurement process unavoidably involves technical, administrative, statistical, instrumental, and personnel aspects, establishing each of these within their own control parameter that ensure accurate data obtained during said process. An ideal measurement process will always provide "true" measurements, which implies having statistical properties of zero variance, zero errors and, consequently, zero probability of wrong decisions. Unfortunately, these types of measurement processes do not exist, which allows the existence of systems or measurement processes according to the precision required, costs, ease of use, etc. A measurement process has a vast diversity of considerations or points of its own interpretation; said understanding of the process varies according

to the area of application where it will be carried out. For example, metrology experts will use VIM3 to interpret and apply the definitions to said process; engineers in industry will base themselves on the definitions and terms most commonly used in management systems, and mathematicians will interpret said process according to established limits and boundaries⁷.

According to the International Metrology Vocabulary, in its third translation (VIM3), 'measurement' is defined as:

"A process that consists in experimentally obtaining one or several values that may be reasonably attributed to a magnitude".

Notes:

- 1. Measurements do not apply to qualitative properties.*
- 2. A measurement supposes a comparison of magnitudes or the count of entities.*
- 3. A measurement supposes a description of the magnitude compatible with the foreseen use of a measurement result, a measurement procedure, and a measurement system calibrated according to a specified measurement procedure, including the measurement conditions.*⁸

Continuing with the scheme of the measurement process, Fig. 1 illustrates analogies of said process seen by.

If the process is analyzed by stages, we may establish that in "A" and "C" there are no problems in identifying and understanding said processes, given that in these stages the elements under study are clearly identified, including the analogies can be carried out without problem; unfortunately, in stage "B" a problem emerges due to causes like:

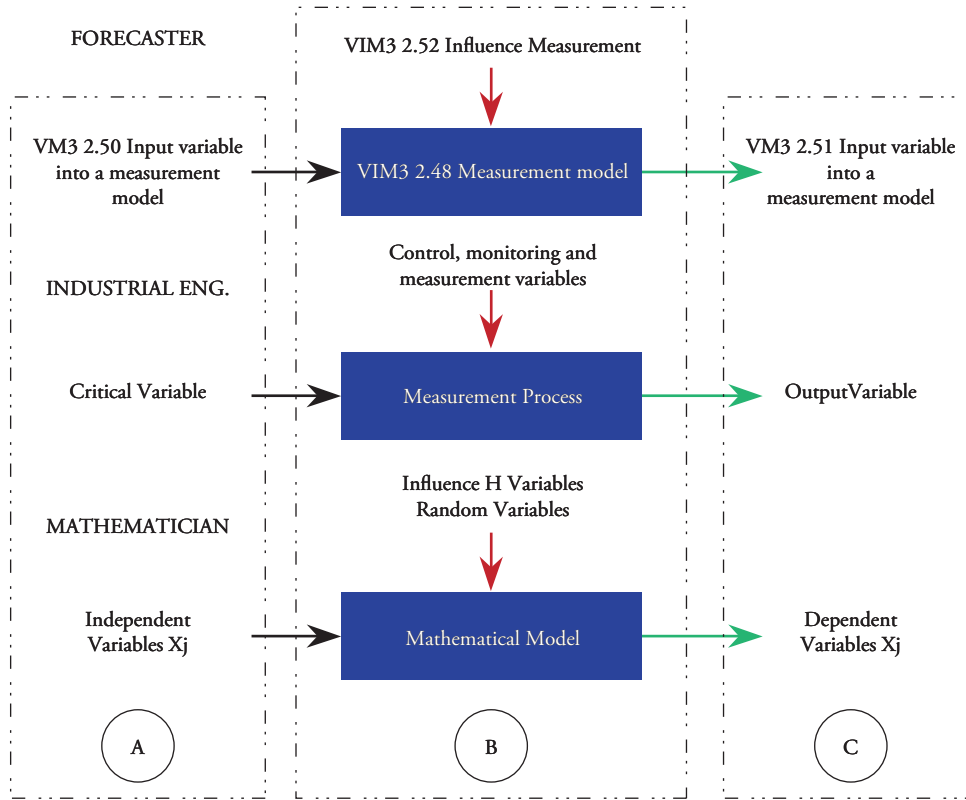
- Level of precision required in C, which results in the complexity of the process in B,
- Recognition and validation of stage B,
- Integration and separation of critical instruments,

⁶ <https://fernandoveyretou.files.wordpress.com/2011/06/validacion-y-confirmacion-de-metodos26.pdf>. Ingeniería en Calidad – Fernando Veyretou. Temas de Calidad. Laboratorio. 2011-06-10.

⁷ <http://www.metras.com.mx/guiametas/La-Guia-MetAs-07-09-proceso-de-medicion.pdf>. MetAs & Metrólogos Asociados. La Guía MetAs. Septiembre de 2007.

⁸ International Metrology Vocabulary. VIM-3rd edition (2012).

Fig. 1.



Source: MetAs & Metrólogos Asociados.

magnitudes, and elements of influence,

- Required variability of the process,
- Among others.

This demonstrates that stage B is an area of transformation, which should be analyzed and studied in greater depth⁹. From the concept of “measurement”, the calibration concept is generated that according to VIM3 is:

“Operation that under specified conditions establishes, in a first stage, a relationship among the values and their associated measurement uncertainties obtained from the measurement patterns, and the corresponding indications with their associated uncertainties and, in a second stage, utilizes this information to establish a relationship that permits obtaining a

measurement result from an indication”.

Notes:

1. *A calibration may be expressed through a statement, a calibration function, a calibration diagram, a calibration curve, or a calibration table. In some cases, it may consist of an additive or multiplicative correction of the indication with its corresponding uncertainty.*
2. *It is convenient not to confuse calibration with the adjustment of a measuring system, often incorrectly called “self-calibration”, or with a verification of the calibration.*
3. *Frequently, it is interpreted that only the first stage of this definition corresponds to calibration.*¹⁰

Then, it may be stated that calibration is the comparison of a standard of measurement, or equipment, with a standard or equipment of greater

⁹ <http://www.metas.com.mx/guiametas/La-Guia-MetAs-07-09-proceso-de-medicion.pdf>. MetAs & Metrólogos Asociados. La Guía MetAs. Septiembre de 2007.

¹⁰ International Metrology Vocabulary. VIM-3rd edition (2012).

precision, to detect and quantify inaccuracies and report or eliminate them through an adjustment. Hence, within the measurement process, calibration is the most important quality control activity, given that it establishes the relationship of the value measured by equipment with a real conventional value, giving the measurement validity and traceability. The following image shows that previously mentioned, a digital calliper gauge is calibrated by using a set of pattern blocks with greater precision than that of the equipment.

Fig. 2.



When using measuring equipment continuously, precision and measurement precision vary gradually due to wear of its parts or due to interference caused by the accumulation of dust or dirt, among other causes or reasons, which is why it is necessary to validate them through calibration and correct them if necessary. All equipment must be calibrated by following the operating conditions, pursuant to procedures based on the specific instructions of the equipment's operation manual, as well as on the general guidelines provided by the normalized or non-normalized methods.

During the execution of the calibration program, different types of calibrations take place, whose complexity and application may vary in function of the circumstances and objectives established. However, it is important for the calibrations to consider the following aspects:

- Traceability of the standards or reference materials;
- Procedures or methods established and validated or confirmed;

- Programming; and
- Documentation of the results.

Analysis strategy: confirmation of methods

The NTC-ISO/IEC 17025 standard (version 2005), applied in COTECMAR's metrology laboratory and through which it obtained its accreditation, in numerals 5.4.2 and 5.4.5.2, respectively, states:

“The laboratory must use the test or calibration methods, including sampling methods, which satisfy the needs of the client and which are appropriate for the tests or calibrations performed. Preferably, methods published as international, regional, or national norms should be used ...”

“The laboratory must validate the non-normalized methods, the methods it designs or develops, the normalized methods used beyond the foreseen reach, as well as extensions and modifications of the normalized methods, to confirm that the methods are suitable for the purpose sought. The validation must be as broad as necessary to satisfy the needs of the given type of application or field of application...”

The confirmation of methods is the validation of normalized methods issued by international normalization organizations (e.g., ISO), regional organizations (European norms, EN, or MERCOSUR, NM), or national organizations like ICONTEC, etc. Methods issued by internationally recognized organizations like EPA, AOAC, etc., are also considered 'normalized' methods. The results of this confirmation show us the veracity and accuracy of the method and of the results of the measurements

In the metrology laboratory at COTECMAR this strategy is adequate for the methods used in the calibration process and its calculation and analysis basis of the results is founded on the NTC 3529-2 standard of 1999, identical to the ISO 5725-3 standard of 1994.

Methodology

The activity was basically carried out in four phases:

Phase 1: Election of the measurand

COTECMAR's metrology laboratory calibrates measuring equipment in two main magnitudes, which are dimensional magnitude and pressure magnitude; within the reach of its management system, the equipment object of this confirmation of methods were chosen bearing in mind the following:

- That they are within the reach of laboratory accreditation.
- Their state of preservation; physical and operating conditions.
- Result of prior calibrations (if equipment is not new).

Phase 2: Selection of analysis method

The methodology selected to obtain and analyze the results of the confirmation of the method in the graphic consistency technique called "Mandel's h and k statistics", documented in the NTC 3529-2 standard of 1999, requisite 7.3.1. It is worth mentioning that this requisite is segregated in the content of the norm in other applicable requirements, which is why it is recommended to revise the text.

Phase 3: Calibration of the measurand

Execution of the standardized calibration process the laboratory performs for the selected

measurement equipment, bearing in mind the laboratory's internal guidelines (calibration instructions and applicable technical norms) and the confirmation of the method regarding repetition conditions of the calibrations and order of calibration stipulated in the NTC 3529-2 standard of 1999, requisite 7.3.1.

Phase 4: Obtaining and analyzing the results

The results of calibrations performed were analyzed according to that stipulated in the NTC 3529-2 standard of 1999, requisite 7.3.1. Upon ending the activity, we must obtain the lowest of the uncertainties reported for the calibrations made for each measurand; this uncertainty is denominated Capacity for Measurement and Calibration (CMC).

Note: for greater reference on the CMC, visit: www.onac.org.co.

Results

Phase 1: Election of the measurand

Owing to the vast scope of the laboratory for confirmation methods, a measurand was selected within the accreditation limits of COTECMAR's metrology laboratory. to show its whole development. The measurand selected is the Calliper gauge in its different presentations according to the laboratory's capacity, thus:

Table 1.

Magnitude	Range of measurement	Instrument to calibrate	Pattern equipment used	Normative document
Length	0 – 150 mm	Calliper calibrator Type: M and CM Division of scale: 0.01 mm	Pattern block set Class 1 and 2	JIS B 7507 – 1993 (Numeral 6.1, Table 1 – Numeral 12, Table 9)
Length	0 – 300 mm	Calliper calibrator Type: M and CM Division of scale: 0.01 mm	Pattern block set Class 1 and 2	JIS B 7507 – 1993 (Numeral 6.1, Table 1 – Numeral 12, Table 9)
Length	0 – 500 mm	Calliper calibrator Type: M and CM Division of scale: 0.01 mm	Pattern block set Class 1 and 2	JIS B 7507 – 1993 (Numeral 6.1, Table 1 – Numeral 12, Table 9)
Length	0 – 900 mm	Calliper calibrator Type: M and CM Division of scale: 0.02 mm	Pattern block set Class 1 and 2	JIS B 7507 – 1993 (Numeral 6.1, Table 1 – Numeral 12, Table 9)

Fig. 3. Digital calliper gauge.



Phase 2: Selection of analysis method

The methodology selected to obtain and analyze the results of the confirmation of the method is the graphic consistency technique called “Mandel’s h and k statistics”, documented in the 1999 NTC 3529-2 standard, requisite 7.3.1. This methodology was chosen because adjusted to the laboratory capacities and, mainly, because it belongs to a nationally accepted reference norm.

Phase 3: Calibration of the measurand

For each of the equipment mentioned in item 5.1,

respective calibrations were carried out according to COTECMAR’s internal calibration instructions, which corresponds to each of them. In this case, the calliper corresponds to internal instruction code N° I-COPSER-001.

Phase 4: Obtaining and analyzing the results

The graphic consistency technique was used to analyze the results; this uses two measurements called Mandel’s h and k . This technique is described in numeral 7.3.1 of the NTC 3529-2:1999 standard. The values of Mandel’s h and k measurements were obtained from Table 7, in the NTC 3529-2:1999 standard, with 95% confidence level (5% significance), for three operators and three repetitions per operator.

The following show the results obtained for each measurement interval supported by each pattern instrument used, as shown in numeral 4.1 of this report.

Table 2. Measurement range up to 150 mm, division of scale 0.01 mm.

Operator	Indications (mm)					
	0	30	70	100	120	150
Delwin Velandia	0.000	30.000	69.998	99.998	119.994	149.994
	0.000	30.004	69.996	100.000	119.996	150.002
	0.000	29.998	70.002	99.996	119.998	150.000
Mean	0.000	30.0007	69.9987	99.9980	119.9960	149.9987
Deviation	0.000	0.003	0.003	0.002	0.002	0.004
h	0.00000	0.00006	0.00000	0.00000	0.00000	-0.00001
k	0.00000	1.00000	1.00000	0.68825	1.50000	1.14018
Majer Atequera	0.000	29.998	69.998	99.996	119.998	149.996
	0.000	29.998	69.998	100.002	119.996	150.004
	0.000	29.996	70.000	99.994	119.996	150.002
Mean	0.000	29.9973	69.9987	99.9973	119.9967	150.0007
Deviation	0.000	0.001	0.001	0.004	0.001	0.004
h	0.00000	-0.00005	0.00000	0.00000	0.00000	0.00000
k	0.00000	0.37796	0.37796	1.43270	0.86603	1.14018
Ronald Argote	0.000	30.000	69.996	99.998	119.996	149.998
	0.000	30.002	69.998	100.000	119.996	150.002
	0.000	29.994	70.004	99.996	119.996	150.002
Mean	0.000	29.9987	69.9993	99.9980	119.9960	150.0007
Deviation	0.000	0.004	0.004	0.002	0.000	0.002
h	0.00000	-0.00001	0.0001	0.00000	0.00000	0.00000
k	0.00000	1.36277	1.36277	0.68825	0.00000	0.63246

Fig. 4. Graph of h.

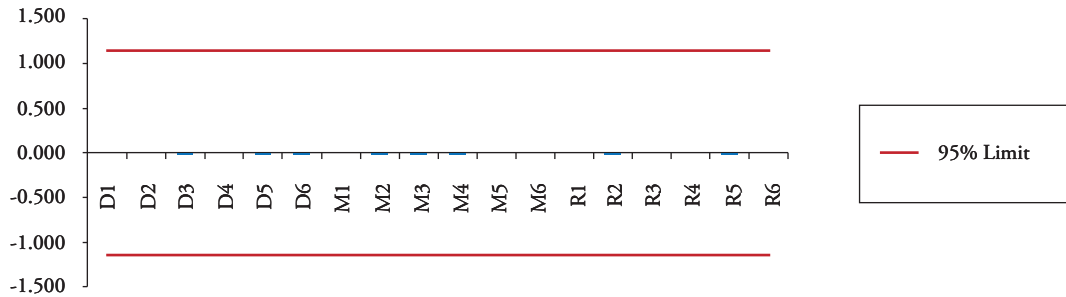
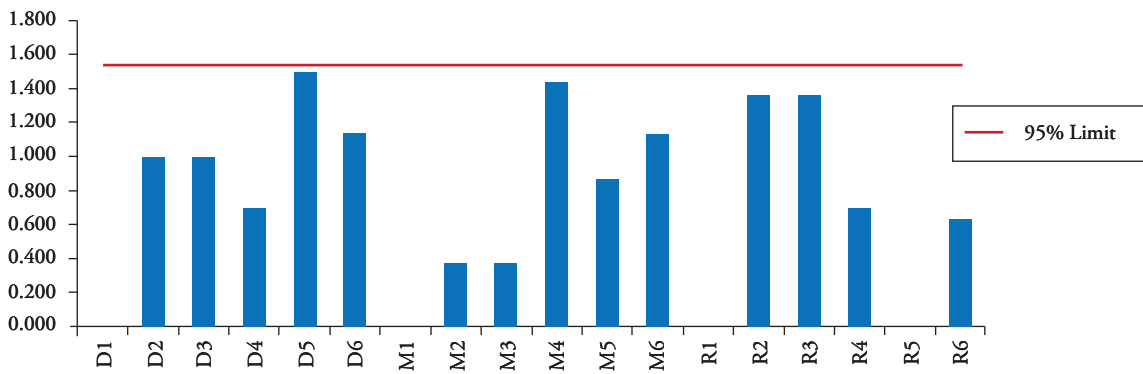


Fig. 5. Graph of k.



From the analysis of the results yielded during the confirmation of methods for caliper gauges of 150 mm measurement range, we may observe in the repeatability graphic that the measurement values are within the specifications for this process and a slight variation noted in the results from the three operators (M and R) is attributed to the operators, given that they are not constant among them.

Regarding the reproducibility analysis, it is observed that the three operators (D, M, and R), present variability in the measurements; this may be attributed to the operator’s skill when performing the measurement and it is derived from the equipment. These are within the specifications of the process.

Table 3. Measurement range up to 300 mm, division of scale 0.01 mm.

Operator	Indications (mm)					
	0	50	100	150	200	300
Delwin Velandia	0.000	49.996	99.996	149.994	199.996	299.994
	0.000	49.992	99.996	149.996	199.996	299.996
	0.000	49.994	99.996	199.994	200.000	299.996
Mean	0.0000	49.9940	99.9960	149.9947	199.9973	299.9953
Deviation	0.0000	0.002	0.000	0.001	0.002	0.001
h	0.00000	-0.00002	0.00000	-0.00001	0.00000	0.00000
k	0.00000	1.13389	0.00000	0.70711	1.04447	0.70711
Majer Atequera	0.000	49.998	99.994	149.996	199.996	299.994
	0.000	49.994	99.996	149.998	199.996	299.998
	0.000	49.996	99.998	149.996	200.000	299.998

Mean	0.000	49.9960	99.9960	149.9967	199.9973	299.9967
Deviation	0.000	0.002	0.002	0.001	0.002	0.002
h	0.00000	0.00002	0.00000	0.00000	0.00000	0.00000
k	0.00000	1.13389	1.50000	0.70711	1.04447	1.41421
Ronald Argote	0.000	49.996	99.998	149.998	199.996	299.996
	0.000	49.996	99.996	149.998	199.998	299.998
	0.000	49.994	99.998	149.994	200.000	299.998
Mean	0.000	49.9960	99.9960	149.9967	199.9973	299.9967
Deviation	0.000	0.002	0.002	0.001	0.002	0.002
h	0.00000	0.00000	0.00001	0.00000	0.00000	0.00000
k	0.00000	0.65465	0.86603	1.41421	0.90453	0.70711

Fig. 6. Graph of h.

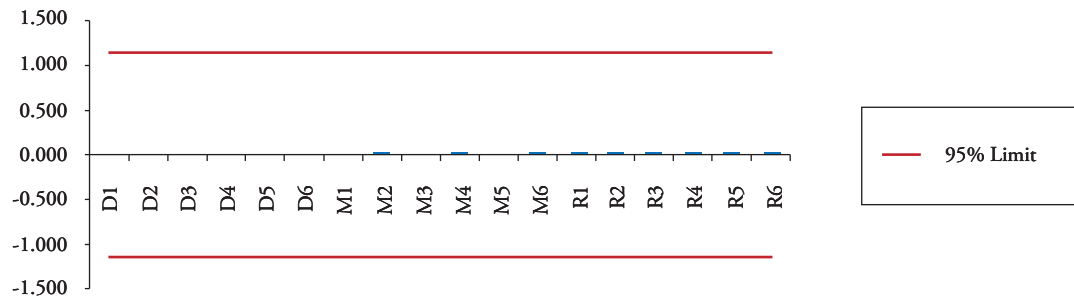
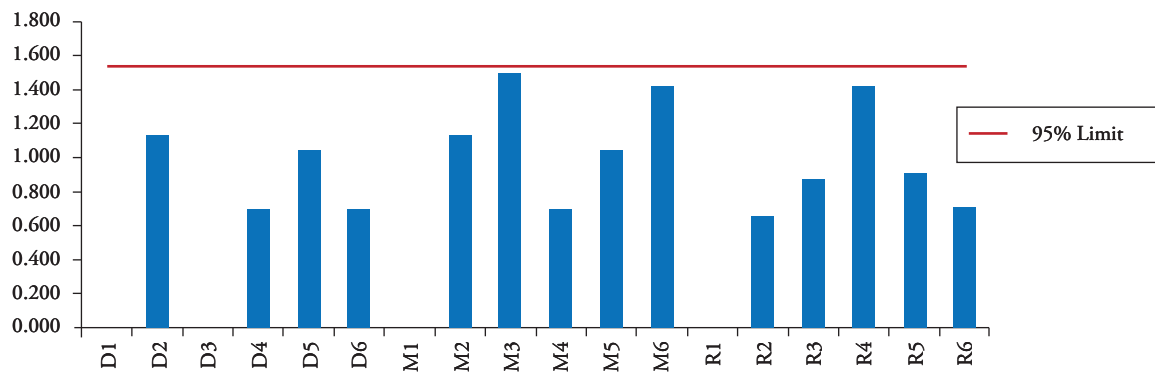


Fig. 7. Graph of k.



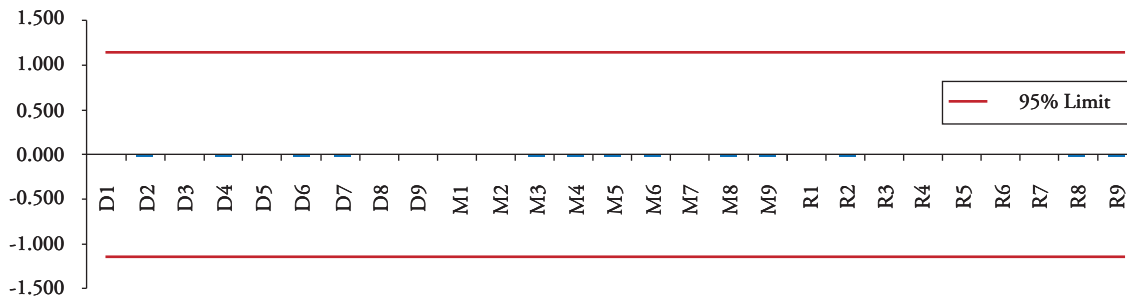
From the analysis of the results yielded during the confirmation of methods for caliper gauges of 300 mm measurement range, we may observe in the repeatability graphic that the measurement values are within the specifications for this process and a slight variation noted in the results from two operators (M and R) is attributed to the operators.

Regarding the reproducibility analysis, it is observed that the three operators (D, M, and R), present variability in the measurements; this may be attributed to the operator's skill when performing the measurement and it is derived from the equipment. These are within the specifications of the process.

Table 4. Measurement range up to 500 mm, division of scale 0.01 mm.

Operator	Indications (mm)								
	0	50	100	150	200	250	300	400	500
Delwin Velandia	0.000	49.986	99.988	149.990	199.992	249.996	299.992	399.998	499.998
	0.000	49.988	99.994	149.992	199.994	249.994	299.994	399.998	500.000
	0.000	49.988	99.992	149.990	199.990	249.996	299.992	400.000	499.998
Mean	0.0000	49.9873	99.9913	149.9907	199.9920	249.9953	299.9927	399.9987	499.9987
Deviation	0.000	0.001	0.003	0.001	0.002	0.001	0.001	0.001	0.001
h	0.00000	-0.00002	0.00001	-0.00001	0.00000	0.00000	-0.00001	0.00000	0.00000
k	0.00000	0.77460	1.18322	1.22474	0.63960	1.22474	1.00000	0.70711	0.86603
Majer Atequera	0.000	49.990	99.998	149.992	199.994	249.996	299.996	399.998	499.998
	0.000	49.990	99.990	149.990	199.990	249.996	299.994	399.998	500.000
	0.000	49.998	99.988	149.992	199.988	249.996	299.994	399.994	499.996
Mean	0.0000	49.9893	99.9887	149.9913	199.9907	249.9960	299.9947	399.9967	499.9980
Deviation	0.000	0.001	0.001	0.001	0.003	0.000	0.001	0.002	0.002
h	0.00000	0.00002	-0.00002	-0.00001	0.00000	0.00000	0.00000	0.00000	0.00000
k	0.00000	0.77460	0.44721	1.22474	0.97701	0.00000	1.00000	1.41421	1.50000
Ronald Argote	0.000	49.986	99.988	149.996	199.996	249.998	299.996	399.996	499.998
	0.000	49.998	99.990	149.996	199.988	249.996	299.994	399.998	499.998
	0.000	49.990	99.994	149.996	199.992	249.998	299.996	399.996	499.998
Mean	0.0000	49.9880	99.9907	149.9960	199.9920	249.9973	299.9953	399.9967	499.9980
Deviation	0.000	0.002	0.003	0.000	0.004	0.001	0.001	0.001	0.000
h	0.00000	0.00000	0.00000	0.00002	0.00000	0.00000	0.00000	0.00000	0.00000
k	0.00000	1.34164	1.18322	0.00000	1.27920	1.22474	1.00000	0.70711	0.00000

Fig. 8. Graph of h.



From the analysis of the results yielded during the confirmation of methods for caliper gauges of 500 mm measurement range, we may observe in the repeatability graphic that the measurement values are within the specifications for this process and a slight variation noted in the results from the three operators (D, M, and R) is attributed to the operators.

Regarding the reproducibility analysis, it is observed that the three operators (D, M, and R), present variability in the measurements; this may be attributed to the operator's skill when performing the measurement and it is derived from the equipment. These are within the specifications of the process.

Fig. 9. Graph of k.

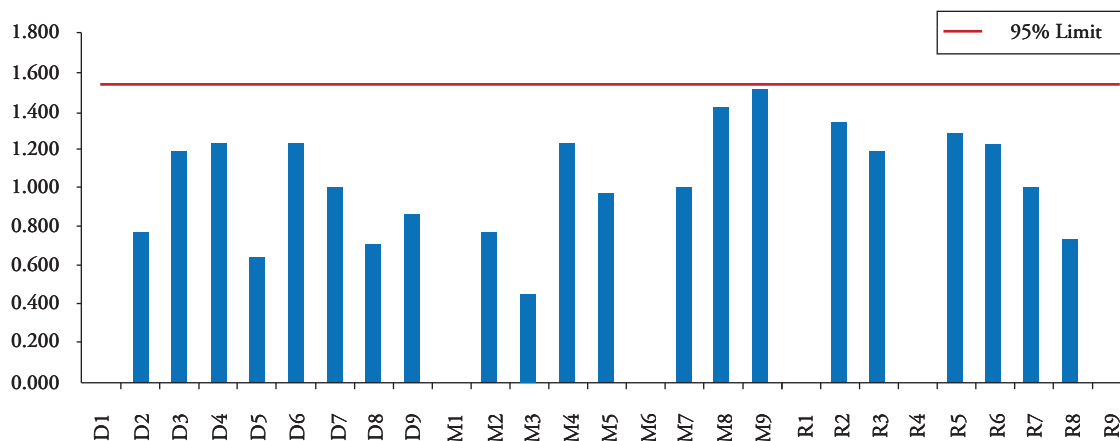


Table 5. Measurement range up to 900 mm, division of scale 0.02 mm.

Operator	Indications (mm)								
	0	50	100	200	300	400	500	750	900
Delwin Velandia	0.000	50.000	100.000	200.000	300.000	400.000	500.000	750.000	900.000
	0.000	50.000	100.000	200.000	300.000	400.000	500.000	750.000	900.000
	0.000	50.000	100.000	200.000	300.000	400.000	500.000	750.004	900.004
Mean	0.0000	50.0000	100.0000	200.0000	300.0000	400.0000	500.0000	750.0013	900.0013
Deviation	0.000	0.000	0.000	0.000	0.000	0.000	0.000	0.002	0.002
h	0.00000	0.00000	0.00000	0.00000	0.00000	0.00000	0.00000	0.00000	0.00000
k	0.00000	0.00000	0.00000	0.00000	0.00000	0.00000	0.00000	1.22474	1.00000
Majer Atequera	0.000	50.000	100.000	200.000	300.000	400.000	500.000	750.000	900.000
	0.000	50.000	100.000	200.000	300.000	400.000	500.000	750.000	900.004
	0.000	50.000	100.000	200.000	300.000	400.000	500.000	750.000	900.000
Mean	0.0000	50.0000	100.0000	200.0000	300.0000	400.0000	500.0000	750.0000	900.0013
Deviation	0.000	0.000	0.000	0.000	0.000	0.000	0.000	0.002	0.002
h	0.00000	0.00000	0.00000	0.00000	0.00000	0.00000	0.00000	0.00000	0.00000
k	0.00000	0.00000	0.00000	0.00000	0.00000	0.00000	0.00000	0.00000	1.00000
Ronald Argote	0.000	50.000	100.000	200.000	300.000	400.000	500.000	750.000	900.004
	0.000	50.000	100.000	200.000	300.000	400.000	500.000	750.004	900.000
	0.000	50.000	100.000	200.000	300.000	400.000	500.000	750.000	900.000
Mean	0.0000	50.0000	100.0000	200.0000	300.0000	400.0000	500.0000	750.0013	900.0013
Deviation	0.000	0.000	0.000	0.000	0.000	0.000	0.000	0.002	0.002
h	0.00000	0.00000	0.00000	0.00000	0.00000	0.00000	0.00000	0.00000	0.00000
k	0.00000	0.00000	0.00000	0.00000	0.00000	0.00000	0.00000	1.22474	1.00000

From the analysis of the results yielded during the confirmation of methods for caliper gauges of 900 mm measurement range, we may observe in the repeatability graphic that the measurement values are within the specifications for this process and

a slight variation noted in the results from the operator (M) is attributed to the operator.

Regarding the reproducibility analysis, it is noted that the three operators (D, M, and R) present

constant variations in some specific points in the measurement; this may be attributed to the measurement instrument and to that derived from the equipment. These are within the specifications of the process.

Fig. 10. Graph of h.

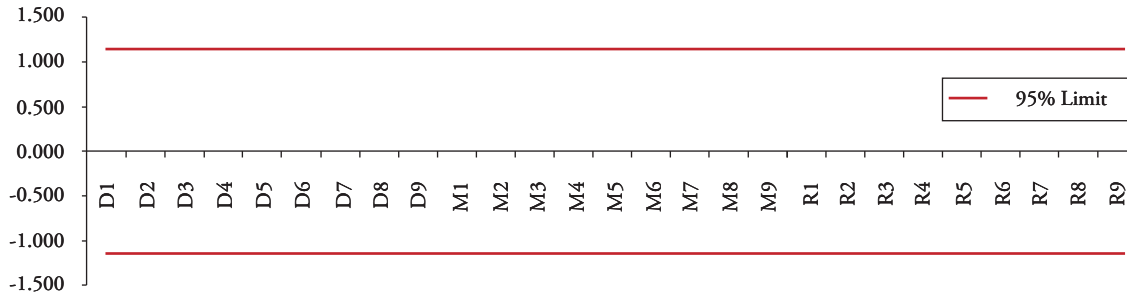
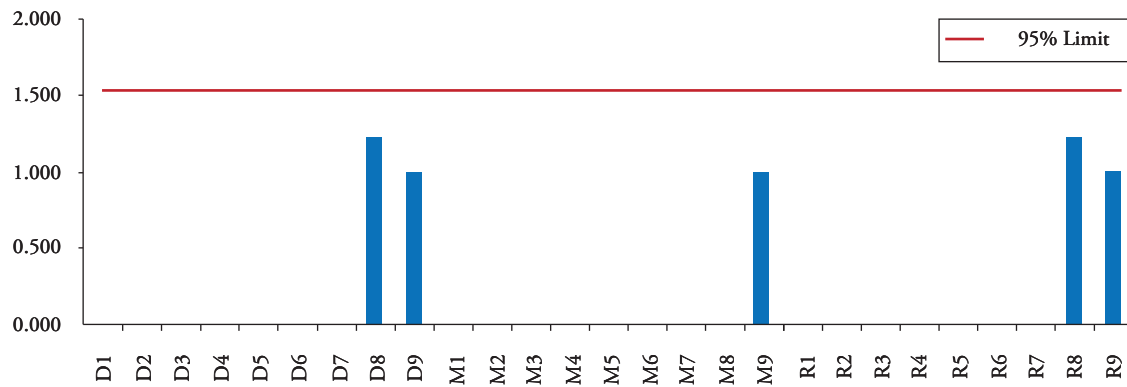


Fig. 11. Graph of k.



Estimation of uncertainty

Estimation of uncertainty during each calibration was determined by following the guidelines from the GTC 51:1997 guide “Guide for the expression of uncertainty in measurements”.

The uncertainties estimated for each measurement interval are shown in the following tables:

a) Interval up to 150 mm, division of scale 0.01 mm

Table 6. Calliper gauge (0-150 mm).

Person selected	Calibration No.	U exp (μ m)	CMC
D	1	8.7	7.7
D	2	7.7	
D	3	7.7	

M	1	7.7
M	2	9.6
M	3	10.0
R	1	8.7
R	2	7.7
R	3	7.7

b) Interval up to 300 mm, division of scale 0.01 mm

Table 7. Calliper gauge (0-300 mm).

Person selected	Calibration No.	U exp (μ m)	CMC
D	1	7.9	7.9
D	2	7.9	
D	3	8.9	
M	1	7.9	
M	2	7.9	
M	3	8.9	

R	1	7.9
R	2	7.9
R	3	8.9

c) Interval up to 500 mm, division of scale 0.01 mm

Table 8. Calliper gauge (0-500 mm).

Person selected	Calibration No.	U exp (μm)	CMC
D	1	11.0	8.1
D	2	9.9	
D	3	12.1	
M	1	9.9	
M	2	9.1	
M	3	9.9	
R	1	9.9	
R	2	9.1	
R	3	8.1	

d) Interval up to 900 mm, division of scale 0.02 mm

Table 9. Calliper gauge (0-900 mm).

Person selected	Calibration No.	U exp (μm)	CMC
D	1	12.1	12.1
D	2	12.1	
D	3	14.5	
M	1	14.5	
M	2	12.1	
M	3	12.1	
R	1	14.5	
R	2	12.1	
R	3	12.1	

According to the results obtained, we have:

a) Interval up to 150 mm, division of scale 0.01 mm.

CMC = 7.7 μm

b) Interval up to 300 mm, division of scale 0.01 mm.

CMC = 7.9 μm

c) Interval up to 500 mm, division of scale 0.01 mm.

CMC = 8.1 μm

d) Interval up to 900 mm, division of scale 0.02 mm.

CMC = 12.1 μm

Conclusions

It may be determined through the confirmation method that the repeatability of the measurements presented by the three operators is within the specifications for each of their measurement ranges; operator D presents a variation per equipment; this may be attributed to the instrument.

It may be determined through the confirmation method that the reproducibility of the measurements presented by the three operators are within specifications for each of their measurement ranges; the three graphics show that the operators presented constant values, which is due to the instrument and method used.

According to the results obtained and exposed in this report, the method remains confirmed. Las CMCs reported clearly show the precision COTECMAR'S metrology laboratory is offering to the different areas performing measurements in the Corporation. This methodology will allow us to reevaluate the corporate measurement processes and make decisions that lead to continuous improvement of production processes.

References

http://www.inocar.mil.ec/web/images/lotaip/2015/literal_a/base_legal/A._Convenio_internacional_solas_1974.pdf. Instituto Oceanográfico de la Armada INOCAR. Ecuador. 2015-05-31.

http://www.inocar.mil.ec/web/images/lotaip/2015/literal_a/base_legal/A._Convenio_internacional_solas_1974.pdf. Instituto Oceanográfico de la Armada INOCAR. Ecuador. 2015-05-31.

<https://www.dimar.mil.co/content/convenio-internacional-sobre-la-seguridad-de-la-vida-humana-en-el-mar>. Dirección General

Marítima, Autoridad Marítima Colombiana. 2015-05-31.

<http://www.semana.com/especiales/articulo/potencia-naval/47869-3>. Revista Semana. 2001-11-05.

<http://www.cotecmar.com/conozcanos.html>. Portal COTECMAR. 2015-05-31.

<https://fernandoveyretou.files.wordpress.com/2011/06/validacion-y-confirmacion-de-metodos26.pdf>. Ingeniería en Calidad – Fernando Veyretou. Temas de Calidad. Laboratorio. 2011-06-10.

<http://www.metas.com.mx/guiametas/La-Guia-MetAs-07-09-proceso-de-medicion.pdf>. MetAs & Metrólogos Asociados. La Guía MetAs. September 2007.

INTERNATIONAL METROLOGY
VOCABULARY. VIM-3rd edition (2012).

<http://www.metas.com.mx/guiametas/La-Guia-MetAs-07-09-proceso-de-medicion.pdf>. MetAs & Metrólogos Asociados. La Guía MetAs. September 2007.

INTERNATIONAL METROLOGY
VOCABULARY. VIM-3rd edition (2012).

Solution to the Anti-aircraft Fire Control Problem on a Naval Platform Using the Direct Geometric Model

Solución al problema de control de tiro antiaéreo sobre una plataforma naval empleando el modelo geométrico directo

Francisco Gil ¹
Andrés Vivas ²

Abstract

To find the kinematic model in applications different from robotics, the free-body diagram and coordinate conversion using Euler angles is frequently used. In robotics the Khalil-Kleinfinger (1986) method is used (and others), which allows coordinate conversions over several joints. In this paper a new application of this method to solve the fire control problem of a naval anti-aircraft gun is proposed. To demonstrate the application a virtual model is built using Virtual Reality Modeling Language (VRML) and controlled by Matlab Simulink[®]. From the direct geometric model the solution of the problem is found, including the detection system, platform, gun and flight of the missile. This model serves as a tool for the design, testing and integration of controllers for the gun and detection system. The prediction algorithms of the trajectory of the target and the missile in flight models can also be integrated. The results show that the geometric model of complex systems with many degrees of freedom can be constructed in a precise, methodical and easy to understand manner.

Key words: Fire control systems, geometric model, modeling.

Resumen

Para hallar el modelo cinemático de un proceso o mecanismo en aplicaciones distintas a la robótica el método frecuentemente usado es el diagrama de cuerpo libre y la conversión de coordenadas mediante ángulos de Euler. En robótica se emplea entre otros el método de Khalil-Kleinfinger el cual permite hacer conversiones de coordenadas sobre varias articulaciones. Este artículo propone una nueva aplicación de este método para la solución del problema de control de tiro antiaéreo de un cañón naval. Para demostrarlo se desarrolla un modelo virtual utilizando Virtual Reality Modeling Language (VRLM) y se implementa el controlador mediante Matlab[®]. A partir del modelo geométrico directo se desarrolla la solución del problema incluyendo el blanco, el sistema de detección, la plataforma, el cañón y el proyectil. El modelo desarrollado sirve como herramienta para el diseño, prueba e integración de controladores para el cañón y el sistema de detección, para desarrollar los algoritmos de predicción de la trayectoria del blanco y modelos del proyectil en vuelo. Los resultados obtenidos muestran que se puede construir el modelo geométrico de sistemas complejos con muchos grados de libertad de una manera precisa, metódica y fácil de comprender.

Palabras claves: Sistemas de control de tiro, modelo geométrico, modelización.

Date Received: October 5th, 2014 - *Fecha de recepción: 5 de octubre de 2014*

Date Accepted: November 25th, 2014 - *Fecha de aceptación: 25 de noviembre de 2014*

¹ Escuela Naval de Cadetes "Almirante Padilla", Colombia. e-mail: francisco.gil@armada.mil.co

² Universidad de Cauca, Colombia. e-mail: avivas@unicauca.edu.co

Introduction

The classic problem of anti-aircraft fire control consists in the correct prediction of the future position of a target over the time in which it is intercepted by a missile (Berg, 1983). For naval anti-aircraft fire, the weapon is on a platform that moves within six degrees of freedom, which requires maintaining the reference in orientation and displacement with respect to the world (Weiss, 1979) through an inertial navigator (I.N.S.) (Woodman, 2007). Additionally, the cannon, the detection system, the inertial navigator, and the platform's center of gravity are in different places; thus, requiring further corrections.

A solution consists in employing numerical methods to correct the cannon's orientation with respect to the line of sight (Elnashar, 2013), using the relative velocity between the target and the platform to predict the future position. This generates error when the platform is mobile, given that the relative velocity to the platform and the target's absolute velocity are different. This error is greater inasmuch as the velocity of the platform is comparable to that of the target. In addition, the derived equations result complex and with many elements.

Wang (2012) employs the free-body diagram and coordinate conversion through Euler angles (Slabaugh, 1999) to find the kinematic model of a system with four stabilized cameras in an air balloon. This method develops conversions of coordinates successively, which also turns out complex due to the large amount of elements to treat. Conversion via Euler angles is used in multiple applications, including control of guided missiles (Ollerenshaw, 2005) and unguided missiles (Hahn, 2009); stabilization of cameras on vehicles (Zayed, 2007), (Kumar, 2008); dynamic models of underwater vehicles (Wadoo, 2011); and models of inertial platforms (Dongsheng, 2011).

A way to simplify the movement equations is to use the matrix representation of vectors. This reduces the number of coefficients necessary for control, making it easier to construct models with multiple inputs and multiple outputs (Fossen, 2011).

Fossen (1991) uses an inverse dynamic model to model a naval artifact with six degrees of freedom. This implementation conceives the artifact as a rigid body and it is used to design controllers for governance and stabilization systems. Cabecinhas (2012) uses a similar strategy for the dynamic model of a four-rotor helicopter.

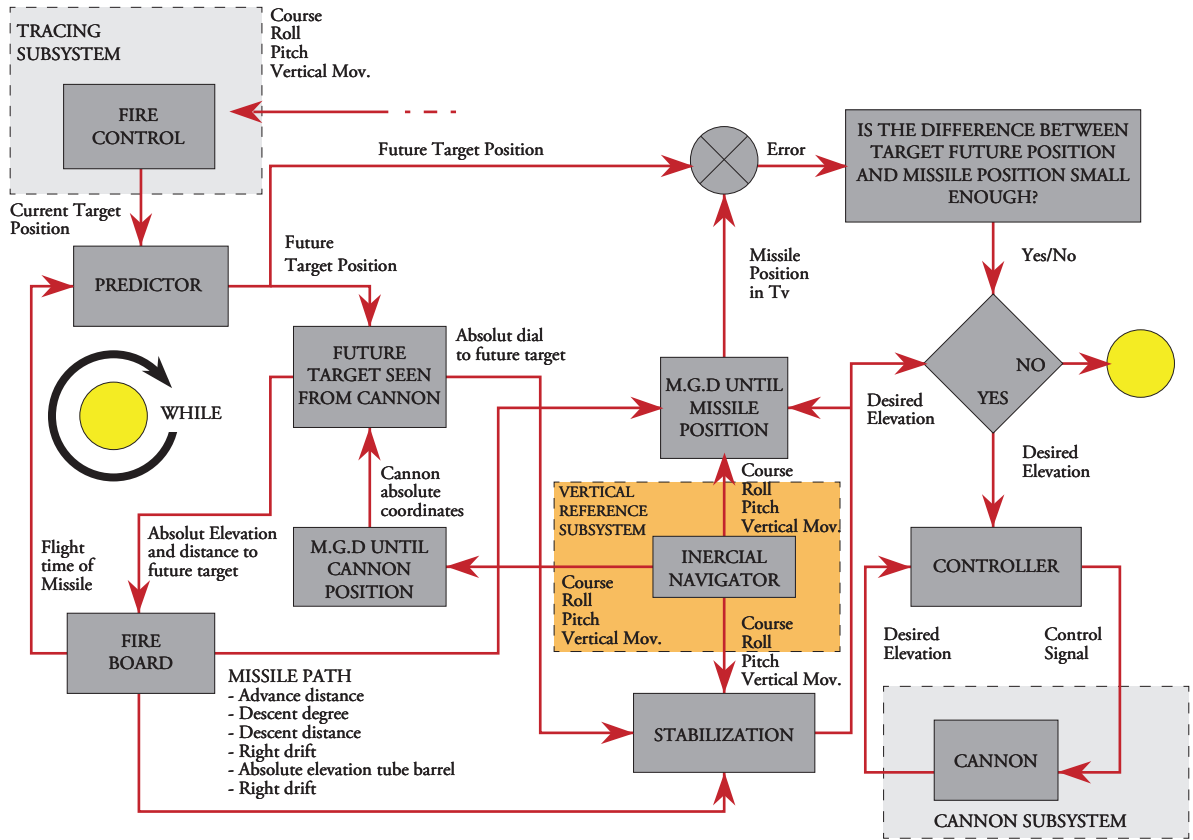
Kim (2008) constructs a virtual model of a stabilization platform that works as a parallel robot capable of moving in six degrees of freedom. Through the inverse geometric model the length of six prismatic articulations is determined. On this virtual model, a drift (ronza) elevation system is tested for a machine gun and its respective sensors. This permits saving resources upon developing part of the field tests on the virtual model. Other tools may be employed to construct virtual models of weapons systems, like in Bo (2011), where Virtool and High-Level Architecture (HLA) are used.

Bearing in mind that the naval fire control problem can contemplate up to 14 degrees of freedom, it turns out complex to find its geometric model by independently performing coordinate transformations, with it being best to take advantage of the methodical manner of performing successive transformations as proposed by Khalil-Kleinfinger (1986). A variation is, then, proposed of this approach to construct a geometric model of the fire control problem, including platform movements and extending to integrate the movements of the target, the cannon located on the platform, and the missile in flight. This model will serve as a framework to design, test, and integrate controllers for the cannon or the direction of fire control. Bao-quan et al. (2010) designed a controller for a cannon's servos on a virtual model. Upon developing a virtual model, huge costs are saved because this allows early detection of possible design problems and tests are reduced by using real surface units, real aircraft targets, and real weapons (Kim, 2008).

Solution to the fire control problem

The following algorithm was designed to solve the fire control problem.

Fig. 1. Algorithm proposed for fire control.



Monitoring Subsystem

This determines the current target position in rectangular coordinates with respect to the platform position over the surface. This position is defined by the point projected by the platform's center of gravity over the surface plane. The target's position is measured through a fire control director that indicates compass bearing, elevation, and distance; thereafter, the coordinates are translated to the point of reference.

The direct geometric model of ${}^0T_{10D}$ is found and the target's coordinates are obtained, thus:

$$\begin{aligned}
 xD = & -R6*(S2*C4 + C2*S3*S4) \\
 & + R5*(S4*S2 + C2*S3*C4) \\
 & - R10*(-C9*(S8*(-S2*C4 + C2*S3*S4) \\
 & + C2*C8*C3) + S9*(S4*S2 + C2*S3*C4)) \\
 & + R7*C2*C3
 \end{aligned} \quad (1)$$

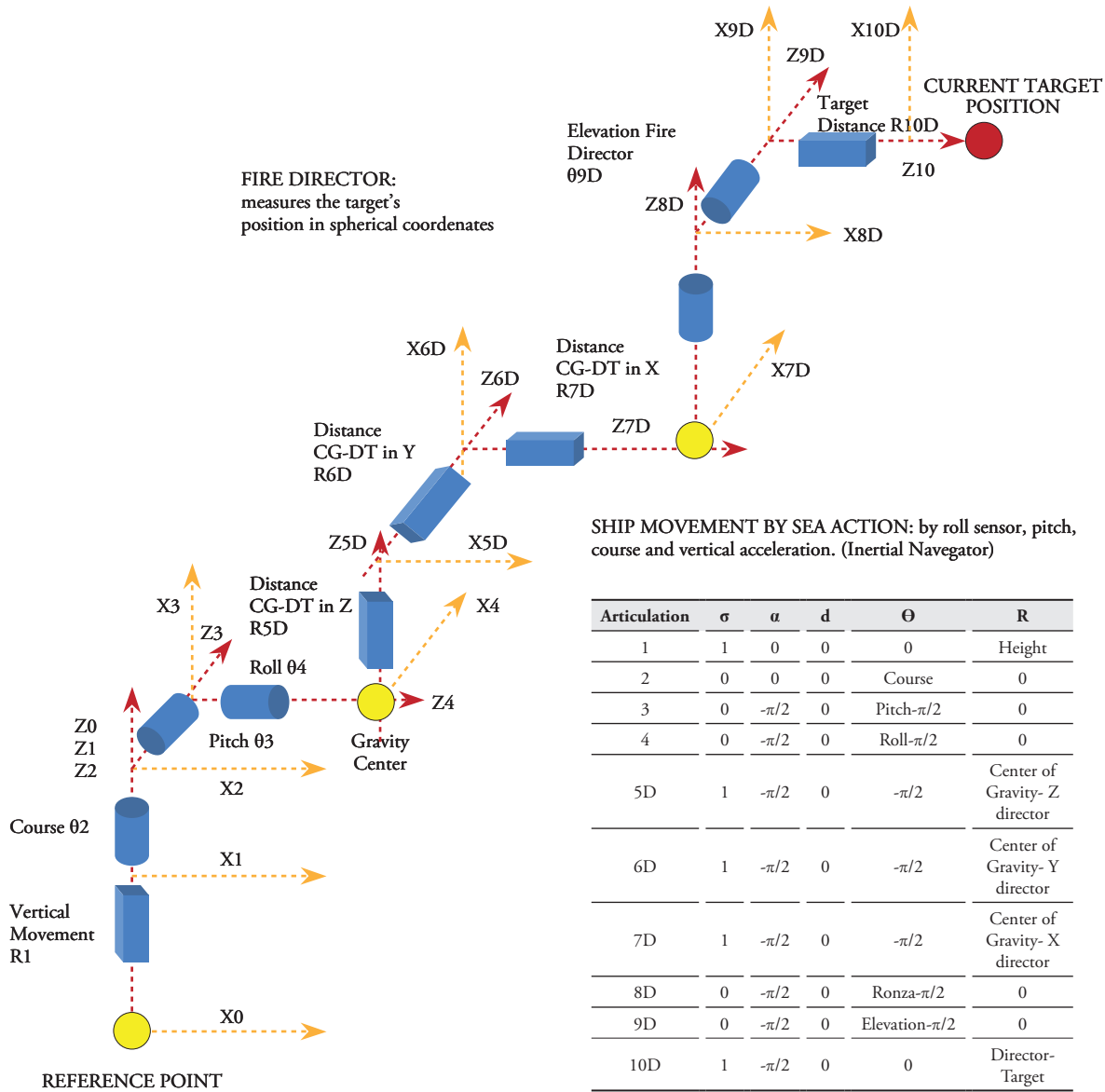
$$\begin{aligned}
 yD = & R10*(-C9*(S8*(-C2*C4 - S3*S4*S2) \\
 & - S2*C8*C3) + S9*(C2*S4 - S3*S2*C4)) \\
 & - R5*(C2*S4 - S3*S2*C4) - R6*(-C2*C4 \\
 & - S3*S4*S2) + R7*S2*C3
 \end{aligned} \quad (2)$$

$$\begin{aligned}
 zD = & R1 - R10*(-C9*(-S3*C8 + S8*S4*C3) \\
 & + S9*C3*C4) - R7*S3 + R6*S4*C3 \\
 & + R5*C3*C4
 \end{aligned} \quad (3)$$

Corrections to maintain the point of reference as fixed point

Unlike the robots normally modeled through the Khalil-Kleininger (1986) technique, in this case the point of reference moves on a plane. Due to this, it is presumed that for each discrete time the point-of-reference position is fixed and the prior target positions are corrected according to the platform's displacement on the plane. It is assumed that the

Fig. 2. Direct geometric model monitoring system and parameters.



inertial navigator is 100% precise; however, in reality a deviation will exist.

A P matrix is defined, which keeps the target's previous positions with respect to the point of reference that is always $[x=0, y=0]$.

$$P_t = \begin{bmatrix} \hat{x}_{t-1} & \hat{y}_{t-1} \\ \hat{x}_{t-2} & \hat{y}_{t-2} \\ \vdots & \vdots \\ \hat{x}_{t-n} & \hat{y}_{t-n} \end{bmatrix} \quad (4)$$

P_t is calculated in the following manner:

$$P_t = P_{t-1} - \Delta P \quad (5)$$

Where ΔP is the platform's displacement in the sampling time, Δt . To find ΔP , measure the instantaneous acceleration delivered by the inertial navigator, a_i , and calculate such through Newton's laws of motion.

$$\Delta P = V_{i_{t-1}} * \Delta t + a_i * \Delta t^2 \quad (6)$$

Where $V_{i_{t-1}}$ is the platform's velocity in the prior time, which is calculated by integrating a_i (Woodman, 2007). P_t and the target's current position $[x_t, y_t]$ are the inputs to the predictor to calculate the target's future position.

Predictor of the target's future position

By using any prediction algorithm, like the Kalman filter (Berg, 1982), from the known trajectory, the target's position is sought in a future time equal to the missile's flight time, t_v . The problem is that the target's future position is a function of the missile's flight time, which in turn is a function of the target's future position. To solve this, we first assume that the target's future position is equal to the current position, hence, the missile's flight time, t_v , is calculated. This flight time serves to calculate a new future position of the target. When repeating this process several times, the difference between the target's future position and the missile's position in t_v is reduced until it gets close to zero (Vila, 2009).

The missile's flight time is obtained from shooting charts. Shooting charts contain the ballistic parameters of a given type of ammunition. These charts are elaborated by manufacturers and are determined experimentally. From the elevation

angle and the distance to target, we find the cannon's elevation angle, missile's angle of fall in its terminal part, and the missile's lateral deviation caused by the rotation on its own axis (Vila, 2009). Another way is to mathematically model the missile's trajectory in the atmosphere based on parameters like the ballistic coefficient, initial velocity, and atmospheric pressure (Carlucci, 2007).

Direct geometric model from the point of reference to the end of the missile's trajectory

The geometric model from the point of reference to the missile's position in t_v permits comparing this last position with the target's future position at the same time, so that we can find a drift position and cannon elevation that reduces the distance between these two points to zero.

The direct geometric model of ${}^0T_{14C}$ is found and the missile's coordinates at moment t_v are obtained, thus equations 7, 8 and 9 (see page 49).

Calculation of drift and cannon elevation

To complete all the parameters of the direct geometric model, determine where the cannon should be aimed with respect to the platform.

Fig. 3. Geometric representation of the parameters provided by the shooting chart.

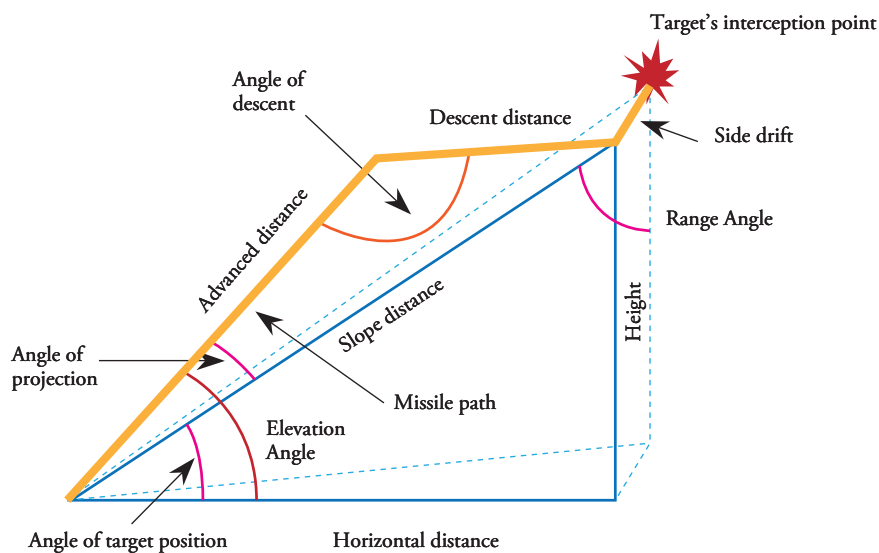
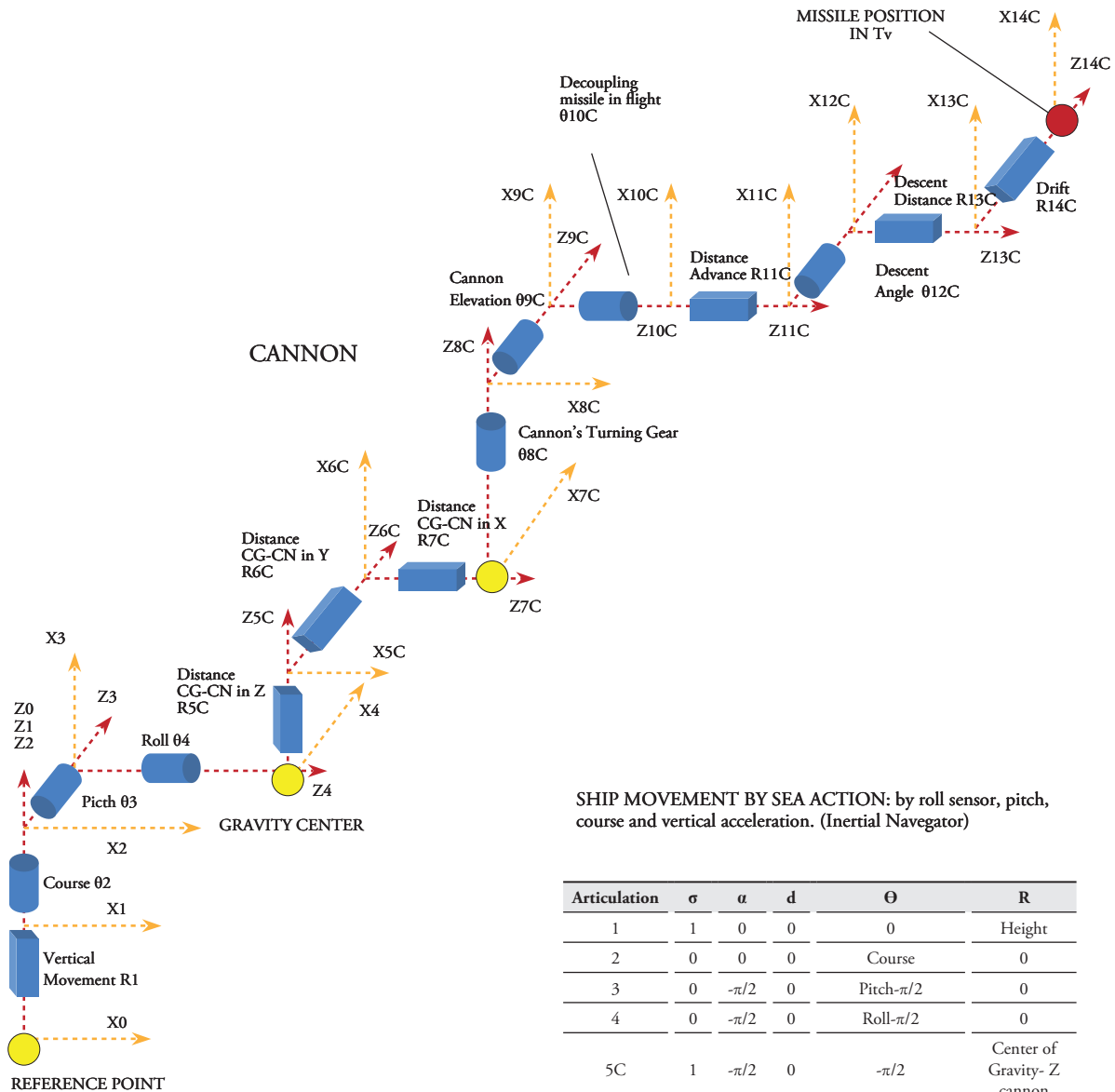


Fig. 4. Direct geometric model from the point of reference to the end of the missile's trajectory and parameters.



SHIP MOVEMENT BY SEA ACTION: by roll sensor, pitch, course and vertical acceleration. (Inertial Navigator)

Articulation	σ	a	d	Θ	R
1	1	0	0	0	Height
2	0	0	0	Course	0
3	0	$-\pi/2$	0	Pitch- $\pi/2$	0
4	0	$-\pi/2$	0	Roll- $\pi/2$	0
5C	1	$-\pi/2$	0	$-\pi/2$	Center of Gravity- Z cannon
6C	1	$-\pi/2$	0	$-\pi/2$	Center of Gravity- Y cannon
7C	1	$-\pi/2$	0	$-\pi/2$	Center of Gravity- X cannon
8C	0	$-\pi/2$	0	Drift- $\pi/2$	0
9C	0	$-\pi/2$	0	Elevation- $\pi/2$	0
10C	0	$-\pi/2$	0	Missile Decoupling	0
11C	1	0	0	0	Rise distance
12C	0	$\pi/2$	0	Angle of descent	0
13C	1	$-\pi/2$	0	0	Descent Distance
14C	1	$\pi/2$	0	0	Deviation

$$\begin{aligned}
 x^P = & R6 * (-S2 * C4 + C2 * S3 * S4) + R5 * (S4 * S2 + C2 * S3 * C4) - R14 * (C10 * (-C8 * (-S2 * C4 + C2 * S3 * S4) \\
 & + C2 * C8 * C3) - S10 * (S9 * (S8 * (-S2 * C4 + C2 * S3 * S4) + C2 * C8 * C3) + C9 * (S4 * S2 + C2 * S3 * C4))) \\
 & - R11 * (-C9 * (S8 * (-S2 * C4 + C2 * S3 * S4) + C2 * C8 * C3) + S9 * (S4 * S2 + C2 * S3 * C4)) \\
 & - R13 * (C12 * (-C9 * (S8 * (-S2 * C4 + C2 * S3 * S4) + C2 * C8 * C3) + S9 * (S4 * S2 + C2 * S3 * C4)) \\
 & + S12 * (S10 * (-C8 * (-S2 * C4 + C2 * S3 * S4) + C2 * S8 * C3) + C10 * (S9 * (S8 * (-S2 * C4 + C2 * S3 * S4) \\
 & + C2 * C8 * C3) + C9 * (S4 * S2 + C2 * S3 * C4)))) + R7 * C2 * C3
 \end{aligned} \tag{7}$$

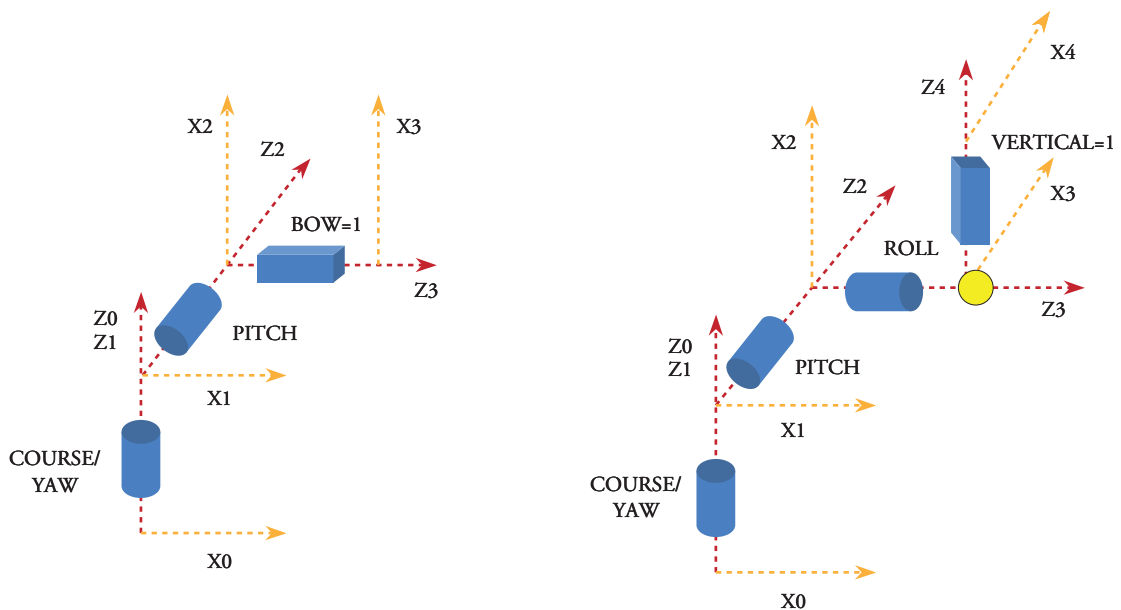
$$\begin{aligned}
 y^P = & R11 * (-C9 * (S8 * (-C2 * C4 - S3 * S4 * S2) - S2 * C8 * C3) - S9 * (C2 * S4 - S3 * S2 * C4)) \\
 & - R5 * (C2 * S4 - S3 * S2 * C4) - R6 * (-C2 * C4 - S3 * S4 * S2) + R14 * (C10 * (-C8 * (-C2 * C4 - S3 * S4 * S2) \\
 & - S8 * S2 * C3) - S10 * (S9 * (S8 * (-C2 * C4 - S3 * S4 * S2) - S2 * C8 * C3) - C9 * (C2 * S4 - S3 * S2 * C4))) \\
 & + R13 * (C12 * (-C9 * (S8 * (-C2 * C4 - S3 * S4 * S2) - S2 * C8 * C3) + S9 * (C2 * S4 - S3 * S2 * C4)) \\
 & + S12 * (S10 * (-C8 * (-C2 * C4 - S3 * S4 * S2) - S8 * S2 * C3) + (C10 * (S9 * (S8 * (-C2 * C4 - S3 * S4 * S2) \\
 & - S2 * C8 * C3) + C9 * (C2 * S4 - S3 * S2 * C4)))) + R7 * S2 * C3
 \end{aligned} \tag{8}$$

$$\begin{aligned}
 z^P = & R1 - R11 * (-C9 * (-S3 * C8 + S8 * S4 * C3) + S9 * C3 * C4) + R14 * (S10 * (S9 * (-S3 * C8 + S8 * S4 * C3) \\
 & + C9 * C3 * C4) + C10 * (S8 * S3 + S4 * C8 * C3)) - R13 * (-C12 * (-C9 * (-S3 * C8 + S8 * S4 * C3) + S9 * C3 * C4) \\
 & + S12 * (C10 * (S9 * (-S3 * C8 + S8 * S4 * C3) + C9 * C3 * C4) - S10 * (S8 * S3 + S4 * C8 * C3))) \\
 & - R7 * S3 + R6 * S4 * C3 + R5 * C3 * C4
 \end{aligned} \tag{9}$$

For this, the platform aspect is characterized with respect to the world through three unit vectors: the vertical that describes the platform plane, the bow that describes the direction, and the starboard

that is perpendicular to the previous two. These are found through the following direct geometric models, from data on course, roll, and pitch.

Fig. 5. Geometric bow and vertical models and parameters.



BOW					
Articulation	σ	α	d	Θ	R
1	1	0	0	Course	0
2	0	$-\pi/2$	0	Pitch- $\pi/2$	0
3	0	$-\pi/2$	0	0	1
VERTICAL					
1	0	0	0	Course	0
2	0	$-\pi/2$	0	Pitch- $\pi/2$	0
3	0	$-\pi/2$	0	Roll- $\pi/2$	0
4	1	$-\pi/2$	0	0	1

Finally, the coordinates of the bow, starboard, and vertical vectors of the platform are obtained, thus:

$$Px = C1 * C2 \tag{10}$$

$$Py = S1 * C2 \tag{11}$$

$$Pz = -S2 \tag{12}$$

$$Vx = S3 * S1 + C1 * S2 * C3 \tag{13}$$

$$Vy = S2 * S1 * C3 - C1 * S3 \tag{14}$$

$$Vz = C2 * C3 \tag{15}$$

$$[Ex, Ey, Ez] = P \times V \tag{16}$$

Upon defining the reference coordinates system, the necessary drift and cannon elevation are determined. For such, we determined the rectangular coordinates of the directions of compass bearing and elevation obtained through the shooting chart by constructing a geometric model equal to that described in Fig. 5 for the bow, except that the articulations are drift, elevation, and cannon tube, obtaining the coordinates of the directions of compass bearing and elevation obtained through the shooting chart, thus:

$$Mx = C (\text{Compass bearing}) * C (\text{Elevation}) \tag{17}$$

$$My = S (\text{Compass bearing}) * C (\text{Elevation}) \tag{18}$$

$$Mz = -S (\text{Elevation}) \tag{19}$$

The components of this last vector are found in the directions of the vertical, bow, and starboard vectors performing the corresponding point products.

$$M_v = \vec{M} \cdot \vec{V} \tag{20}$$

$$M_p = \vec{M} \cdot \vec{P} \tag{21}$$

$$M_e = \vec{M} \cdot \vec{E} \tag{22}$$

Fig. 6a. Cannon direction vector (M) with respect to the point of reference.

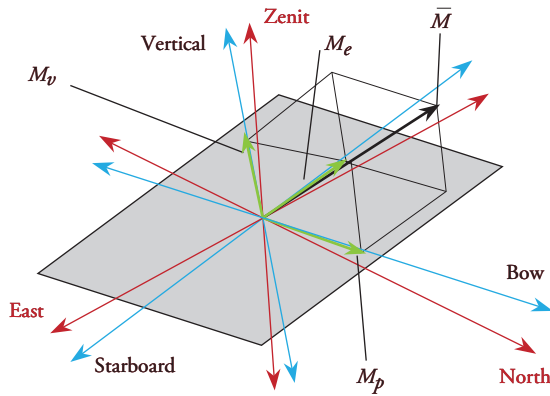
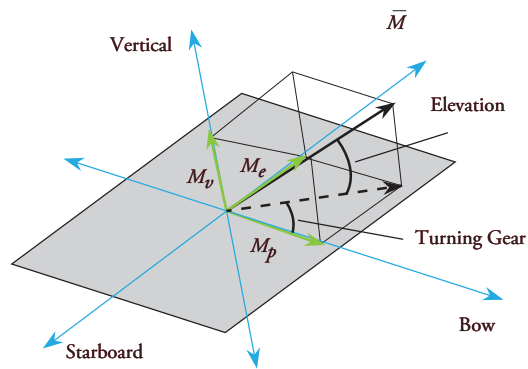


Fig. 6b. Cannon direction vector (M) with respect to the platform.



The component of the compass bearing-elevation vector in direction of the vertical vector permits finding the elevation, while the components in bow and starboard direction permit finding the compass bearing.

$$\text{Elevation} = \arcsin(M_v) \tag{23}$$

$$\text{Ronza} = \pm \arccos \frac{M_p}{C(\text{Elevation})} \tag{24}$$

If vector $M_e \geq 0$ then the drift is toward the right (+), on the contrary it is to the left (-).

Missile decoupling

When the missile abandons the cannon tube to start its flight, it stops depending on the platform's orientation; hence, it is necessary to maintain the

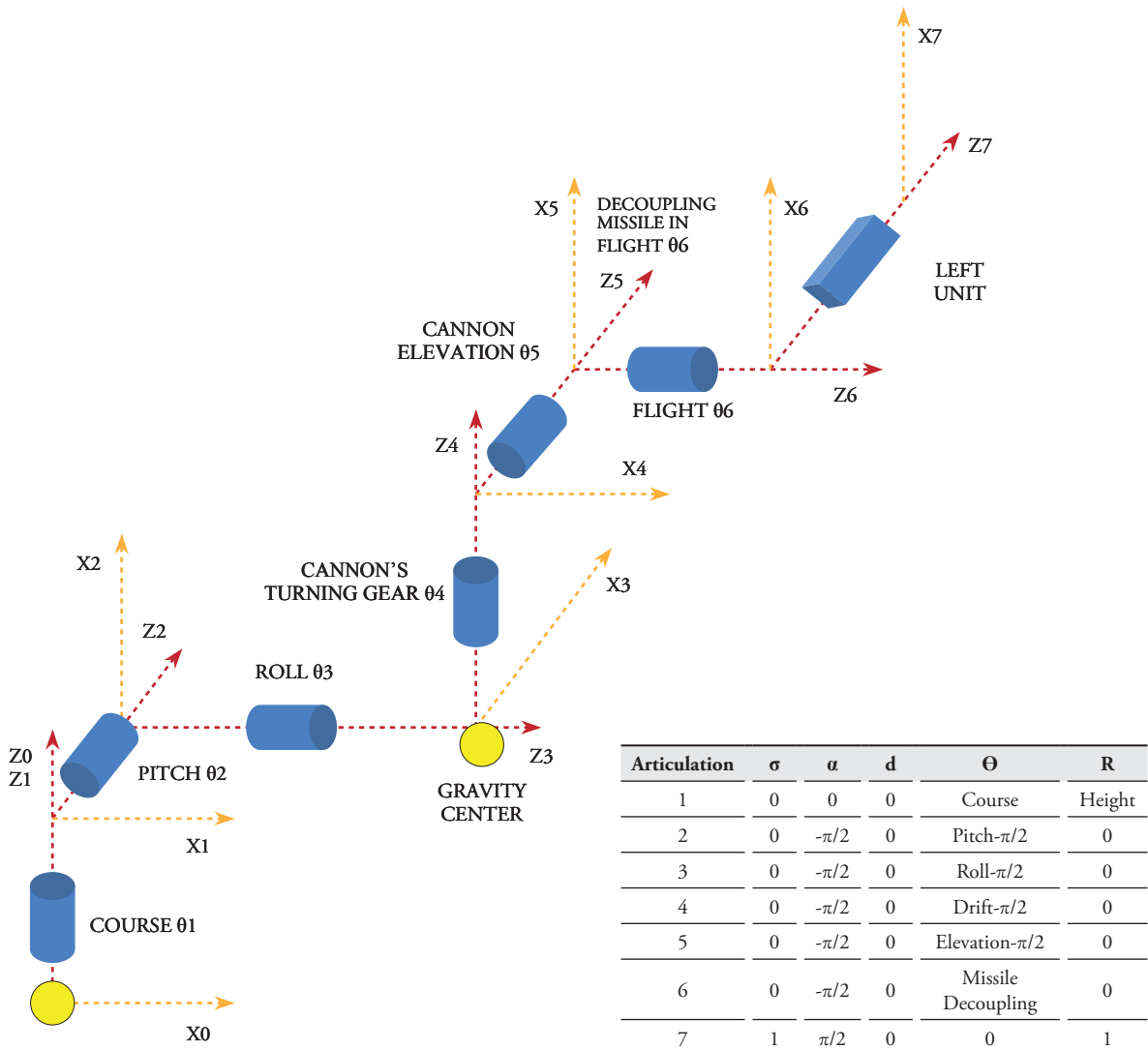
plane formed by the rise distance and the descent distance when turning over the angle of descent, perpendicular to the surface plane. For this, the decoupling articulation must be turned. To find this turn angle, the following geometrical model is constructed. The rise distance-descent distance plane is perpendicular to the surface when the left unit vector (z7) is perpendicular to the zenith. This occurs when:

$${}^0T_7 \cdot Z = 0 \tag{25}$$

$$\begin{bmatrix} {}^0T_{7x}, {}^0T_{7y}, {}^0T_{7z} \end{bmatrix} \cdot \begin{bmatrix} 0, 0, 1 \end{bmatrix} = 0 \tag{26}$$

$${}^0T_{7z} = 0 \tag{27}$$

Fig. 7. Geometric model and parameters of the left unit vector for the missile decoupling in flight.



From the direct geometric model we obtain:

$${}^0 T_7 = S_6*(S_5*(S_3*S_4*C_2 - S_2*C_4) + C_2*C_3*C_5) + C_6*(S_3*C_2*C_4 + S_2*S_4) \quad (28)$$

$$0 = S_6*(S_5*(S_3*S_4*C_2 - S_2*C_4) + C_2*C_3*C_5) + C_6*(S_3*C_2*C_4 + S_2*S_4) \quad (29)$$

$$S_6*(S_5*(S_3*S_4*C_2 - S_2*C_4) + C_2*C_3*C_5) = -C_6*(S_3*C_2*C_4 + S_2*S_4) \quad (30)$$

$$\frac{S_6}{-C_6} = \frac{S_3*C_2*C_4 + S_2*S_4}{S_5*(S_3*S_4*C_2 - S_2*C_4) + C_2*C_3*C_5} \quad (31)$$

$$-tan\delta = \frac{S_3*C_2*C_4 + S_2*S_4}{S_5*(S_3*S_4*C_2 - S_2*C_4) + C_2*C_3*C_5} \quad (32)$$

$$decoupling(z_6) = -tan^{-1} \frac{S_3*C_2*C_4 + S_2*S_4}{S_5*(S_3*S_4*C_2 - S_2*C_4) + C_2*C_3*C_5} \quad (33)$$

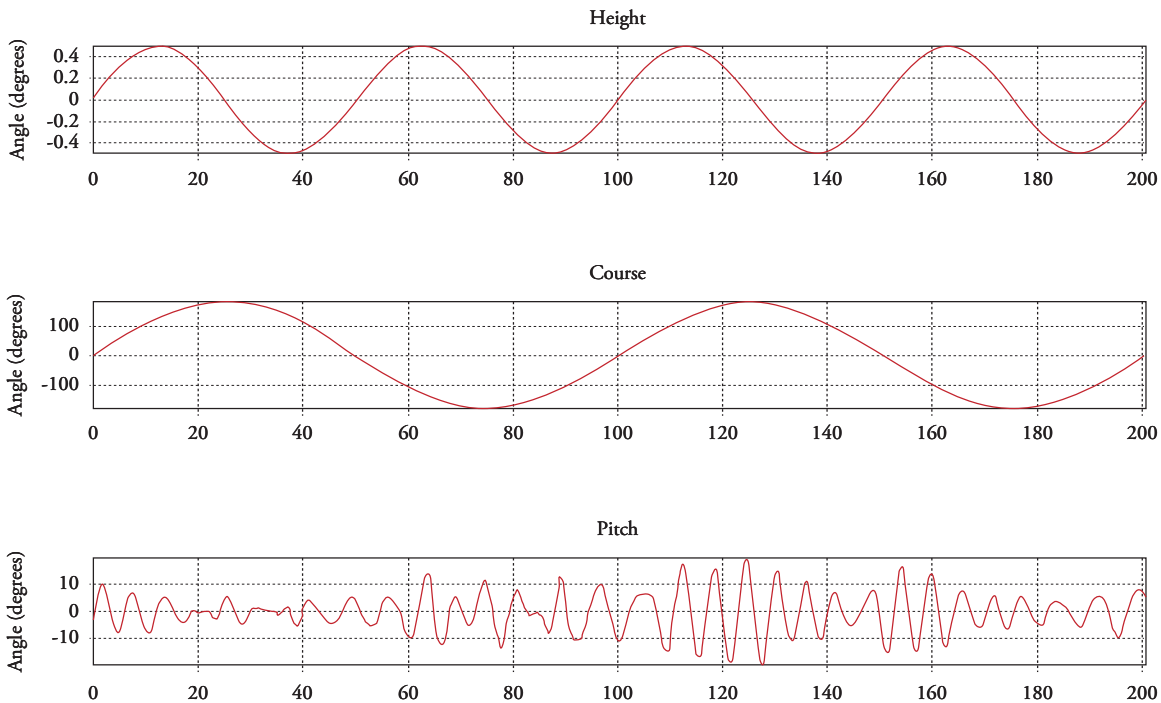
Results

To assess the model's performance, a virtual model is constructed of a surface platform with a shooting director and a cannon, according to the geometric models described previously, using VRML (Cellary, 2012). The algorithm described in Fig. 1 is tested by using Matlab® Simulink®. The target's trajectory

is generated through a free-ware flight simulator, YSflight, (Yamakawa, 2009).

To simplify the predictor it is presumed perfect when taking the target's future position in t_v of the same trajectory recorded from the simulator. Likewise, the cannon's plant model or its controller is not considered.

Fig. 8. Height, course, pitch, and roll signals of the platform movement.



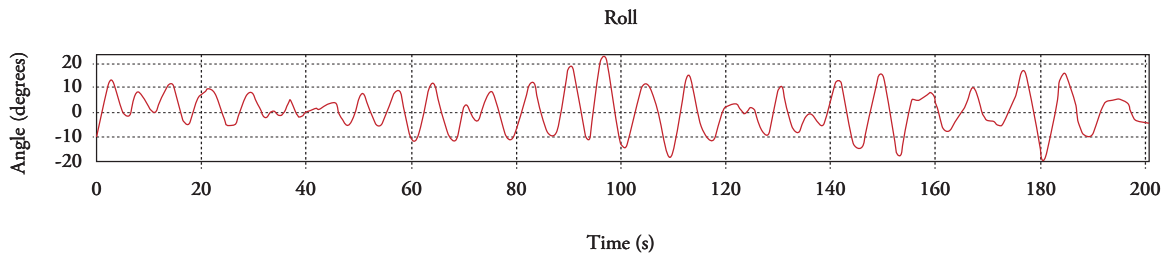


Fig. 9a. Perspective of the virtual model from the east ($x=10.5, y=3.7, z=17.9$).

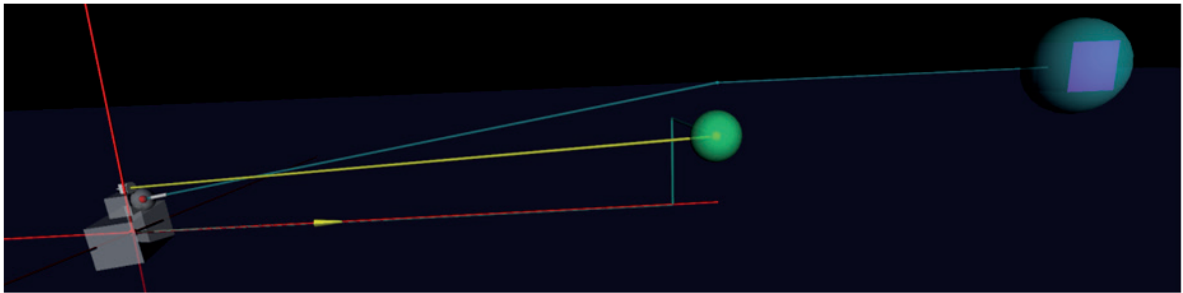
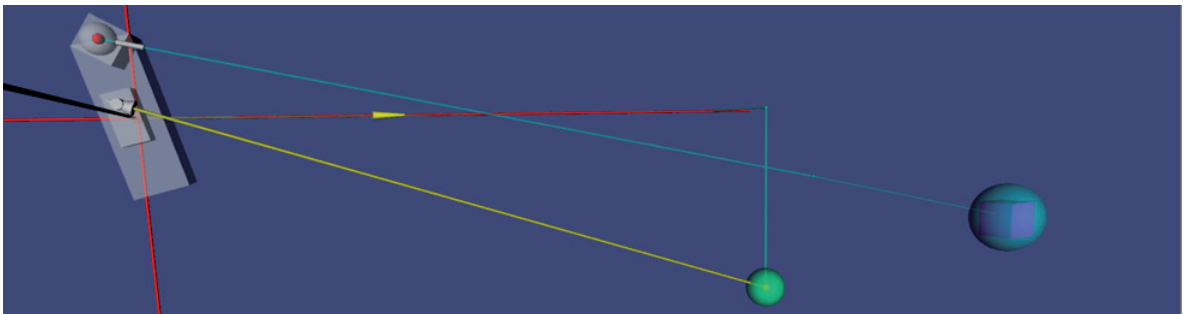


Fig. 9b. Perspective of the virtual model from the top ($x=2.1, y=0.6, z=16.5$).



In the previous images, the cannon is toward the bow and is represented as a sphere with a thin cylinder, the shooting director is over the superstructure and is represented as a cylinder that is the base, and a cone whose flat face represents the sensor that monitors the target. Note that the position of the cannon and shooting director is common and is taken as generic, but in practice it may be any over the platform, being this one of the advantages of this model because it permits modeling the position of the cannon or director in any part of the platform.

From a trajectory of a target and simulated platform movements the algorithm is tested, obtaining the results represented in Figs. 9 to 11.

Fig. 11a shows an error of 8.58×10^{-8} MRS in the missile's position with respect to the target's future position. This error is because the shooting chart uses an approximation in the missile's deviation. In Fig. 11b the deviation is equal to zero to observe the error attributable to the geometric model, with this error being 2.45×10^{-27} MRS.

Conclusions

This article has presented a new application of the Khalil-Kleinfinger method (1986) to geometrically model robots to solve the control problem of a naval anti-aircraft cannon shot, suggesting the applicability of this method to diverse problems.

This method facilitates the construction of the model, given that it simplifies the equations permitting easier design of controllers for the system.

The model developed serves as generic platform to develop a fire control system by integrating all the system's components from the mean of

detection to the missile in flight, being easily adaptable to multiple platforms including air and land.

Future work will include the development of the controller for a cannon and the prediction algorithm of the target's future position.

Fig. 10. Target's future position against missile's position at the end of its flight.

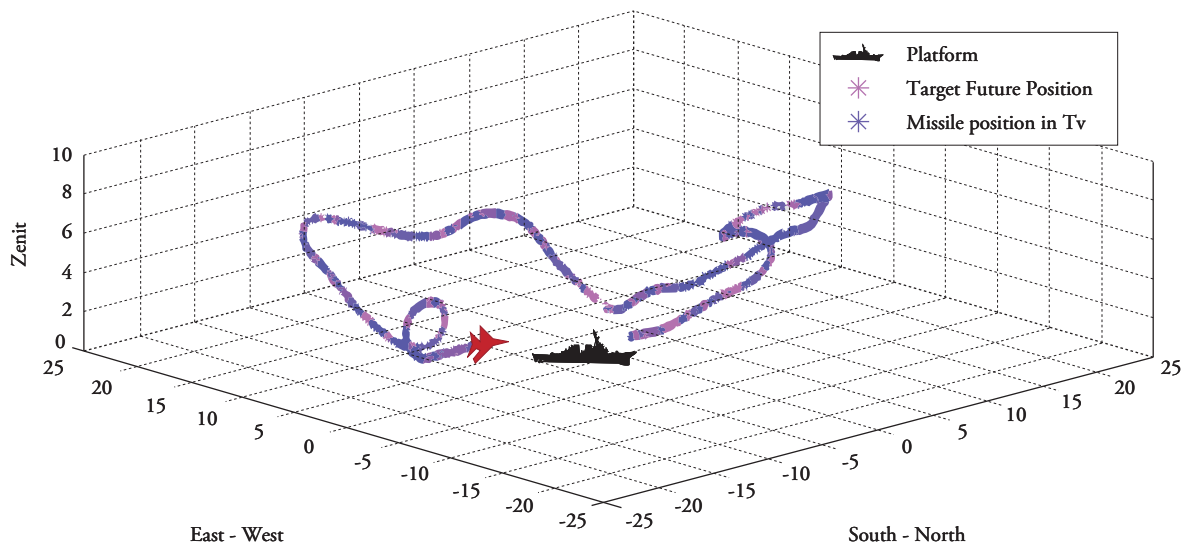


Fig. 11a. Error of the target's future position against the missile's position at the end of its flight, with (a); keep in mind the deviation.

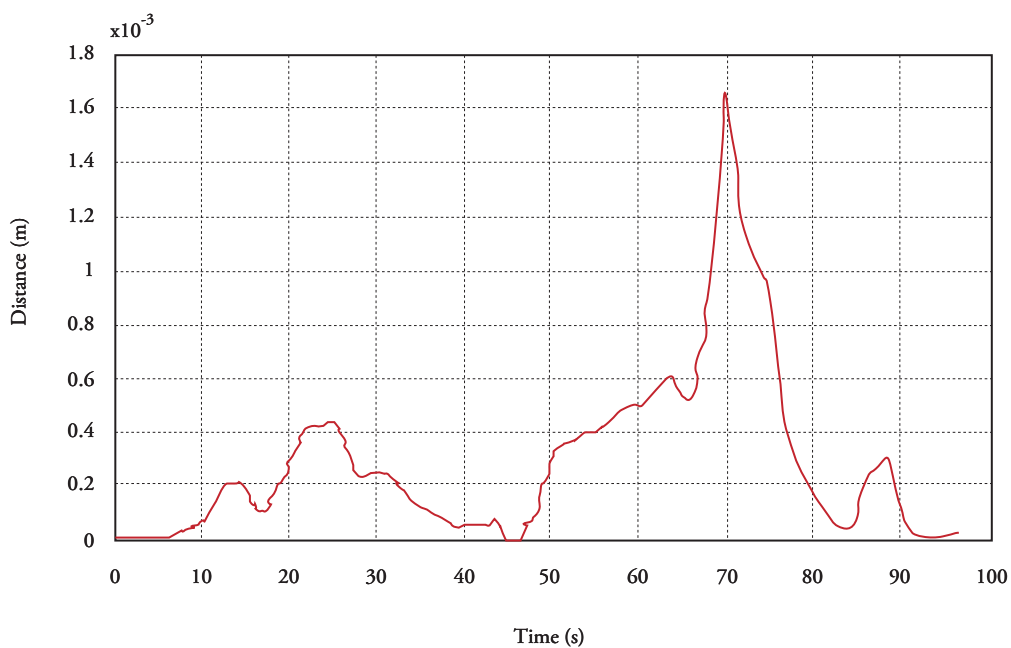
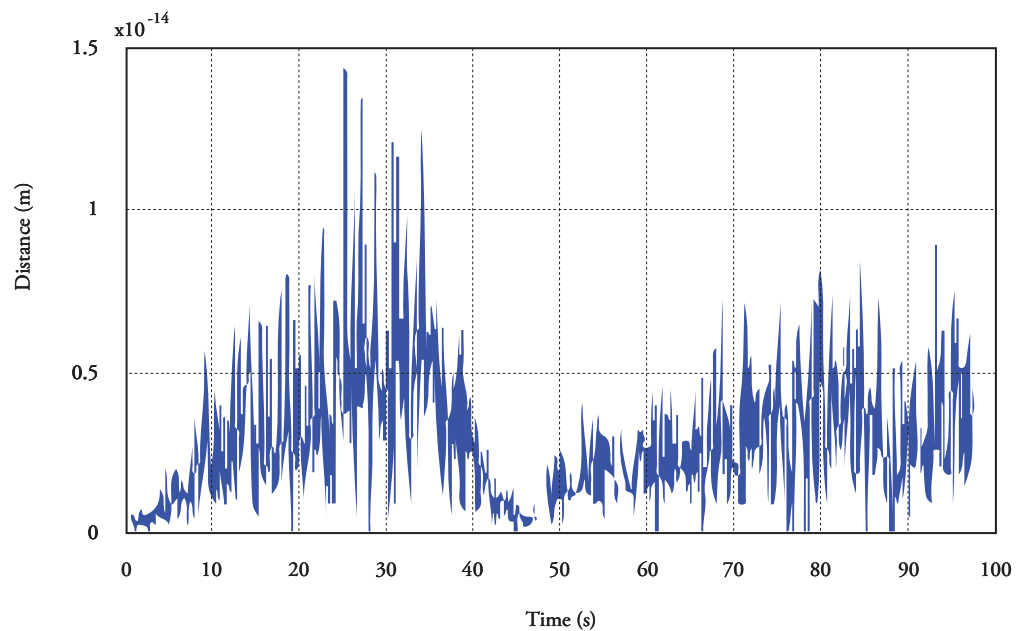


Fig. 11b. Error of the target's future position against the missile's position at the end of its flight, without (b); keep in mind the deviation.



References

- BAO-QUAN, M. *et al.* Research on Dynamic Simulation of Remotely-Operated Weapon Stations Servo Control System. 2010 IEEE International Conference on Intelligent Computation Technology and Automation. China, Changsha, 2010
- BERG, R.F. Estimation and prediction for manoeuvring target trajectories, IEEE Transactions of Automatic Control, Vol. 28, No. 3, March 1983, pp. 294–304.
- BO, B., *et al.* Research of Anti-aircraft Gun Weapon System Simulation Platform Based HLA and Virtools. 2011 International Conference on Electronics, Communications and Control. China, Ningbo, pp. 4455-4457, September, 2011.
- CABECHINHAS, D. Integrated Solution to Quadrotor Stabilization and Attitude Estimation Using a Pan and Tilt Camera. 51st IEEE Conference on Decision and Control. USA, Maui, Hawaii, December, 2012.
- CARTLUCCI, D. and JACOBSON, S. Ballistics Theory and Design of Guns and Ammunition. CRC Press, Taylor & Francis Group. Boca Raton, Florida, USA, 2007. ISBN: 978-1-4200-6618-0.
- CELLARY W. Interactive 3D Multimedia Content, Models for Creation, Management, Search and Presentation. Department of Information Technology Poznan University of Economics. Springer. Poland. 2012. ISBN 978-1-4471-2496-2.
- DONGSHENG L. *et al.* Research on Modelling and Simulation for Pitch/Roll Two-Axis Strap-down Stabilization Platform. The Tenth International Conference on Electronic Measurement & Instruments. The 54th Research Institute of CETC, Shijiazhuang, School of Instrumentation Science and Optoelectronic Engineering Beijing University of Aeronautics and Astronautics, China. 2011.
- ELNASHAR, G. A mathematical model derivation of general fire control problem and solution scenario, School of Engineering-Egyptian

- Armed Forces. Int. Journal of Modelling, Identification and Control, Vol. 20, No. 3, Cairo Egypt, 2013.
- FOSSEN, T. Nonlinear Modelling and Control of Underwater Vehicles. Doctoral Thesis (PhD). Department of Engineering Cybernetics, Norwegian University of Science and Technology. Trondheim, Norway. 1991.
- FOSSEN T, Handbook of Marine Craft Hydrodynamics and Motion Control, First Edition. Norwegian University of Science and Technology Trondheim, Norway. John Wiley & Sons Ltd. Trondheim, Norway. 2011. ISBN: 978-1-119-99149-6.
- HAHN R. *et al.* Predictive Guidance of a Missile for Hit-to-Kill Interception. IEEE Transactions on Control Systems Technology, Vol. 17, No. 4, July 2009. 1063-6536.
- KHALIL, W. Y KLEINFINGER, J.F. A new geometric notation for open and closed-loop robots. 1986 IEEE International Conference on Robotics and Automation, San Francisco, USA, pp. 1174-1180.
- KIM D. *et al.* Stabilization Control for the Mobile Surveillance Robot using Motion Simulator. Chungnam National University, Dodaam Systems Co. International Conference on Control, Automation and Systems. Seoul, Korea. 2008.
- KUMAR J. Stabilization System for Camera Control on an Unmanned Surface Vehicle. Thesis. Naval Postgraduate School. Monterey, California, USA. 2008. NSN 7540-01-280-5500.
- OLLERENSHAW D. and COSTELLO M. Model of Predictive Control of a Direct-Fire Missile Equipped With Canards. Oregon State University. Corvallis, Oregon, USA. 2005.
- WADDOO S. and KACHROO P. Autonomous Underwater Vehicles, Modelling, Control Design and Simulation. CRC Press, Taylor & Francis Group. 2011. ISBN-13: 978-1439818312.
- SLABAUGH G. Downloaded from: <http://www.soi.city.ac.uk/~sbbh653/publications/euler.pdf>. 1999.
- VIVAS O. Diseño y Control de Robots Industriales Teoría y Práctica. Elaleph, Buenos Aires, Argentina. 2010. ISBN 978-987-1581-76-4.
- WOODMAN O. An introduction to inertial Navigation, Technical report Number 696, University of Cambridge, Computer Laboratory. Cambridge UK. 2007. 37p. ISSN 1476-2986.
- WANG, Y., *et al.* Strap-down stabilization for multi-load optoelectronic imaging platform. Beihang University, Chinese Academy of Sciences. Aircraft Engineering and Aerospace Technology: An International Journal. Beijing, China. 2012.
- WEISS I. Y CROSS R. Ship Motion Effects on Gun Fire Control System Design. Naval Engineers Journal, P 75-80. 1979.
- YAMAKAWA S. ysflight. software flight simulator. Available on line in: <http://www.ysflight.com/>. Version 20090611.
- ZAYED M. and BOONAERT J. An Inertial Sensor for Mechanical Compensation of the Vehicle Vertical Movement Impact on In-Vehicle Embedded Camera Orientation. Proceedings of the 2007 IEEE Intelligent Transportation Systems Conference. Seattle, Washington, USA. 1-4244-1396-6.

Fatigue Analysis of the Structural Bottom of an Aluminum Planing Craft through Vibratory Load of the Propeller System

Análisis de fatiga del fondo estructural de una lancha planeadora en aluminio por carga vibratoria del sistema propulsor

José R. Marín ¹
Carlos A. Cuenca ²

Abstract

This work analyzed the structural fatigue of a high-speed craft, which has a propeller system formed by two 493-hp engines connected through speed multipliers to water jet systems. Its aluminum alloy structure has combined-type framing. The useful life of the boat bottom's structure was determined considering the cyclical loads generated by the propulsion system, using the Finite Elements method and applying the effort-number method of cycles to failure. For this, a structural model was developed of the selected zone, which was analyzed with the SAP2000 program, to obtain complex amplitudes of the stress supported by the structure. Thereafter, with these results the stress range was determined and, then, using S-N curves for Aluminum the number of cycles that needed to be carried out by six structural details selected was determined, for its failure. Using Miner's Rule, combined with the craft's assumed work modes, the time of the useful life time of the referential details selected during an hour was determined. Finally, if the craft operates for three hours per day, the bottom structure of the boat analyzed would have a useful life of 14.5 years, when working principally in low speed rating.

Key words: planing craft, fatigue.

Resumen

En este trabajo se analiza la fatiga de la estructura de una lancha rápida, que tiene un sistema propulsor formado por dos motores de 493 hp cada uno, conectados mediante multiplicadores de velocidad a sistemas de chorro de agua. Su estructura de aleación de aluminio tiene cuaternaje de tipo combinado. Se determinó la vida útil de la estructura del fondo de la embarcación, considerando las cargas cíclicas generadas por el sistema de propulsión, utilizando el método de Elementos Finitos y aplicando el método Esfuerzo-Número de ciclos para la falla. Para ello se desarrolló un modelo estructural de la zona seleccionada, el cual es analizado con el programa SAP2000 para obtener las amplitudes complejas de los esfuerzos que soporta la estructura. Luego, con estos resultados se determina el rango de esfuerzos, y posteriormente, usando curvas S-N para aluminio, se determina el número de ciclos que deben desarrollar seis detalles estructurales seleccionados, para su falla. Después, utilizando la regla de Miner, en combinación con modos de trabajo asumidos de la embarcación, se determinó el tiempo de vida útil de los detalles referenciales seleccionados en una hora. Finalmente, si la embarcación operara 3 horas por día, la estructura del fondo de la lancha analizada tendría una vida útil de 14.5 años, cuando trabaja principalmente en régimen de velocidad baja.

Palabras claves: lancha planeadora, fatiga.

Date Received: July 8th, 2014 - *Fecha de recepción:* 8 de julio de 2014

Date Accepted: August 24th, 2014 - *Fecha de aceptación:* 24 de agosto de 2014

¹ ESPOL. 1Facultad de Ingeniería Marítima, Ciencias Biológicas, Oceánicas y RR.NN. Guayaquil, Ecuador. e-mail: jmarin@espol.edu.ec

² SLEM S.A. Guayaquil, Ecuador. e-mail: ccuenca@espol.edu.ec

Introduction

The vibratory forces generated by a ship's propulsion system can cause a reduction of the resistance of the structural material, a phenomenon known as fatigue (Bannantine, 1990). After a high number of cycles, even with low stress level, cracks that disable the structure may be formed. For planing crafts, given the high power installed, the level of the vibratory excitation forces is quite high and the fatigue produced must be analyzed. This effect is magnified by the presence of stress hot points and weld joints, typical of ship structures. All this may lead to an accelerated process of the appearance of fissures after a given number of cycles.

Due to the prior explanation, emphasis must be made on analyzing the phenomenon of fatigue in high-power crafts to determine the number of cycles after which the formation of cracks on the structure may be expected. For this, classifying societies have processes to determine the useful life time of ship structures, applying the Stress-Useful life method. These societies consider the stress range applied to structural details, along with Miner's linear damage rule, see ABS (2011) and DNV (2011).

This work sought to analyze the influence of fatigue on the bottom structure of a planing craft subjected to the vibratory action generated by the torque of the main engines and by the thrust generated by the propeller (Cuenca, 2014). Unfortunately, the literature available locally has few references with details on this type of calculation. Thereby, it is expected that these results provide an additional point of reference to compare the classical requirement, creep failure, to this other failure mode, due to fatigue, in case of small, high-speed crafts.

Structural modeling of the boat bottom

Structural model

The craft analyzed has a length of 11 m and was designed to reach a speed of 32 knots, ASTINAVE (2011). It is completely constructed

in 5086 aluminum alloy and has a structure with combined-type framing, with 'L'-type longitudinals with 48-cm separations and 'L' type with 75-cm separation. The thickness on the bottom is of 4.76 mm. For its propulsion, it has two 493-hp diesel engines and these, through speed multipliers are joined to water jet systems, which work at 3000 rpm, Hamilton (2007).

Table 1. Main characteristics of the planing craft.

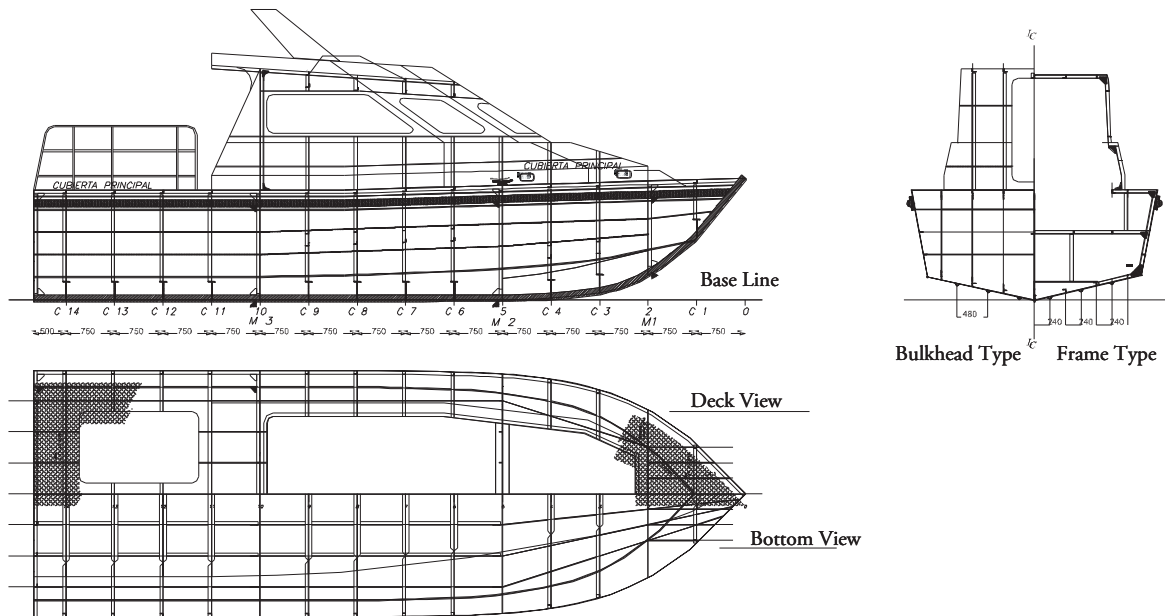
Total length	11.0 m
Maximum breadth	3.80 m
Depth	1.70 m
Draft at maximum load	0.74 m
Maximum displacement	14.9 tons
Design speed	32.0 knots

Fig. 1 presents a structural plan of the craft analyzed, ASTINAVE (2011).

To reduce the size of the structural model to be developed, a segment was taken from the bottom of the structure corresponding to the engine room, from one side; this is the region where the vibratory sources of interest are found for this analysis. The model represents the primary and secondary structural elements, including the perforations on the shell plating for suction and discharge of the water used to propel the craft. The region of the structure analyzed is 3.5 m long, and its width is equal to the semi-breadth to the chine, corresponding to a distance of 1.9 m. The transom was included to analyze the vibratory stress transmitted by the duct of the propeller system. It has been considered that the presence of the keel would help the vibration generated by a propeller system to be manifested only on said side of the structure.

The geometric model is shown in the appendix and served to generate the structural model with MEF, the x axis points in the direction toward the bow, y points toward port, and z points up. In said model, flat areas are defined to then model the shell plating of the bottom and transom, and the reinforcement cores; lines are also defined that will serve to generate, in simplified manner, reinforcement flanges.

Fig. 1. Structure of the craft analyzed, ASTINAVE (2011).



The geometric model is imported from the SAP2000 commercial package, where the structural characteristics of the sections and of the material are added ($E=7.1E10$ N/m², $\nu=0.33$), taken from the web site: asm.matweb. Finally, simple support boundary conditions are imposed on the model edges. On the centerline plane, upon restricting the rotation in axial direction, high levels of stress were produced, which appeared incorrect, which is why it was decided to impose simple support conditions in said nodes. By restricting the lateral translation (y Global) of various nodes located vertically, a restriction is represented of the rotation in x direction. The characteristics of the structural elements are presented in Table 2.

To represent the inertia of the engine propeller mass, solid elements covering the volume of said equipment are included, and with adequate density to recover its original mass. Besides, to represent the duct of the water jet system, steel beam elements were included, joining the nodes around the perforations of the bottom with those of the transom perforation. Thus, bottom and transom vibrate in phase, as a result of the high rigidity of the propeller duct.

Table 2. Scantlings of the structure, mm.

Location	Element	Section	Dimensions
Bottom	Shell plating	-----	4.76
	Frame	Alma	4.76
		Ala	50.8 x 4.76
	Principal Long. stiffener	Alma	6.36
		Ala	127.0 x 12.7
Sec. Transverse stiffener	Ele	50.8 x 50.8 x 6.36	
Transom	Shell plating	-----	4.76
	Transverse stiffener	Platina	50.8 x 6.36
	Long. stiffener	Platina	50.8 x 6.36
	Long. stiffener	Ele	50.8 x 50.8 x 6.36
Joint	Lodging knee	-----	4.76

Fig. 3 shows an image of the bottom and the corresponding structural model, as a way of proving their similarity.

Added Mass

The bottom of the boat analyzed, when submerged in water, supports the hydrodynamic effect, denominated added mass, generated by the interaction between the bottom's vibrating

Fig 2. Structural model used.

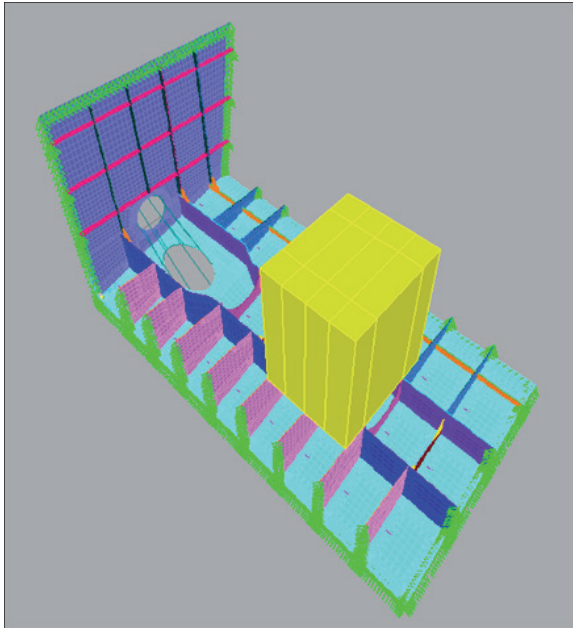


Fig 3. Real structure and detail of the model.

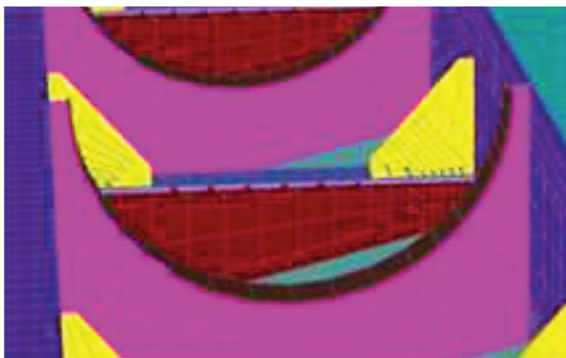


plate and the fluid in which it is immersed. The following formula taken from Korotkin (2009)

was used to estimate the added mass per unit of area:

$$m = \mu \left(\frac{l}{nb} \right) \frac{l}{n} (\rho + \rho_1) \quad (1)$$

where μ is a parameter that depends on the plate's aspect ratio, which has dimensions $l \times b$, n is the number of half waves formed by the plate when oscillating, and ρ and ρ_1 are the densities of the fluids at each side of the plate.

By applying formula (1), the added mass per unit of area is 140 kg/m^2 , considering vibration with a half wave and the interior fluid's density as null. By dividing this value for the bottom's thickness, an "added density" will result that will be added to that of the structural material. The resulting value, 32103 kg/m^3 is the density included as data for the bottom's plates. This value is quite high and deserves future corroboration.

Typically, for the present analysis was assumed 2% structural dampening, which results from applying the model, available in the structural analysis program used.

Analysis of vibratory stress

Vibratory load to apply

The engine room of the craft analyzed has the engine propellers seated on the primary longitudinal reinforcements; also, on said structural elements are the water jet systems, which are attached to the craft's bottom and transom. These two will be the vibration sources acting directly on the boat's structure. The resulting alternative stresses will affect the useful life of the craft's structure.

This work considered the load due to the sixth harmonic of the torque generated by the cylinders, given that they are in phase among each other; the frequency of this harmonic is $3 \cdot \text{rpm}$, given that it is a four-stroke engine. It is also considered that the water jet produces a load due to the variation the thrust has with the ratio frequency

Table 3. Characteristics of the propeller system.

Engine power (2)	493
Type of engine	4T
Number of cylinders	6L
Diameter x Stroke	11.4 x 13.5 cm
Reduction ratio	0.923:1
Number of pump blades	3

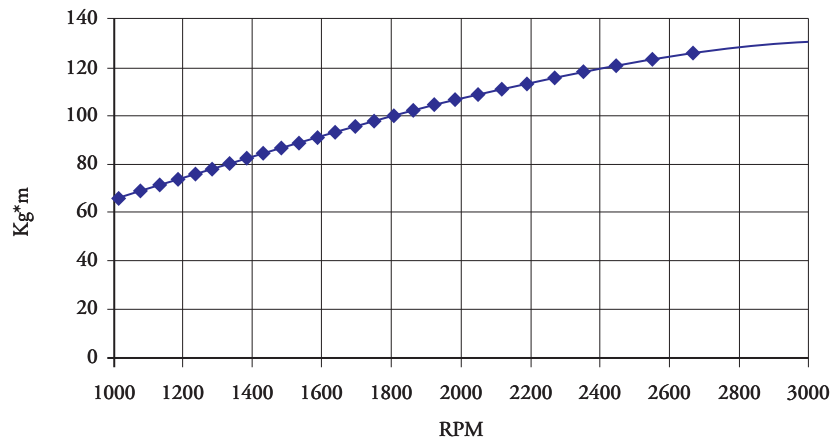
of the blades (rotation frequency by the number of blades).

To estimate the amplitude of the oscillating torque, the tangential stress was taken for different values of

indicated medium pressure, using the graphics by Moreno (1980). From the effective medium pressure, 85% mechanical efficiency is assumed, to estimate pmi, and assuming quadratic variation with rpm, the tangential stress is calculated for the engine's different rotation rates. The tangential stress multiplied by the area and by the piston stroke produces the vibratory torque. Fig. 4 shows the amplitude of the sixth harmonic of the torque in function of the rotation rate, considering that the harmonics of each cylinder are in phase with each other.

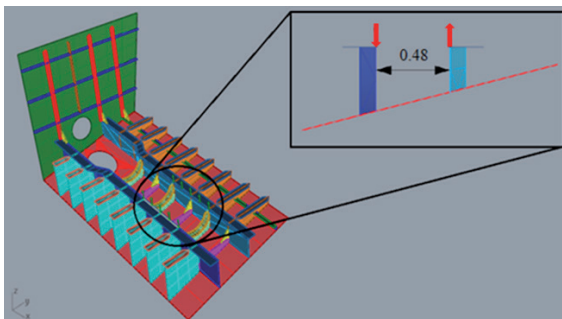
To apply the vibratory moment over the structure, it is considered that the engine is seated on the primary

Fig. 4. Variation of the sixth harmonic amplitude of the engine torque.



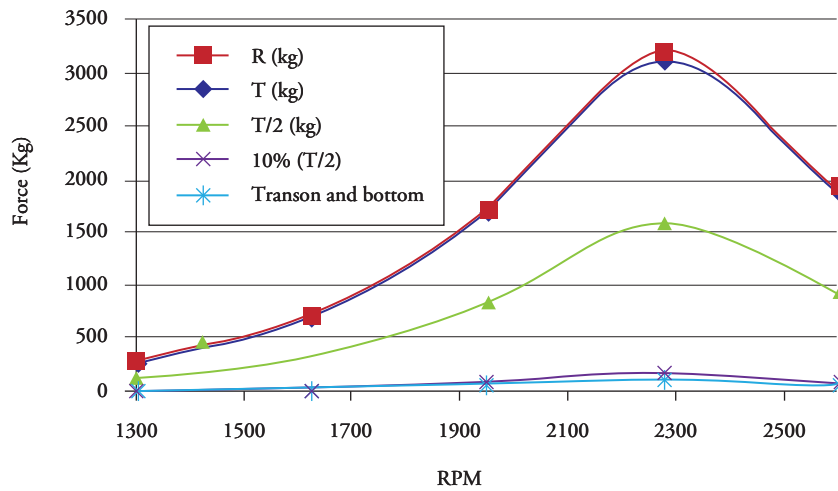
longitudinal reinforcements, which are separated by 0.48 m. An equivalent force is then applied to the ratio of the torque amplitude and the separation between reinforcements, with 180° offset. This force is distributed uniformly among the five nodes where said forces are applied, as shown in Fig. 5.

Fig. 5. Application of the vibratory torque.



For alternative thrust, it was assumed an amplitude equal to 10% of the mean value developed by each driver, a typical value in the case of open propellers, according to the figures published in Long (1992). This value is considered representative for the case of conventional propellers. The average thrust for different rotation rates is estimated from strength calculations by applying the classic Savitsky method for planing boats, Marín *et al* (2011); a value of -0.02 is used of the deduction of thrust, t . Given that the system has two propellers, this amplitude was divided by two and, then, by the number of nodes of the connection of the duct with the craft's bottom and transom. The frequency of this excitation corresponds to what is known as the axis blade:rpm ratio for the number of blades of the propeller.

Fig. 6. Assumed vibratory thrust.



Originally, the plan was to also include as excitation the water pump impeller imbalance. However, according to Long (1992), said load may be in the order of 1% of the propeller’s weight, which results in a low value compared to the other two excitations, and due to this it was discarded.

Selection of structural details to analyze in fatigue

By applying the two excitations to each of their corresponding frequency, then the zones of maximum alternative stress were identified to estimate the operation time necessary for the appearance of cracks due to fatigue. Fig. 7 shows a typical amplitude distribution of normal stress through excitation of the engine’s vibratory torque at a rotation rate of 2600 rpm; in the case shown, the amplitudes of the excitation forces acting on each node are taken as 1 kg and then they are corrected linearly according to the real amplitude of excitation. A similar process was carried out for the excitation due to the vibratory thrust generated by the propeller systems.

Upon obtaining the results of the normal stress distributions and observing where the maximum values are six structural details were selected for fatigue analysis:

- The plate from the bottom between the longitudinal reinforcements, under the engine.

- The main longitudinal reinforcement near the joint between the bottom and the transom.
- The shell plating from the bottom under the side main reinforcement, in the union with discontinuity in direction toward the stern.
- The bottom’s shell plating under the main reinforcement toward the keel, in the joint with the discontinuity in direction toward the stern;
- The shell plating above the duct’s clamping perforation edge on the transom.
- The bottom’s shell plating under the main reinforcement toward the keel, close to the stern.

Table 4 (see pag. 64) presents the different maximum stress zones, when they appear as vibratory torque excitation and the oscillatory thrust.

Calculation of stress in the hot points

In the bottom of the boat analyzed, a structural analysis was performed by applying cyclical loads generated by engine torque and propeller thrust. From these results, it was determined that the highest stress is produced for the cyclic load due to engine torque, in “detail 1”, at a frequency of 107.5

Fig. 7. Typical distribution of normal stress in x direction (Bow-Stern).

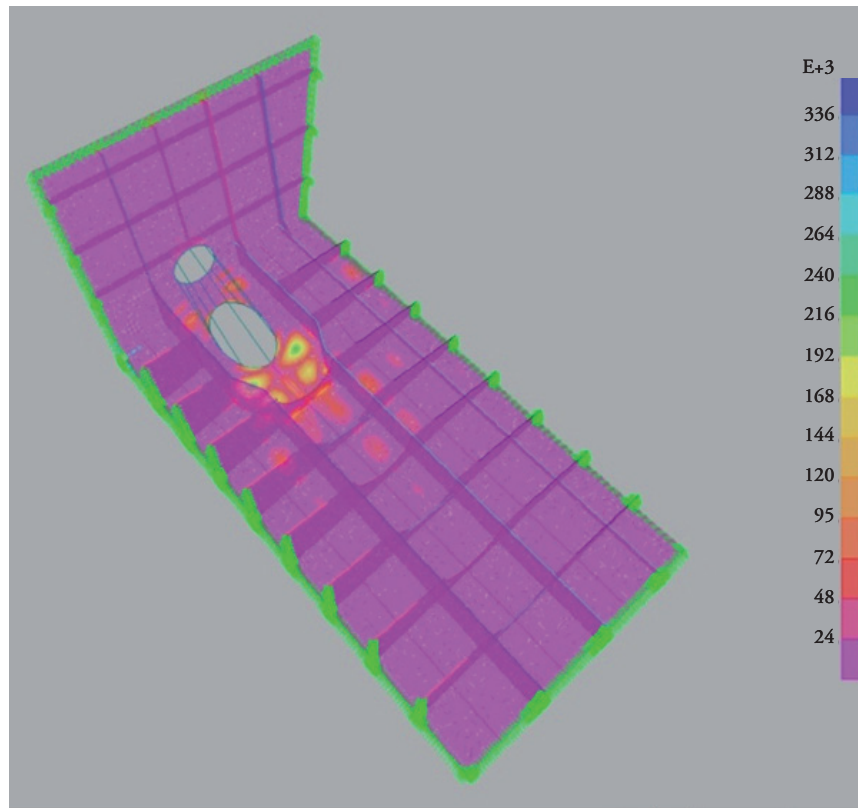


Fig. 8. Location of the details selected.

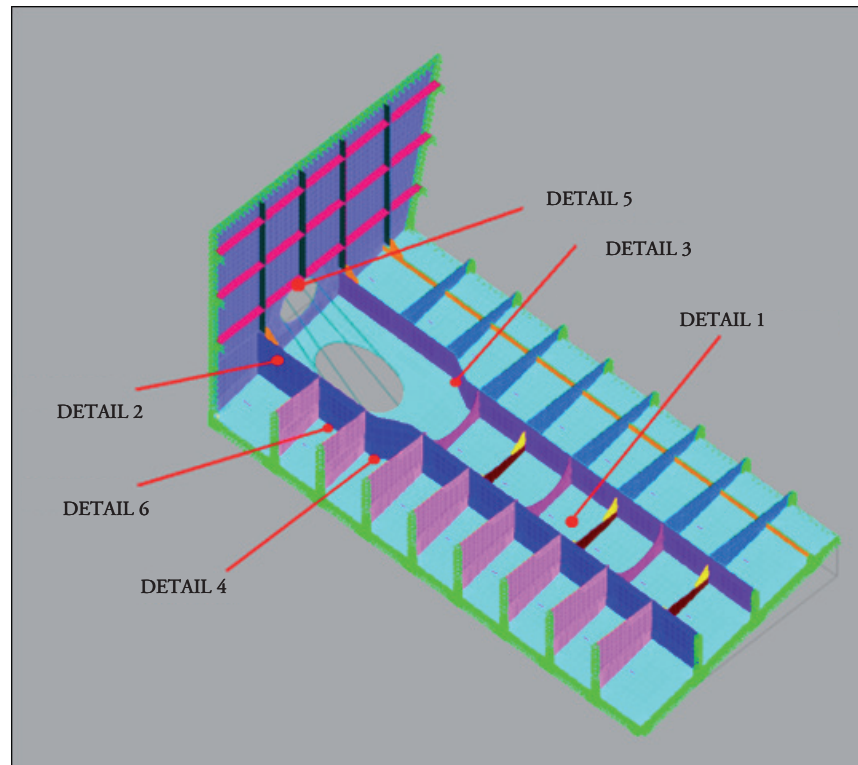
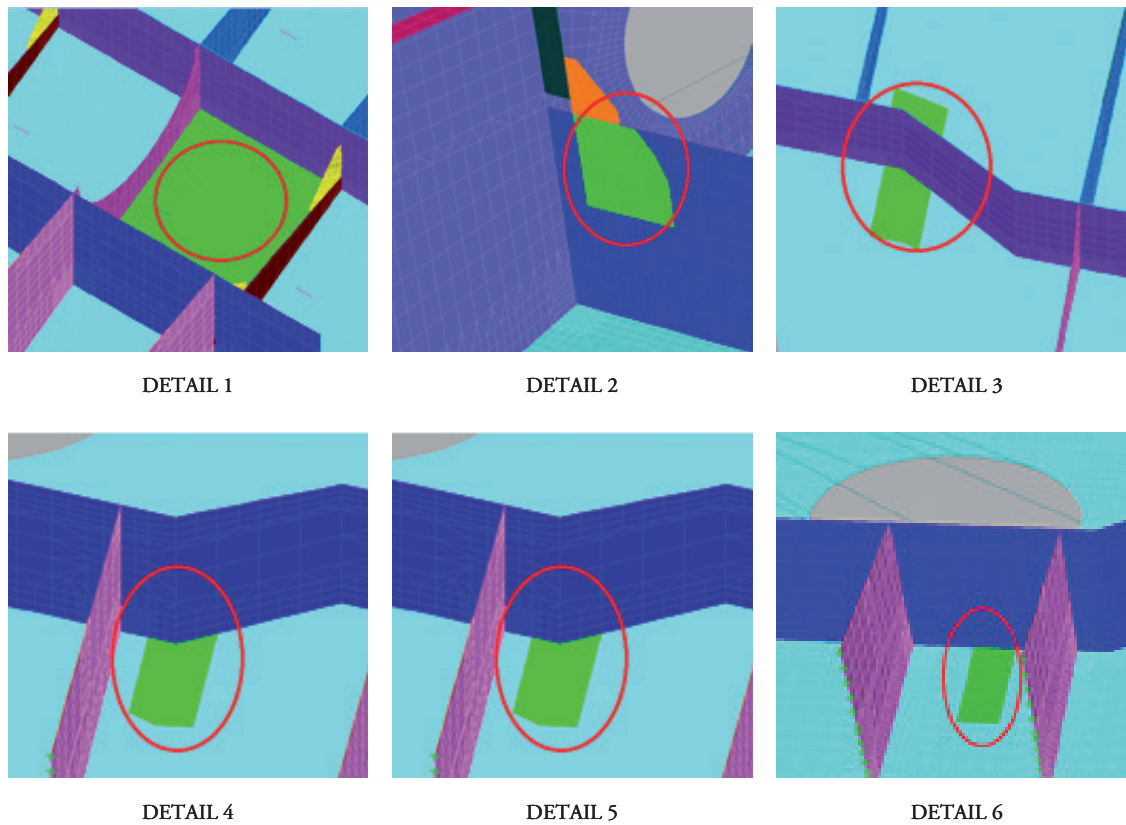


Table 4. Zones of maximum normal stress through the engine's vibratory torque (nodal load of 1 Kg).

Item	N_motor RPM	F_excitation CPS	Load caused by engine torque			Zone
			Node	Direction	Pressure (Kg/cm ²)	
1	2000	100.0	6440	S11	6.34E-2	Plate on the posterior zone near to principal stiffener of broadside
2			6440	S22	4.46E-2	Plate on the posterior zone near to principal stiffener of broadside
3	2150	107.5	6440	S11	8.07E2	Plate on the posterior zone near to principal stiffener of broadside
4			122-16	S22	4.30E-2	Bottom plate between principal stiffeners under engine
5	2300	115.0	122-16	S11	5.80E-2	Bottom plate between principal stiffeners under engine
6			122-16	S22	-1.90E-1	Bottom plate between principal stiffeners under engine
7	2450	122.5	13738	S11	3.15E-1	Bottom plate between longitudinal principal stiffener of broadside and longitudinal secondary stiffener
8			13738	S22	3.12E-1	Bottom plate between longitudinal principal stiffener of broadside and longitudinal secondary stiffener
9	2600	130.0	122-16	S11	-8.47E-1	Bottom plate between principal stiffeners under engine
10			122-16	S22	2.80E-1	Bottom plate between principal stiffeners under engine

Fig. 9. Details analyzed.



CPS with a value of 47 Kg/cm². Additionally, it was obtained that, in general, the load due to thrust generates minor stress compared to those obtained due to the load from the engine's cyclical torque.

Thereafter, the so-called hot-spot stress (HSS) was calculated for the details analyzed, depending

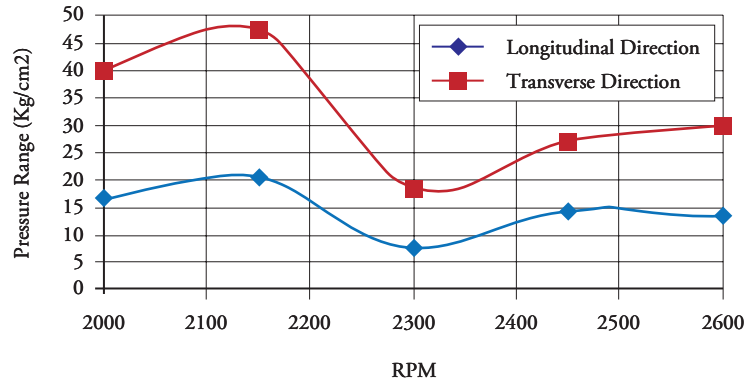
on the type of axial or bending load, following the process explained in DNV (2011). Table 5 summarizes the stress range (2*amplitude), for the different details, for both excitations, considering that the craft's engines operate at different rotation rates.

Table 5. Summary of the stress range in each detail analyzed.

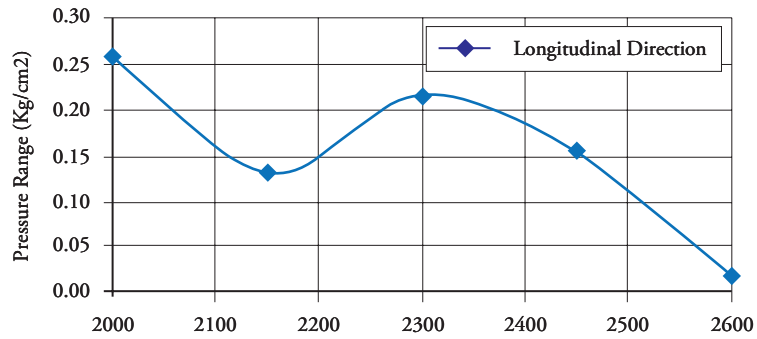
	Cyclic load of engine torque				Cyclic load of propeller thrust		
	N_motor RPM	f_ excitation CPS	Longitudinal direction Range Pressure (Kg/cm ²)	Transverse direction Range Pressure (Kg/cm ²)	f_ excitation CPS	Longitudinal direction Range Pressure (Kg/cm ²)	Longitudinal direction Range Pressure (Kg/cm ²)
DETAIL 1	2000	100.00	16.75	39.92	108.34	0.70	0.80
	2150	107.50	20.26	47.46	116.47	0.88	3.02
	2300	115.00	7.87	18.59	124.60	1.18	1.53
	2450	122.50	14.54	26.99	132.73	0.95	3.89
	2600	130.00	13.45	30.00	140.86	5.79	14.98
DETAIL 2	2000	137.50	0.26	-----	108.34	0.21	-----
	2150	145.00	0.13	-----	116.47	0.07	-----
	2300	152.50	0.22	-----	124.60	0.05	-----
	2450	160.00	0.15	-----	132.73	0.08	-----
	2600	167.50	0.02	-----	140.86	0.11	-----
DETAIL 3	2000	100.00	1.00	10.99	108.34	1.18	0.59
	2150	107.50	1.75	10.60	116.47	3.21	4.32
	2300	115.00	0.81	3.46	124.60	2.43	2.83
	2450	122.50	2.09	5.42	132.73	1.57	0.99
	2600	130.00	0.69	0.92	140.86	2.99	4.29
DETAIL 4	2000	137.50	1.21	2.22	108.34	0.87	1.17
	2150	145.00	1.21	2.48	116.47	1.28	1.71
	2300	152.50	0.33	0.89	124.60	1.50	2.91
	2450	160.00	0.18	1.11	132.73	1.03	2.91
	2600	167.50	0.16	0.12	140.86	1.13	0.96
DETAIL 5	2000	100.00	11.47	3.98	108.34	23.72	8.02
	2150	107.50	37.51	13.13	116.47	5.76	1.78
	2300	115.00	6.25	2.09	124.60	4.42	1.38
	2450	122.50	1.69	0.53	132.73	3.43	1.05
	2600	130.00	0.46	0.16	140.86	4.17	1.27
DETAIL 6	2000	100.00	0.85	1.45	108.34	0.47	1.28
	2150	107.50	0.87	1.97	116.47	0.66	1.66
	2300	115.00	0.28	0.79	124.60	0.76	3.90
	2450	122.50	0.99	1.61	132.73	0.63	3.90
	2600	130.00	0.46	0.65	140.86	0.70	1.49

Fig. 10. Stress range due to engine's cyclical torque.

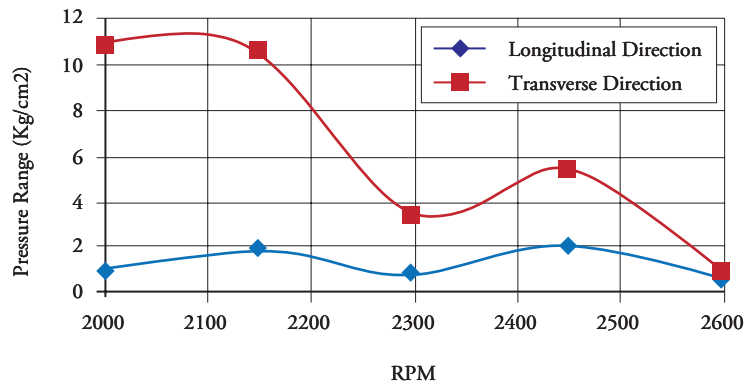
Pressure Range
D1 vs RPM.



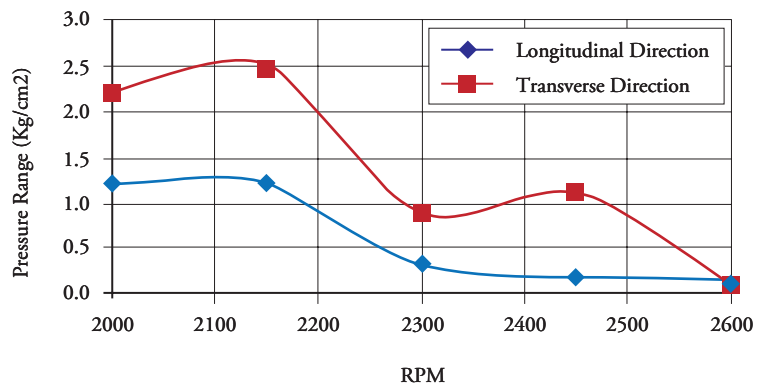
Pressure Range
D2 vs RPM.



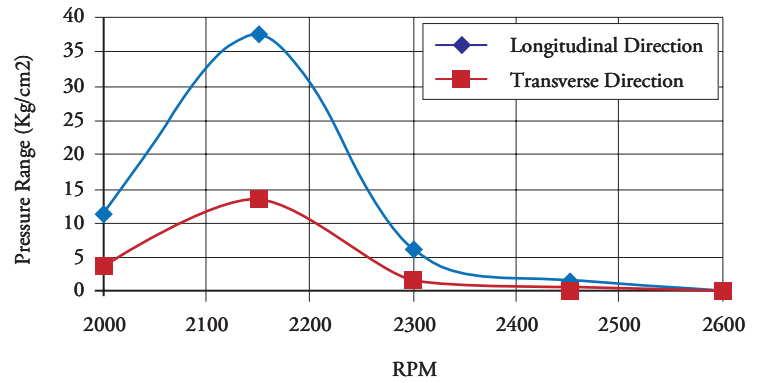
Pressure Range
D3 vs RPM.



Pressure Range
D4 vs RPM.



Pressure Range D5 vs RPM.



Pressure Range D6 vs RPM.

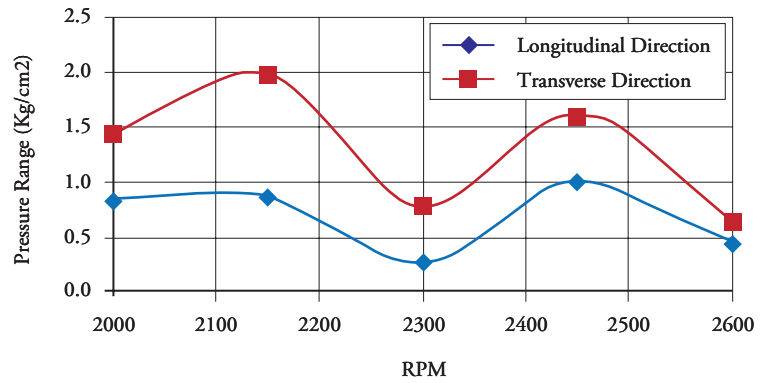
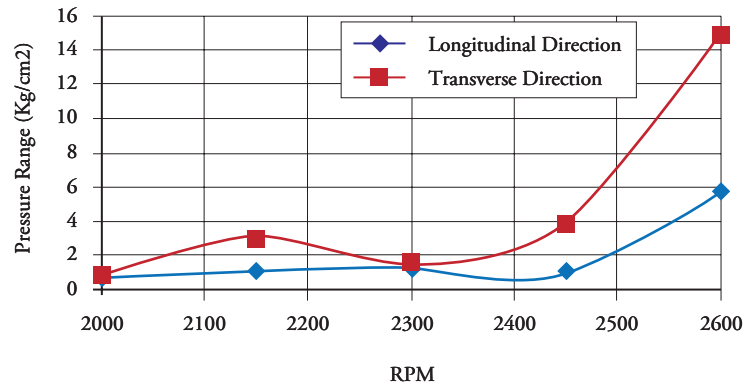
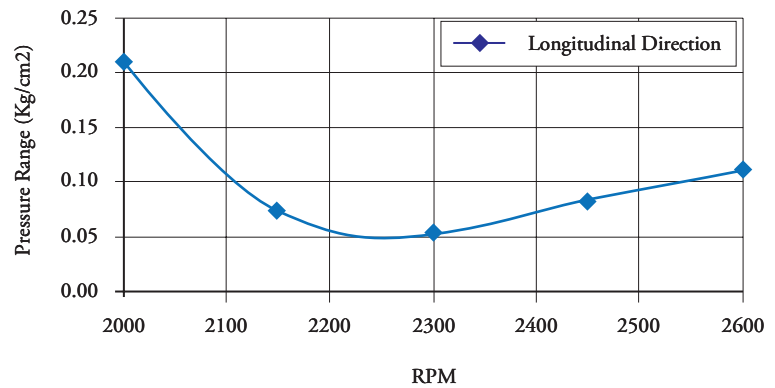


Fig. 11. Stress range due to cyclical propeller thrust.

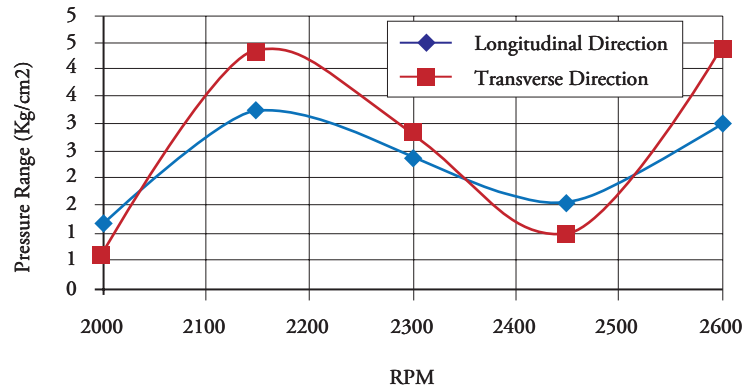
Pressure Range D1 vs RPM.



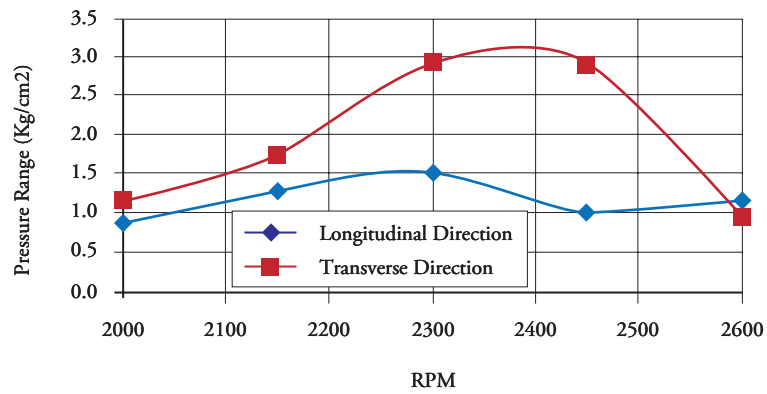
Pressure Range D2 vs RPM.



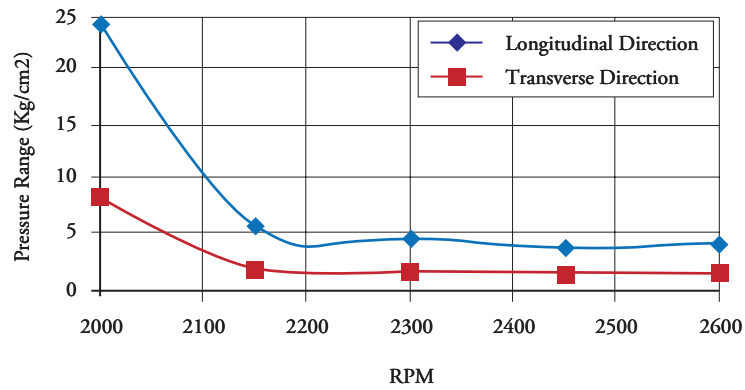
Pressure Range D3 vs RPM.



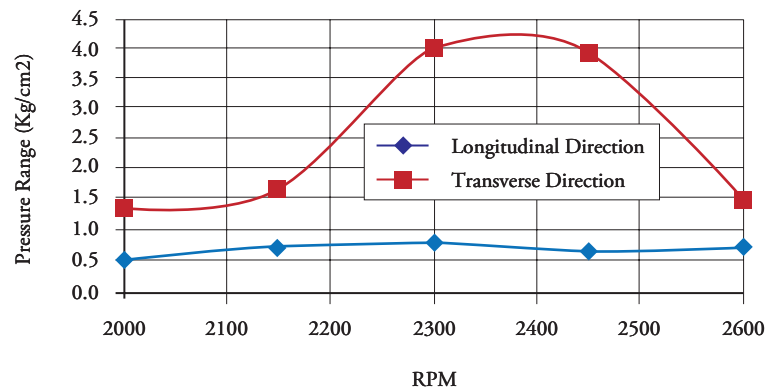
Pressure Range D4 vs RPM.



Pressure Range D5 vs RPM.



Pressure Range D6 vs RPM.

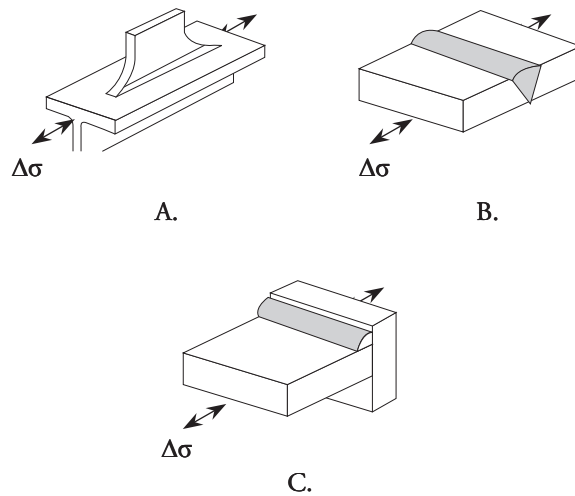


Note that in spite of increasing the rotation rate the excitation amplitudes grow; the responses do not follow that pattern. This is probably due to the presence of local resonant situations.

Calculation of the useful life of the boat's bottom

For the fatigue analysis of the structure from the bottom of the boat analyzed, Stress-Life and S-N curves were used for the 5086 aluminum alloy published in the Eurocode (2011). The S-N curves used depend on the type of detail (plate and welded joint), and on the flexural and axial type load to which they are subjected:

Fig 12. Types of details to select S-N curves, Eurocode, (2011).



Figs. 13 show the evaluations of the number of cycles for the failure, N_f , according to the type of load for each detail. In this study, given the influence of the structure's operating environment, the second region of the S-N curve is prolonged without limit, that is, a stress limit due to fatigue is not recognized.

With the frequency of each excitation, the number of cycles developed in one hour were estimated, n_i . Then, with the values of the number of cycles for the failure, N_f , previously determined, the

contribution of the damage in each detail was estimated with the following relation:

$$D_i = \frac{n_i}{N_i} \quad (2)$$

Thereafter, by applying Miner's rule of cumulative linear damage, Bannantine (1990), the useful life time consumed was determined for each referential detail analyzed. Given that both vibration sources act simultaneously, their life reduction is added:

$$D_c = \left(\sum_{i=1}^5 \frac{n_i}{N_i} \right)_{\text{Cyclical Torque}} + \left(\sum_{i=1}^5 \frac{n_i}{N_i} \right)_{\text{Cyclical Thrust}} \quad (3)$$

where i denotes the speed rating considered.

The damage percentage according to equation (3) was calculated for different rpm of the main engine, but the craft does not operate a single speed. Then, due to the lack of information on how to use the propeller installations, three ways to operate the boat were established:

- Navigation principally at low speed,
- Navigation principally at high speed, and
- Uniform navigation at several speeds.

Accumulated damage per hour corresponds to the previous sum, equation (2), but multiplied by the percentage of use, according to the work mode. The inverse of this parameter would correspond to the number of hours of operation it would take to reach failure in each detail; the results are shown in Table 6 (See Pag. 73).

The referential element reduced in greatest percentage in its useful life is detail 1, for work mode 1. Finally, the number of years it would take each structural detail to reach its failure will be estimated.

Useful life of the boat's bottom

The useful life of the bottom of the boat is analyzed, using the values of total hours until failure for each structural detail calculated for which the boat's hours of work per year were assumed.

Fig. 13a. Stress-Life range curves ($\Delta\sigma$ vs N). Detail 1: Cyclic load of engine torque.

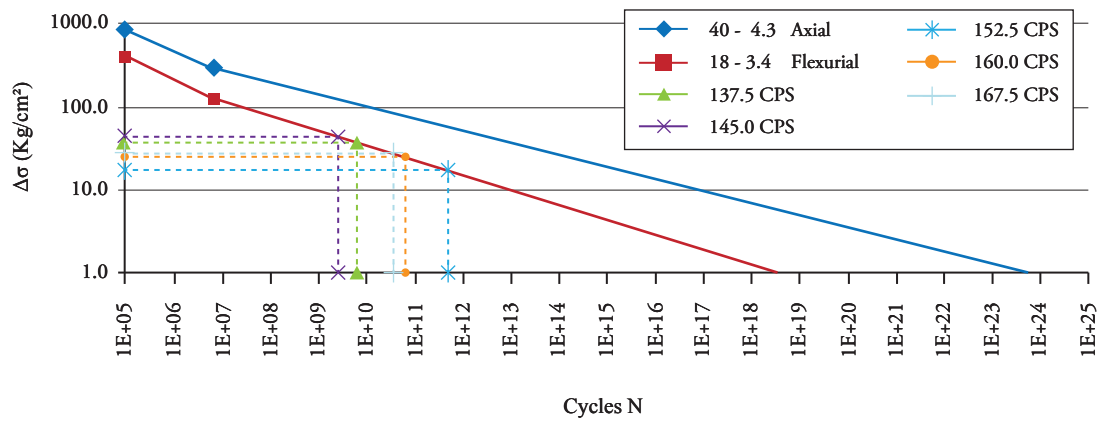


Fig. 13b. Stress-Life range curves ($\Delta\sigma$ vs N). Detail 1: Cyclic load of engine torque.

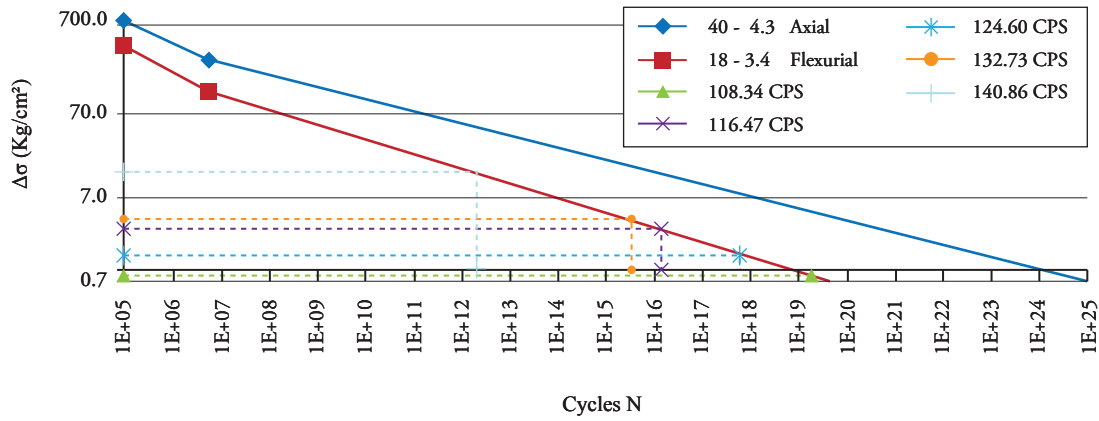


Fig. 13c. Stress-Life range curves ($\Delta\sigma$ vs N). Detail 2: Cyclic load of engine torque.

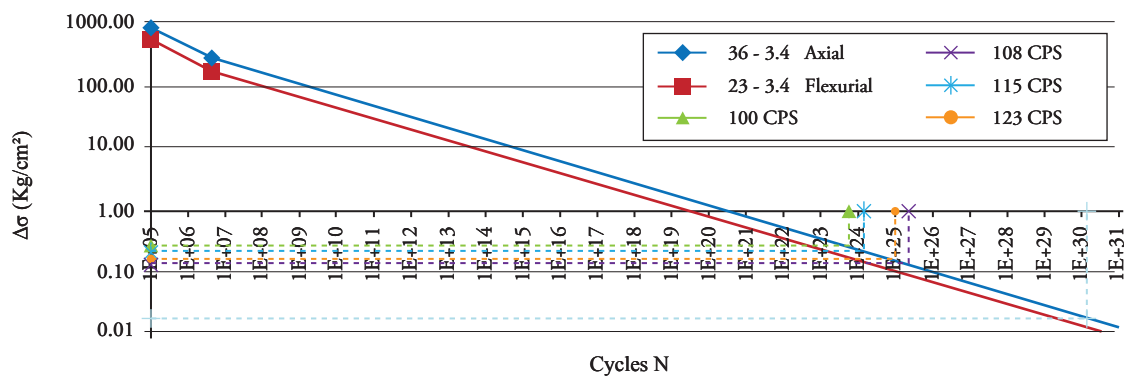


Fig. 13d. Stress-Life range curves ($\Delta\sigma$ vs N). Detail 2: Cyclic load of thrust.

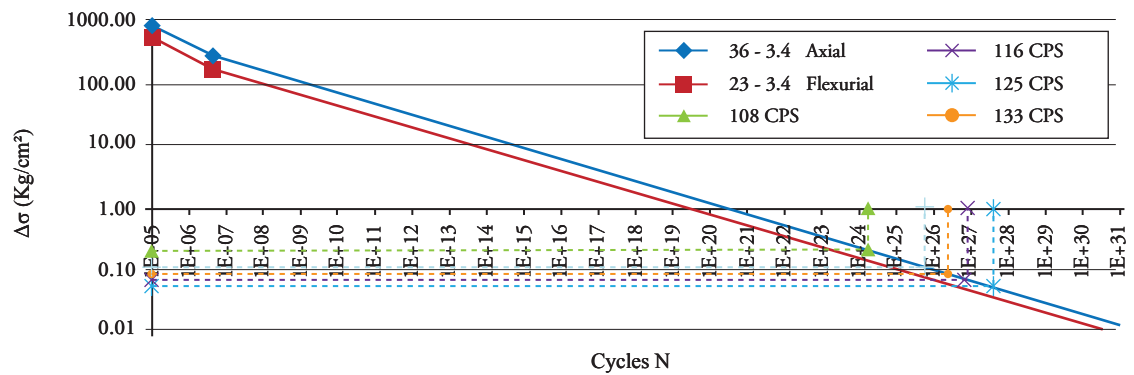


Fig. 13e. Stress-Life range curves ($\Delta\sigma$ vs N). Detail 3: Cyclic load of engine torque.

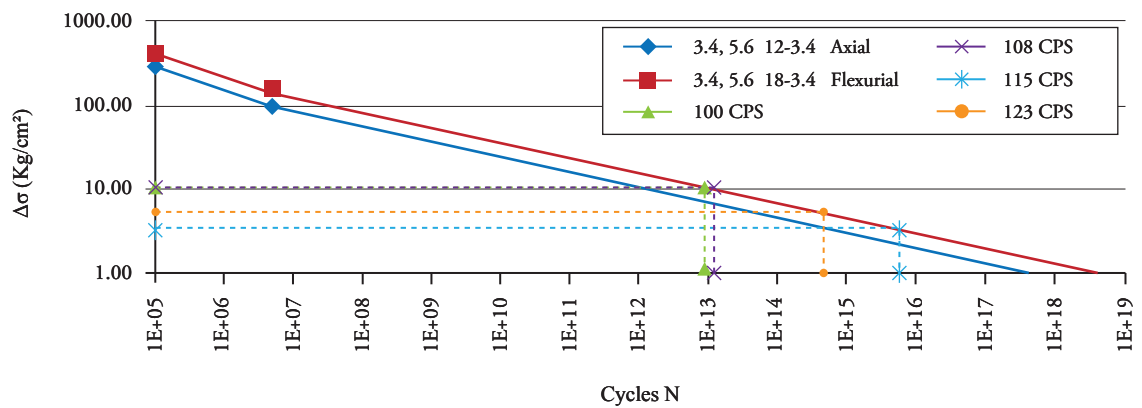


Fig. 13f. Stress-Life range curves ($\Delta\sigma$ vs N). Detail 3: Cyclic load of thrust.

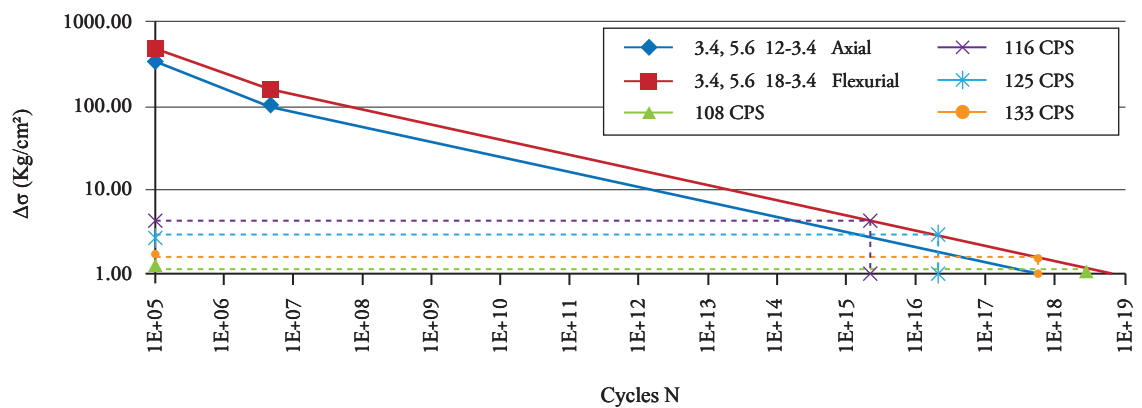


Fig. 13g. Stress-Life range curves ($\Delta\sigma$ vs N). Detail 4: Cyclic load of engine torque.

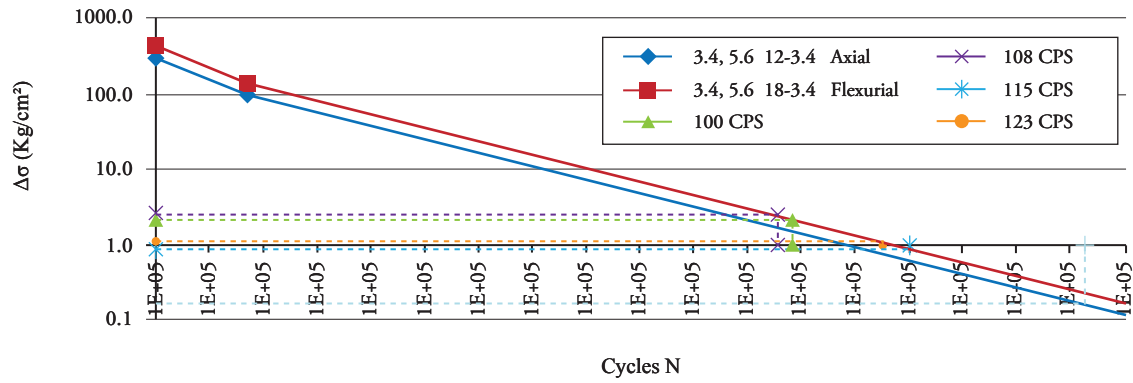


Fig. 13h. Stress-Life range curves ($\Delta\sigma$ vs N). Detail 4: Cyclic load of thrust.

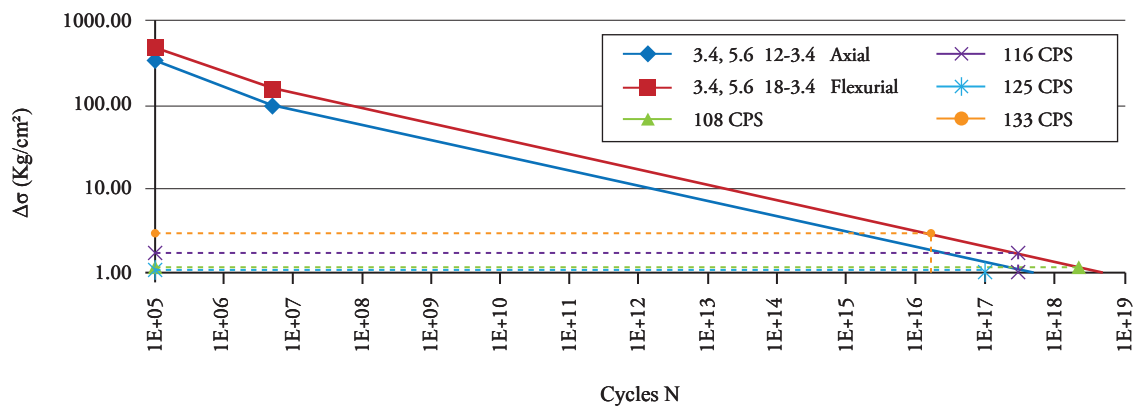


Fig. 14. Work modes assumed.

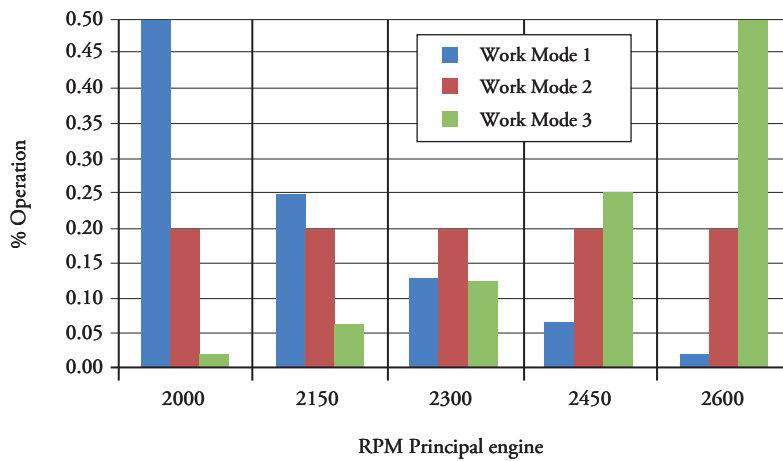


Table 6. Accumulated damage per hour.

	Work Mode 1	Work Mode 2	Work Mode 3
	(Hours)	(Hours)	(Hours)
DETAIL 1	1.59E+04	5.04E+04	2.39E+04
DETAIL 2	2.19E+18	1.29E+19	4.27E+18
DETAIL 3	3.54E+07	2.55E+08	6.83E+07
DETAIL 4	8.29E+10	7.04E+10	6.23E+10
DETAIL 5	8.59E+04	3.68E+05	1.23E+05
DETAIL 6	3.08E+10	1.56E+10	1.57E+10

Three cases were taken for this analysis: the boat navigating for three, four, and five hours

per day, during the whole year. These represent 1095, 1460, and 1825 hours of operation in one year. Upon conducting this analysis, it was obtained that the boat’s bottom has a useful life restricted by “detail 1”, which corresponds to the bottom’s shell plating, located between the main reinforcements under the main engine, which has a useful life time of 5.4 years, navigating a fourth part of the day, in work mode 1. The inverse of the accumulated damage per hour will correspond to the number of hours to reach failure through fatigue of each structural detail.

Table 7. Useful life of each detail.

		DETAIL 1	DETAIL 2	DETAIL 3	DETAIL 4	DETAIL 5	DETAIL 6
Work Mode 1	[(3 h/Day)]	14.5	2.0E+15	3.2E+04	7.6E+07	78.4	2.81E+07
	[(4 h/Day)]	10.9	1.5E+15	2.4E+04	5.7E+07	58.8	2.11E+07
	[(5 h/Day)]	8.7	1.2E+15	1.9E+04	4.5E+07	47.1	1.69E+07
Work Mode 2	[(3 h/Day)]	46.0	1.2E+15	2.3E+05	6.4E+07	335.8	1.42E+07
	[(4 h/Day)]	34.5	8.9E+15	1.7E+05	4.8E+07	251.8	1.07E+07
	[(5 h/Day)]	27.6	7.1E+15	1.4E+05	3.9E+07	201.5	8.55E+06
Work Mode 3	[(3 h/Day)]	21.8	3.9E+15	6.2E+04	5.7E+07	112.6	1.43E+07
	[(4 h/Day)]	16.4	2.9E+15	4.7E+04	4.3E+07	84.4	1.07E+07
	[(5 h/Day)]	13.1	2.3E+15	3.7E+04	3.4E+07	67.5	8.59E+06

The detail that would most rapidly reach failure would be number 1, in work mode 1, that is, operating a longer time at low speed. If the craft operated continuously three hours per day, the failure of detail 1 would occur in 14.5 years.

Conclusions

This project determined the useful life of the structural bottom of a planing patrol boat, using the method of Range of Stress-Number of Cycles for the failure, which includes an estimation of stresses, developed through a structural analysis using finite elements. The model analyzed included the structural details found in the zone selected, and the cyclical loads due to the propeller system (engine torque and thrust), and according to that obtained the following is concluded:

It is considered that the structural model developed is suitable, given that it includes all the details with the characteristics shown in the structural plans provided by the manufacturing shipyard. In addition, the aspect ratio of the plate elements used in the discretization is below 3.0, and the element of greater dimension used in the whole numerical model is of 47 x 41 mm. The acting loads were methodically estimated and have been applied in realistic manner in the numerical model.

The stress distributions obtained are acceptable, given their normally continuous behavior in the referential details selected, for both types of loads analyzed in the different excitation frequencies applied.

Miner’s rule of linear accumulated damage was used to determine the number of hours it would

take the structural details to fail. With this, it was determined that the boat has a lower useful life for a work mode in which it navigates most of the time at low speeds. Finally, it was determined that detail 1 of the craft analyzed will have a useful life time of 14.5 years navigating three hours per day continuously.

Recommendations

The evaluation of the added mass in the bottom panels produced very high values, leading to recommend experimental works to test said results.

The vibration analyzed is developed at high frequencies, possibly with high local effects; therefore, to confirm the numerical results, it is recommended to measure the vibratory response of the boat's bottom structure during navigation, or it would be convenient to conduct experiments with models and excitation of the type herein considered.

Finally, it is recommended to also determine real spectra of work modes for these types of crafts.

Acknowledgments

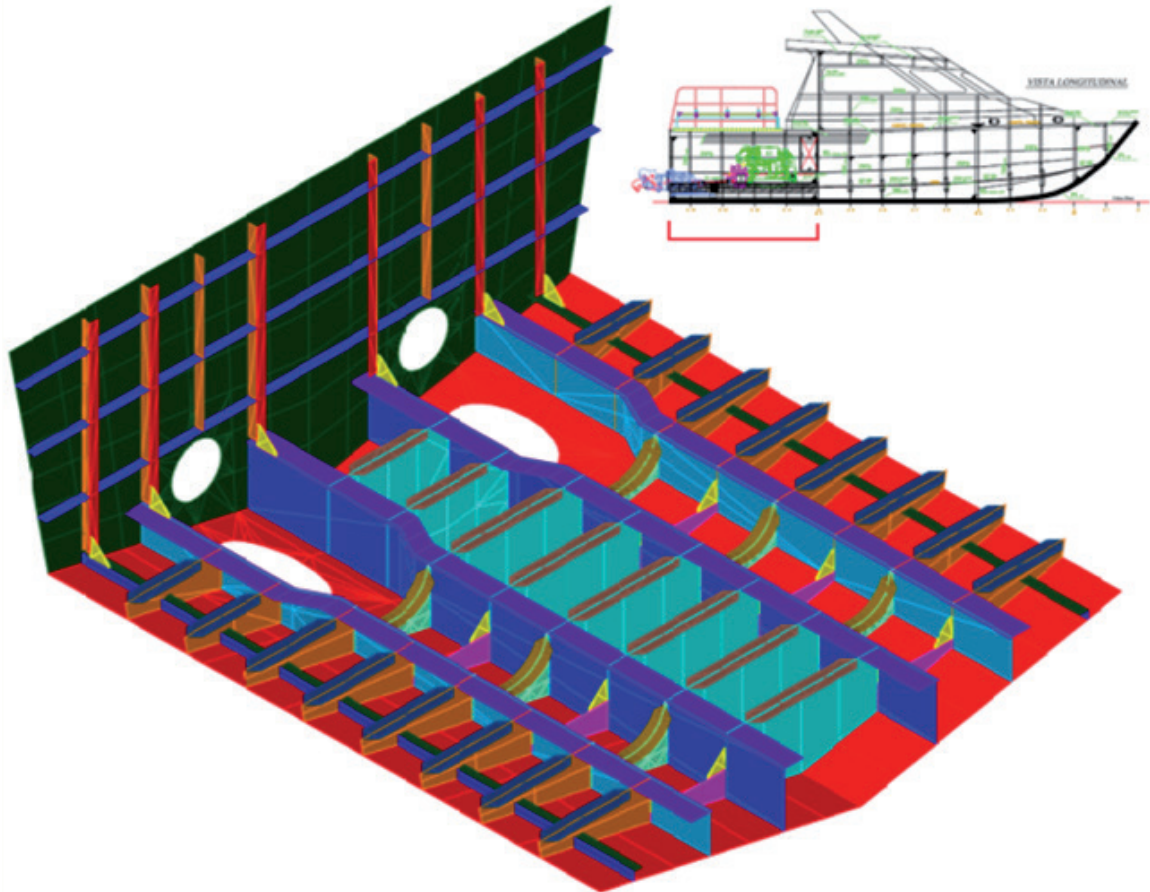
The authors thank ASTINAVE for providing the technical information to carry out this project.

Bibliography

- AEROSPACE SPECIFICATION METALS Inc. MatWeb. [Online]. <http://asm.matweb.com/search/SpecificMaterial.asp?bassnum=MA5086H116>
- AMERICAN BUREAU OF SHIPPING, "Guide for Building and Classifying High-speed Craft". ABS, 2012.
- AMERICAN BUREAU OF SHIPPING, "Structural Direct Analysis for High Speed Craft". ABS, 2011.
- ASTINAVE E.P., Memoria Técnica de la Lancha Guayas. Guayaquil, 2011.
- BANNANTINE, J., COMER, J., and HANDROCK, J., Fundamentals of Metal Fatigue Analysis. Pearson Edition, 1990.
- CUENCA, C., Determinación de la Vida Útil del fondo de una embarcación construida en Aluminio por Carga Vibratoria del Sistema Propulsivo. Tesis de Ingeniería Naval, FIMCBOR, ESPOL, Guayaquil, 2014
- DET NORSKE VERITAS, Rules for Classification of Speed, Light Craft, and Naval Surface Craft, DNV, 2011.
- European Committee for Standardization, Eurocode 9: Design of Aluminium Structures, Brussels, 2011.
- HAMILTON JET, Manual de diseño de la serie HJ de Hidrojets, 2007.
- KOROTKIN, A., Added Masses of Ship Structures. Springer, 2009.
- LONG, CH., Propellers, Shafting, and Shafting System Vibration Analyses, Cap. X en Marine Engineering, Harrington, Ed., SNAME, 1992.
- MARÍN, J., MIRANDA, L., and MACAS, F., Análisis de resultados propulsivos en una lancha planeadora de 11 m. Jornadas Técnicas sobre Propulsión de Buques, Colegio de Ingenieros Navales del Ecuador, Guayaquil, 2011.
- MORENO, V., Motores de Combustión Interna, Vol. II. Escuela Técnica Superior de Ingenieros Navales, Madrid, 1980.
- OTERO, C., Tipología y análisis de fallos en la estructura de los buques mercantes, 2ª parte. Revista Ingeniería Naval, Nov. 2004.

Appendix

Fig. 15. Geometric model of the structure.



Editorial Guidelines for Authors

Thematic Interest

The *Ship Science and Technology* Journal accepts for publication original engineering contributions in English language on ship design, hydrodynamics, dynamics of ships, structures and materials, vibrations and noise, technology of ship construction, marine engineering, standards and regulations, ocean engineering and port infrastructure, as well as results of scientific and technological research. Every article shall be subject to consideration by the Editorial Council of The *Ship Science and Technology* Journal deciding on the pertinence of its publication.

Typology

The *Ship Science and Technology* Journal accepts to publish articles classified within the following typology (COLCIENCIAS 2006):

- *Scientific and technological research articles.* Documents presenting detailed original results of finished research projects. Generally, the structure used contains four important parts: introduction, methodology, results, and conclusions.
- *Reflection Articles.* Documents presenting results of finished research as of an analytical, interpretative, or critical perspective of the author on a specific theme, resorting to original sources.
- *Revision Articles.* Documents resulting from finished research in the field of science or technology in which published or unpublished results are analyzed, systemized, and integrated to present advances and development trends. These are characterized by presenting an attentive bibliographic revision of at least 50 references.

Format

All articles must be sent to the editor of The *Ship Science and Technology* Journal accompanied by a letter from the authors requesting their publication. Every article must be written in *Microsoft Word* in single space and sent in magnetic form.

Articles must not exceed 10,000 words (9 pages).

File must contain all text and any tabulation and mathematical equations.

All mathematical equations must be written in *Microsoft Word Equation Editor*. This file must contain graphs and figures; additionally, they must be sent in a modifiable format file (soft copy). Also, abbreviations and acronyms have to be defined the first time they appear in the text.

Content

All articles must contain the following elements that must appear in the same order as follows:

Title

It must be concise (no more than 25 words) with appropriate words so as to give readers an idea of the contents of the article. It must be sent in English and Spanish language.

Author and Affiliations

The author's name must be written as follows: last name, initial of first name . Affiliations of author must be specified in the following way and order:

- Business or institution (including department or division to which he/she belongs).
- Street mailing address.
- City (Province/State/Department).
- Country.

Abstract

A short essay of no more than one hundred fifty (150) words, specifying content of the work, scope, and results. It must be written in such a way so as to contain key ideas of the document. It must be sent in English and Spanish language.

Key Words

Identify words and/or phrases (at least three) that recover relevant ideas in an index. They must be sent in English and Spanish language.

Introduction

The text must be explanatory, clear, simple, precise, and original in presenting ideas. Likewise, it must be organized in a logical sequence of parts or sections, with clear subtitles to guide readers. The first part of the document is the introduction. Its objective is to present the theme, objectives, and justification of why it was selected. It must contain sources consulted and methodology used, as well as a short explanation of the status of the research, if it were the case, and form in which the rest of article is structured.

Body Article

It is made up of the theoretical framework supporting the study, statement of the theme, status of its analysis, results obtained, and conclusions.

Equations, Tables, Charts and Graphs

All of these elements must be numbered in order of appearance according to their type and must have their corresponding legends, along with the source of the data.

Equations must be numbered on the right hand side of the column containing it, in the same line and in parenthesis. The body of the text must refer to it as "(Equation x)". When the reference starts a sentence it must be made as follows: "Equation x". Equations must be written so that capital letters can be clearly differentiated from lower case letters. Avoid confusions between the letter "l" and the number one or between zero and the lower case letter "o". All sub-indexes, super-indexes, Greek letters, and other symbols must be clearly indicated.

All expressions and mathematical analyses must explain all symbols (and unit in which they are measured) that have not been previously defined in the nomenclature. If the work is extremely mathematical by nature, it would be advisable to develop equations and formulas in appendixes instead of including them in the body of the text.

Figure/Fig. (lineal drawings, tables, pictures, figures, etc.) must be numbered according to the order of appearance and should include the number of the graph in parenthesis and a brief description. As with equations, in the body of the text, reference as "(Fig. X)", and when reference to a graph is the beginning of a sentence it must be made as follows: "Fig. x".

Charts, graphs, and illustrations must be sent in modifiable vector file format (*Microsoft Excel*, *Microsoft Power Point*, and/or *Microsoft Visio*).

Pictures must be sent in TIF or JPG format files, separate from the main document in a resolution higher than 1000 dpi.

Foot Notes

We recommend their use as required to identify additional information. They must be numbered in order of appearance along the text.

Acknowledgment

Acknowledgments may be made to persons or institutions considered to have made important contributions and not mentioned in any other part of the article.

Bibliographic References

The bibliographic references must be included at the end of the article in alphabetical order and shall be identified along the document. To cite references, the Journal uses ISO 690 standards, which specify the mandatory elements to cite references (monographs, serials, chapters, articles, and patents), and ISO 690-2, related to the citation of electronic documents.

Quotations

They must be made in two ways: at the end of the text, in which case the last name of author followed by a comma and year of publication in the following manner:

“Methods exist today by which carbon fibers and prepregs can be recycled, and the resulting recycle retains up to 90% of the fibers’ mechanical properties” (*Davidson, 2006*).

The other way is:

Davidson (2006) manifests that “Methods exist today by which carbon fibers and prepregs can be recycled, and the resulting recycle retains up to 90% of the fibers’ mechanical properties”.

List of References

Bibliographic references of original sources for cited material must be cited at the end of the article in alphabetical order and according to the following parameters:

In the event of more than one author, separate by commas and the last one by an “and”. If there are more than three authors write the last name and initials of the first author and then the abbreviation “*et al.*”.

Books

Last name of author followed by a comma, initial(s) of name followed by a period, the year of publication of book in parenthesis followed by a comma, title of publication in italics and without quotation marks followed by a comma, city where published followed by a comma, and name of editorial without abbreviations such as Ltd., Inc. or the word “editorial”.

Basic Form:

LAST NAME, N.I. *Title of book*. Subordinate responsibility (optional). Edition. Publication (place, publisher). Year. Extent. Series. Notes. Standard Number.

Example:

GOLDBERG, D.E. *Genetic Algorithms for Search, Optimization, and Machine Learning*. Edition 1. Reading, MA: Addison-Wesley. 412 p. 1989. ISBN 0201157675.

If a corporate author

Write complete name of entity and follow the other standards.

Basic form:

INSTITUTION NAME. *Title of publication*. Subordinate responsibility (optional). Edition. Publication (place, publisher). Year. Extent. Series. Notes. Standard Number.

Example:

AMERICAN SOCIETY FOR METALS. *Metals Handbook: Properties and Selection: Stainless Steels, Tool Materials and Special-Purpose Metals*. 9th edition. Asm Intl. December 1980. ISBN: 0871700093.

When book or any publication have as author an entity pertaining to the state, write name of country first.

Basic form:

COUNTRY, ENTITY PERTAINING TO THE STATE. *Title of publication*. Subordinate responsibility (optional). Edition. Publication (place, publisher). Year. Extent. Series. Notes. Standard Number.

Example:

UNITED STATES OF AMERICA. EPA - U.S. Environmental Protection Agency. Profile of the Shipbuilding and Repair Industry. Washington D.C. 1997. P. 135.

Journal Article

Basic form:

Last name, N.I. Title of article, *Name of publication*. Edition. Year, issue designation, Page number of the part.

Graduation Work

Basic form:

Primary responsibility. *Title of the invention*. Subordinate responsibility. Notes. Document identifier: Country or issuing office. *Kind of patent document*. Number. Date of publication of cited document.

Example:

CARL ZEISS JENA, VEB. *Anordnung zur lichtelektrischen Erfassung der Mitte eines Lichtfeldes*. *Et-finder*: W. FEIST, C. WAHNERT, E. FEISTAUER. Int. Cl.3 : GO2 B 27/14. Schweiz Patentschrift, 608 626. 1979-01-15.

Presentation at conferences or academic or scientific event

Basic form:

LAST NAME, N.I. Title of the presentation. In: Sponsor of the event. *Name of the event*. Country, City: Publisher, year. Pagination of the part.

Example:

VALENCIA, R., et al. Simulation of the thrust forces of a ROV En: COTECMAR. *Primer Congreso Internacional de Diseño e Ingeniería Naval CIDIN 09*. Colombia, Cartagena: COTECMAR, 2009.

Internet

Basic form:

LAST NAME, N.I. *Title of work*, [on-line]. Available at: http://www.direccion_completa.com, recovered: day of month of year.

Example:

COLOMBIA. ARMADA NACIONAL. COTECMAR gana premio nacional científico, [web on-line]. Available at: <http://www.armada.mil.co/?idcategoria=545965>, recovered: 5 January of 2010.

Acceptance

Articles must be sent by e-mail to the editor of The *Ship Science and Technology Journal* to otascon@cotecmar.com or in CD to the journal's street mailing address (COTECMAR Mamonal Km 9 Cartagena Colombia), accompanied by the "Declaration of Originality of Written Work" included in this journal.

The author shall receive acknowledgement of receipt by e-mail. All articles will be submitted to Peer Review. Comments and evaluations made by the journal shall be kept confidential. Receipt of articles by The Ship Science and Technology Journal does not necessarily constitute acceptance for publishing. If an article is not accepted it shall be returned to the respective author. The Journal only publishes one article per author in the same number of the magazine.

Opinions and declarations stated by authors in articles are of their exclusive responsibility and not of the journal. Acceptance of articles grants The Ship Science and Technology Journal the right to print and reproduce these; nevertheless, any reasonable petition by an author to obtain permission to reproduce his/her contributions shall be considered.

Further information can be obtained by:

Sending an e-mail to sst.journal@cotecmar.com

Contacting Oscar Dario Tascon (Editor)

The Ship Science and Technology (Ciencia y Tecnología de Buques) office located at: COTECMAR Mamonal Km. 9, Cartagena Colombia.

Phone Number: 57 - 5 - 6685377.

Statement of Originality of Written Work

Title of work submitted

I hereby certify that the work submitted for publication in The *Ship Science and Technology* journal of Science and Technology for the Development of Naval, Maritime, and Riverine Industry Corporation, COTECMAR, was written by me, given that its content is the product of my direct intellectual contribution. All data and references to material already published are duly identified with their respective credits and are included in the bibliographic notes and quotations highlighted as such.

I, therefore, declare that all materials submitted for publication are completely free of copyrights; consequently, I accept responsibility for any lawsuit or claim related with Intellectual Property Rights thereof.

In the event that the article is chosen for publication by The *Ship Science and Technology* journal, I hereby state that I totally transfer reproduction rights of such to Science and Technology for the Development of Naval, Maritime, and Riverine Industry Corporation, COTECMAR. In retribution for the present transfer I agree to receive two issues of the journal number where my article is published.

In witness thereof, I sign this statement on the _____ day of the month of _____ of year _____, in the city of _____.

Name and signature:

Identification document:



Km. 9 Vía Mamonal - Cartagena, Colombia
www.shipjournal.co

Vol. 8 - n.º 16

January 2015

Development of a Comparison Method of
Sonar Systems for Surface Platforms

Andrés Cortes Ciro, Ennio Emanuel Pinzón Villarroel

Fuel-Cell Integration on Board Surface Ships

David Ignacio Fuentes, Hernán de Lavalle Pérez

Implementation of the Confirmation of Methods in the calibration of
Measuring Equipment as Standardized Strategy to Assure the Quality
of Measurements Made in the Construction, Repair, and Modernization of
Ships and Naval Artifacts in COTECMAR

Ronald Yesid Argote Guzmán

Solution to the Anti-aircraft Fire Control Problem on a Naval
Platform Using the Direct Geometric Model

Luis Guerrero Gómez, Montserrat Espín García

Fatigue Analysis of the Structural Bottom of an Aluminum
Planing Craft through Vibratory Load of the Propeller System

José R. Marín, Carlos A. Cuenca



COTECMAR

www.shipjournal.co